TRYPTOPHAN REGULATION OF THE *ESCHERICHIA COLI* TRYPTOPHANASE (*TNA*) OPERON

A Dissertation

by

ALLYSON KENDALL MARTINEZ

Submitted to the Office of Graduate and Professional Studies of
Texas A&M University
in partial fulfillment of the requirements for the degree of

DOCTOR OF PHILOSOPHY

Chair of Committee,	Matthew Sachs
Committee Members,	Michael Benedik
	Deborah Siegele
	Margaret Glasner
Head of Department,	Tom McKnight

December 2013

Major Subject: Microbiology

Copyright 2013 Allyson Kendall Martinez

ABSTRACT

Free L-tryptophan induces the expression of the *Escherichia coli tna* operon that specifies proteins necessary for catabolizing tryptophan. Regulation is effected by a transcriptional attenuation mechanism requiring translational arrest at the TnaC regulatory leader peptide in the 5' leader of the *tna* transcript. Interactions between the TnaC nascent regulatory peptide and the elements constituting the ribosomal peptide exit tunnel are implicated in the inhibition of the translating ribosome by free L-tryptophan.

In this study, genetic and biochemical analyses were used to investigate the role of specific residues of the TnaC peptide and of 23S rRNA regions that line the ribosomal exit tunnel in TnaC-mediated ribosome arrest. Highly conserved amino acids of TnaC and the 23S rRNA nucleotides predicted by structural models to interact with those TnaC residues were selected for analysis. TnaC residues Trp-12, Asp-16, and Ile-19 and 23S rRNA nucleotides A748-A752 as well as U2609 and A2058 are crucial for L-tryptophan-induced TnaC-mediated ribosome arrest. Interactions between the TnaC peptide and 23S rRNA residues are affected by mutations to either molecule. These interactions, specifically between Ile-19 of TnaC and the 23S rRNA A2058 nucleotide, are required for L-tryptophan binding and/or action. Finally, both *cis*-acting and *trans*-acting mutations can suppress the loss-of-function TnaC D16E mutation, supporting the model that both the TnaC peptide and the ribosome exit tunnel are active participants in the inhibition of peptidyl-transferase activity in response to L-tryptophan.

Taken together, the findings of this study suggest that the highly conserved nature of specific amino acids of TnaC can be explained by the requirement for interactions between these residues with 23S rRNA nucleotides within the ribosomal exit tunnel. These interactions likely induce conformational changes within the TnaC peptide, the ribosomal exit tunnel or both that contribute to the formation of a free L-tryptophan binding site, locking the peptidyl-transferase center in an inactive conformation resulting in ribosome arrest.

DEDICATION

To Nana

ACKNOWLEDGEMENTS

I express my deepest gratitude to my graduate advisor Dr. Matthew Sachs for his mentoring, guidance, patience, and support throughout my graduate career. I have grown so much professionally under his guidance and it has been an honor being part of his lab.

I also thank the other members of my committee Dr. Michael Benedik, Dr. Deborah Siegele, and Dr. Margaret Glasner for their support. I would especially like to thank Dr. Benedik for giving me a space to work in his lab and for all of his guidance.

And a very special thanks to Dr. Luis Rogelio Cruz-Vera and Dr. Charles Yanofsky for advise, collaboration, and weekly conference calls throughout my graduate work.

I also thank the current and former members of the Sachs' lab, especially Dr. Cheng Wu, Dr. Ying Zhang, and Dr. Jiajie Wie and a special thanks to Dr. Benedik's former graduate student and my best friend Dr. Mary Abou Nader Crum.

I give my love and gratitude to my family, especially my husband Alejandro Martínez II, our first child Alejandro Martínez III, my father Frederick Wakefield, and my grandmother Mary Wakefield. Many thanks for their love, patience, and support throughout my life. Without them, I would not be who I am today.

To my husband: I could not have done this without you. Thank you for the helpful discussions, kind reassuring words, and your amazing Illustrator abilities.

Finally, to Baby Alex, who I carried with me during the final year of my graduate career: thank you for waiting patiently and coming after my Dissertation Defense.

NOMENCLATURE

β-gal	β-galactosidase
Ery	erythromycin
L-Trp	L-tryptophan
PTC	peptidyl transferase center
r-protein	ribosomal protein
rRNA	ribosomal RNA
SD	Shine-Dalgarno

TABLE OF CONTENTS

Page

LIST OF FIGURES

Page

LIST OF TABLES

Page

CHAPTER I

INTRODUCTION AND LITERATURE REVIEW

OVERVIEW

The ribosome has the remarkable ability to synthesize all of the proteins that cells produce. To accomplish this task, the ribosome must synthesize myriad of peptide/protein sequences without discrimination. This requirement has historically led to the view that the ribosome was a nonspecific translational machine, without any regulatory function. However, it has become evident that during translation the exit tunnel of the ribosome monitors the structure of the peptide being synthesized and can modulate translation in response to specific peptide sequences. Peptide-dependent translational arrest, or ribosome stalling, is now known to control the expression of a number of bacterial and eukaryotic genes (1-11).

Ribosome arrest peptides (RAPs) are often encoded in the 5'-leader region of bacterial transcripts (termed leader peptides), and in upstream open reading frames (uORFs) in eukaryotic transcripts. By stalling ribosomes during their own synthesis, such RAPs can regulate expression of downstream genes transcribed on the same transcript. There are two classes of RAPs. The first class of RAPs stalls the ribosome only when an inducing level of a required small molecule is present. The bacterial leader peptides TnaC and ErmCL, and the eukaryotic Arginine Attenuator Peptide (AAP) and MAGDIS, fall into this class of RAPs (4,5,7,8). The second class of RAPs contain intrinsic arrest sequences that mediate ribosome stalling without the requirement

for small molecules. The bacterial leader peptides SecM and MifM, and the cytomegalovirus (CMV) gp48 uORF2 fall into the second class (10,12). The bacterial leader peptides TnaC, ErmCL, SecM, and MifM, and their role in gene expression regulation, are the focus of this introduction and literature review. TnaC will be reviewed because it is the focus of my research; ErmCL, SecM, and MifM regulation will be reviewed because the mechanism of TnaC-mediated ribosome arrest will be compared to the mechanism used by each of the other bacterial leader peptide systems in the discussion section of this dissertation.

My research has focused on understanding additional features of the molecular basis for TnaC-mediated L-tryptophan (L-Trp)-dependent ribosome arrest—how ribosome stalling is achieved through the interactions between the ribosomal exit tunnel, TnaC, and the amino acid, L-Trp. Through genome-wide studies it has become evident that leader peptides and uORFs play more of a role in regulating gene expression than was first realized (13,14). Furthermore, continuing studies have revealed the variety of regulatory features used by translating ribosomes, in regulating gene expression. As a result, understanding how RAPs function in concert with the ribosome to cause translational arrest is now more of a priority than it was ever before. Therefore, the techniques used and the results of this study can be applied to understanding the arrest mechanisms of newly discovered RAPs, especially those implicated in human diseases and regulation of antibiotic resistance genes in bacteria.

PROKARYOTIC RIBOSOME

The prokaryotic 70S ribosome is a 2.3 MDa ribonucleoprotein complex, composed of a large (50S) subunit and the small (30S) subunit, their combined action functions to translate mRNA into proteins. A total of 54 proteins and 3 ribosomal RNAs (rRNAs) make up the prokaryotic 70S ribosome, with 33 proteins and 2 rRNAs (23S and 5S) in the 50S subunit and 21 proteins and 1 rRNA (16S) constituting the 30S subunit (15). Ribosomal proteins are located primarily within the shell of the ribosome and serve a variety of functions such as aiding in the assembly and maintenance of the structure of the ribosome, lining the mRNA entry pore, and providing binding sites for translation factors, chaperones, and protein export machinery. The rRNA forms most of the core of the ribosome, which contains the functional centers of the ribosome: the decoding center, the peptidyl-transferase center (PTC), and the exit tunnel.

During translation initiation, the functional 70S ribosome is formed by the binding of the 50S subunit to the pre-initiation complex (which is composed of the 30S subunit, initiation factors, and fMet-tRNA), bringing together at the interface the decoding center of the 30S subunit and PTC of the 50S subunit. Within the decoding center, the 30S subunit contains three binding sites for tRNA: the aminoacyl site (A-site), the peptidyl site (P-site), and the exit site (E-site). The A-site accepts incoming aminoacylated-tRNA, the P-site contains tRNA with attached peptide chain (peptidyl-tRNA), and the E-site holds deacylated-tRNA before it leaves the ribosome. The A-site is mainly tasked with maintaining the fidelity of translation by monitoring base-pairing between the codon of the mRNA and the anti-codon loop of the tRNA (16).

Specifically, the 16S rRNA nucleotides G530, A1492, and A1493 in this region are responsible for distinguishing between cognate and near-cognate tRNA, which is important for maintaining translational fidelity (17). After the codon:anticodon interaction within the A-site of the decoding center, the PTC of the ribosome functions to catalyze peptide bond formation, transferring the growing nascent peptide from the peptidyl-tRNA to the amino acid of the newly bound aminoacyl-tRNA. 23S rRNA nucleotides within the PTC bind the acceptor arms of the incoming aminoacyl-tRNA and the peptidyl-tRNA, positioning them in a manner conducive to peptide bond formation (18). Interactions among nucleotides A2602, U2584, and G2553 and the aminoacyl- and peptidyl-tRNAs influence peptide bond formation. Through the concerted action of the two subunits at the interface—that is, decoding of the mRNA by the 30S subunit, peptide bond formation by the 50S subunit, and the involvement of both subunits in translocation—proteins are synthesized by adding one amino acid at a time.

All newly formed proteins must traverse the exit tunnel of the ribosome, which spans approximately 80-100 Å from the peptidyl-transferase center through the body of the large ribosomal subunit and opens at the opposite side (Figure 1) (19). Along its length, the diameter of the exit tunnel varies between 10-20 Å (19). The walls of the ribosome exit tunnel are composed almost entirely of 23S rRNA except at the constriction site where regions of ribosomal proteins (r-proteins) L4 and L22 protrude into the exit tunnel decreasing the diameter in this region (19,20). The constriction site thus provides an opportunity for interactions between exit tunnel components and the nascent peptide. Some proteins, instead of passing passively through the exit tunnel,

actively interact with and induce conformational changes within the exit tunnel as well as the PTC. Therefore, the mechanism of how these interactions and conformational changes elicit translational arrest are subject to experimental analysis.

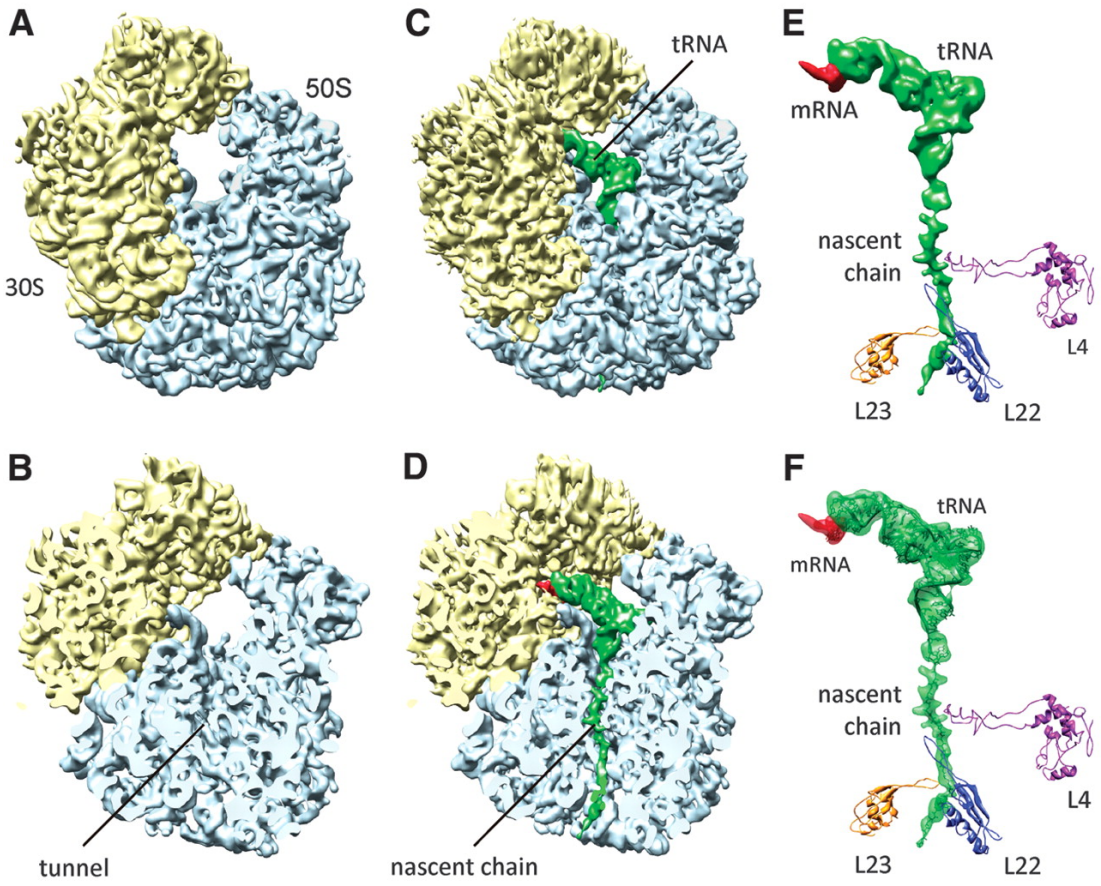

Figure 1. Cryo-EM reconstruction of the TnaC•70S complex. (**A and B**) Cryo-EM reconstruction of the control E. coli 70S ribosome at 6.6 Å resolution, with small and large subunit colored yellow and blue, respectively. (**C and D**) The 5.8 Å resolution cryo-EM density of the TnaC•70S complex, with density for the TnaC-tRNA shown in green. (**E**) Isolated density for the TnaC-tRNA (green) and mRNA (red) from (**C**). The relative positions of ribosomal proteins L4 (purple), L22 (blue), and L23 (yellow) are indicated. (**F**) Fitting of molecular models for the TnaC-tRNA^{Pro} into the cryo-EM density from (**E**). Figure was reprinted with permission from "Structural insight into nascent polypeptide chain-mediated translational stalling" by Birgit Seidelt, Axel C. Innis, Daniel N. Wilson, Marco, Gartmann, Jean-Paul Armache, Elizabeth Villa, Leohardo G. Trabuco, Thomas Becker, Thorsten Mielke, Klaus Schulten, Thomas A. Steitz, and Roland Beckman. 2009. *Science*, 326, 1412-1415, Copyright [2009] by The American Association for the Advancement of Science.

TNAC

The *tna* operon of *Escherichia coli* contains a 319-nt transcribed leader region and two structural genes *tnaA*, which encodes tryptophanase, and *tnaB*, which encodes a tryptophan-specific permease (Figure 2) (21,22). Tryptophanase is a catabolic enzyme that breaks down L-Trp into indole, pyruvate, and ammonia (23). Pyruvate and ammonia can be used as carbon and nitrogen sources, respectively, which allow bacteria with a functional *tna* operon to use L-Trp as their sole carbon and nitrogen source. Indole is a volatile signaling molecule that has been shown to function in both quorum sensing and biofilm formation (24,25). Recently, tryptophanase, through the production of indole, has been implicated in exotoxin-induced lethality caused by Enteropathogenic *E.coli* (26).

Transcription initiation of the *tna* operon is controlled by catabolite repression and is L-Trp-independent (27). The CRP-cAMP complex is a positive acting element that is required for activation of catabolite sensitive promoters. Glucose concentration and cAMP concentration in the cell are inversely related. Therefore, when glucose, the preferred carbon source of *E.coli*, is limiting, cAMP levels increase. Under limiting glucose, CRP-cAMP activates a number of catabolite sensitive promoters, including the promoter of the *tna* operon (27).

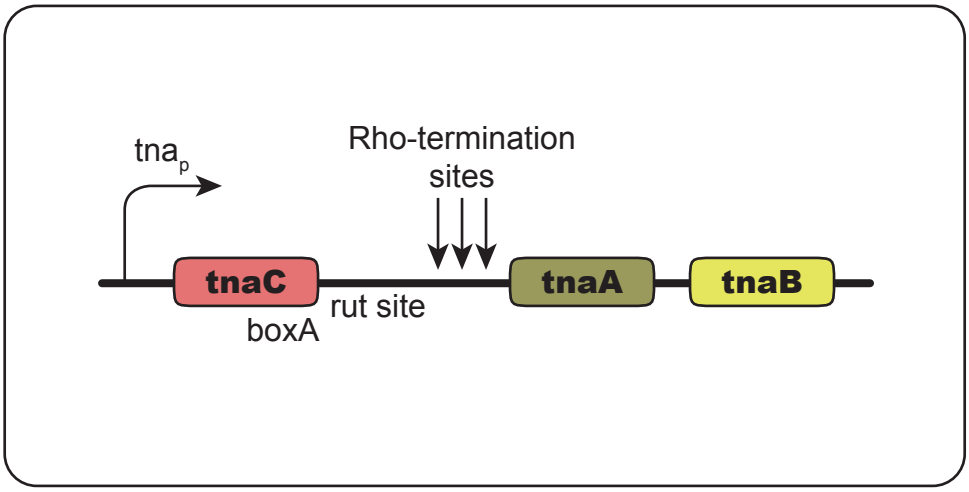

Figure 2. Arrangement of the *E.coli tna* operon. The *tna* operon of *E.coli* consist of the coding region for the 24 amino acid leader peptide TnaC, followed by the two structural genes of the operon, *tnaA* and *tnaB*. The *boxA* site is contained within *tnaC* and is immediately followed by the *rut* site. The 220 nucleotide transcribed region between *tnaC* and *tnaA* also contains several Rho-termination sites. The *boxA* site, *rut* site, and Rho-termination sites all work in concert to terminate transcription in the leader region in the absence of inducing levels of tryptophan.

Continuation of transcription into the structural genes of the operon is regulated by L-Trp-dependent inhibition of Rho Factor-dependent transcription termination (1). Previous analysis of *tna* mRNA levels showed that in the absence of tryptophan transcription is terminated prematurely resulting in shorter transcripts that are rapidly degraded. L-Trp decreases transcription termination and thus increases the presence of the read-through transcripts containing *tnaA* and *tnaB* coding regions (28,29). The transcribed leader region contains important regulatory elements that work in concert to regulate the L-Trp-dependent increase of read-through transcription and subsequent translation of *tnaA* and *tnaB*. The regulatory elements within the leader region include: (i) the coding region for the 24 amino acid leader peptide, *tnaC*, which functions as a

RAP, (ii) a presumed *boxA* site, (iii) a Rho utilization (*rut*) site, and (iv) transcription pause sites (30). The *boxA* site, *rut* site, and transcription pause sites function together to reduce the expression of *tnaA* and *tnaB* in the absence of inducing levels of L-Trp by attenuating transcription. In the presence of inducing levels of L-Trp, the TnaC leader peptide, through its RAP function, causes transcription to continue into *tnaA* and *tnaB*.

The specific functions of the last nine nucleotides of *tnaC*, which resemble a *boxA* site, which in bacteriophage λ early regions and rRNA operons prevents Rho-dependent transcription termination through binding of Nus factors, remains obscure (31,32). It was hypothesized that the presumed *boxA* sequence in the leader region of the *tna* operon might function similarly to decrease termination. However, both *in vivo* and *in vitro* studies on the effect of NusA on anti-termination in the *tna* operon showed that NusA may actually increase Rho-dependent termination (32). Introduction of specific point mutations or deletion of the *boxA* sequence results in decreased termination and constitutive expression of tryptophanase (1,31,32). However, whether this is a consequence of changes to the *boxA* sequence at the nucleotide level or a change in the amino acid sequence of TnaC has not been resolved. Additionally, the roles of NusA and the identified *boxA* sequence in *tna* operon regulation remain unclear.

The functions of the other regulatory elements are clearer. The *rut* site and the transcription pause sites in the intergenic region between *tnaC* and *tnaA* are important for Rho-dependent transcription termination (1,28,32). Rho is an RNA-binding protein that is required for transcription termination by RNA polymerase at certain sites in the *E.coli* genome (33,34). The observation that basal tryptophanase levels were increased

upon the addition of bicyclomycin, a Rho inhibitor, and the identification of a *rut* site immediately following *tnaC* suggested that Rho-dependent transcription termination reduced expression of *tnaA* and *tnaB* in the absence of inducing levels of L-Trp (32,35). Furthermore, Rho mutations and deletion of the *rut* site result in constitutive reporter operon expression (31,32,35). Together, these results support the requirement for Rho-dependent transcription termination in controlling basal level expression of the structural genes of the *tna* operon. The transcription pauses sites in the intergenic region between *tnaC* and *tnaA* function to slow the progress of RNA polymerase. This allows sufficient time for Rho to bind to the transcript and interact with RNA polymerase, which is required for transcription termination.

Translation of *tnaC* is required for L-Trp induction of *tna* operon expression. In the absence of translation, when the start codon of *tnaC* is changed to a stop codon, L-Trp induction of *tna* operon expression is abolished (28,36). In the absence of inducing levels of L-Trp, translation termination at the *tnaC* stop codon occurs through RF2-mediated cleavage of the peptidyl-tRNA. The peptide is released from the ribosome and the ribosome dissociates from the mRNA (28). After efficient translation termination at the *tnaC* stop codon, the *rut* site, which immediately follows the *tnaC* stop codon, is exposed and is available for Rho binding. Rho-dependent transcription termination occurs in the leader region before transcription of the structural genes of the *tna* operon (Figure 3A) (31,37). Therefore, in the absence of inducing levels of L-Trp, the expression of *tnaA* and *tnaB* is reduced. In the presence of inducing levels of L-Trp, RF-2 binding and/or action are inhibited causing the ribosome to stall at the stop codon of

tnaC. The stalled ribosome blocks Rho's access to the *rut* site decreasing transcription termination and increasing read-through transcription into the structural genes of the operon (Figure 3B) (31,37).

The amino acid sequence of TnaC is important for free L-Trp-mediated induction (31). Mutations in *tnaC* that alleviated L-Trp-mediated induction changed the amino acid sequence. However, changes to the nucleotide sequence that did not change the amino acid sequence had little to no affect on L-Trp-mediated induction (31). Genome-wide comparisons of species that contain *tnaC* and mutational analysis of highly conserved residues identified W12, D16, I19, and P24 to be crucial for L-Trp-mediated induction of *tna* operon expression (31,32,38) (Figure 4). These residues in combination with L-Trp either directly interfere with translation termination at the PTC or indirectly as a consequence of interactions within the ribosome exit tunnel.

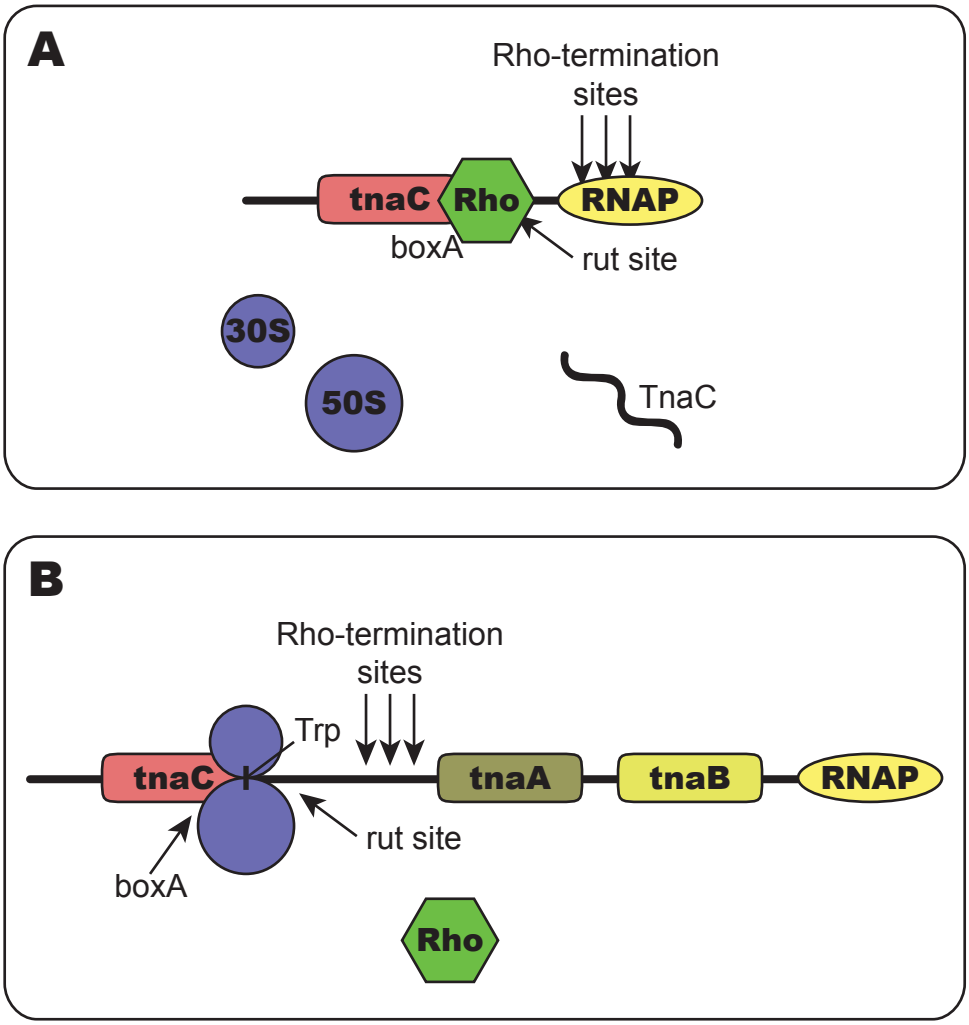

Figure 3. Regulation of the *E.coli tna* operon by an attenuation of transcription mechanism. (**A**) In the absence of inducing levels of L-Trp, after synthesis of TnaC, translation is efficiently terminated resulting in the dissociation of the nascent TnaC peptide and the ribosomal subunits from the transcript. The dissociation of the ribosome from the transcript uncovers the *rut*-site. The Rho transcription termination factor can then bind to the *rut*-site allowing Rho to interact with paused RNA polymerase in the intergenic region between *tnaC* and *tnaA* leading to premature transcription termination before the structural genes of the *tna* operon are transcribed. (**B**) In the presence of inducing levels of L-Trp, TnaC translation termination is inhibited, leading to ribosome arrest at the end of the *tnaC* coding sequence. The arrested ribosomes at the end of the *tnaC* sequence blocks Rho's access to the *rut*-site allowing RNA polymerase to continue transcription into the structural genes of the *tna* operon, thus increasing the expression of *tnaA* and *tnaB*.

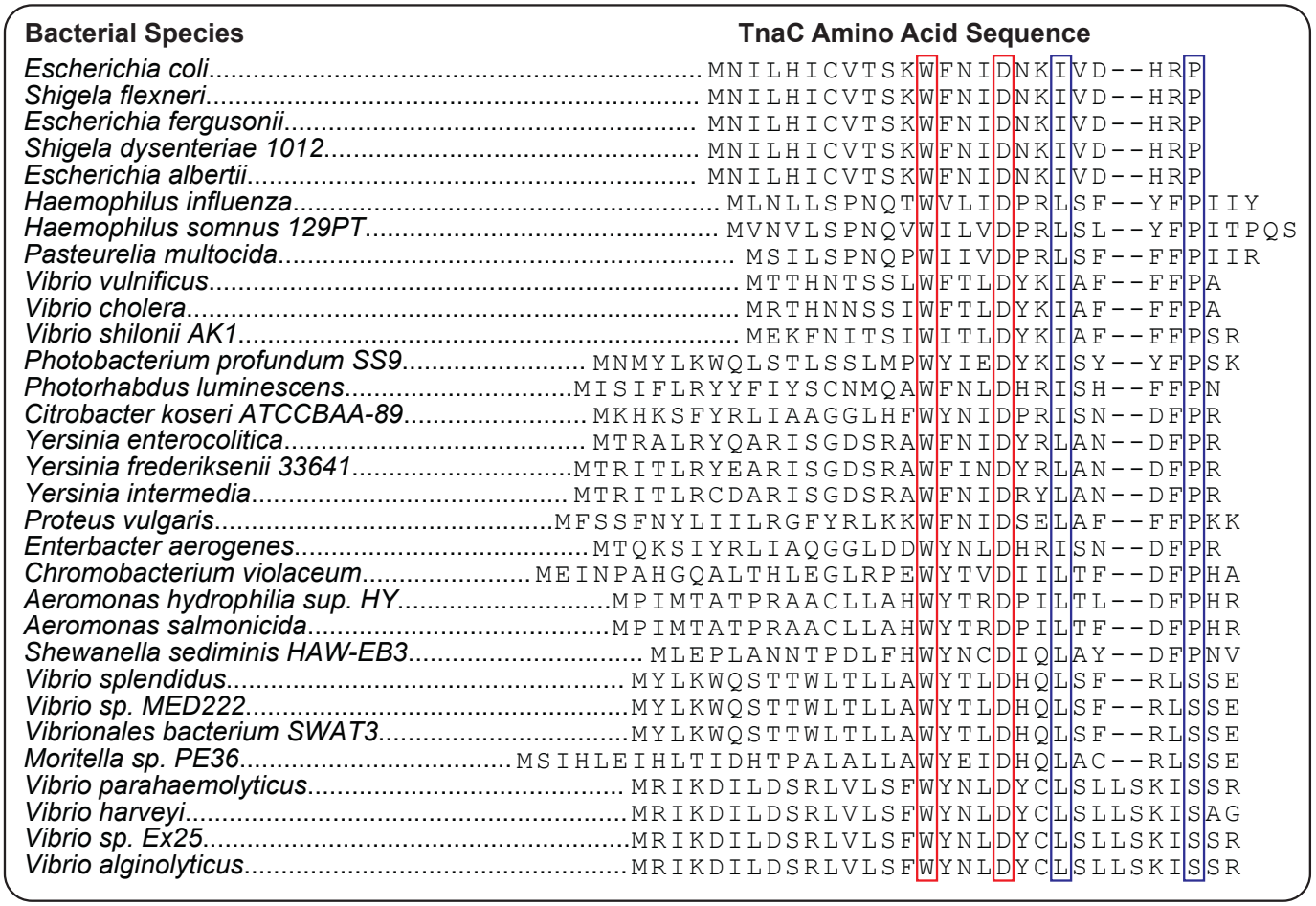

Figure 4. Alignment of TnaC sequences from different bacterial species. Residues boxed in red are fully conserved across examined species and residues boxed in blue are semi-conserved. Figure was reprinted with permission from "Conserved residues Asp16 and Pro24 of TnaC-tRNA^{Pro} participate in tryptophan induction of *tna* operon expression" by Luis R. Cruz-Vera and Charles Yanofsky. 2008. *Journal of Bacteriology*, 14, 4791-4797, Copyright [2008] by American Society for Microbiology.

Although the P24 codon and the UGA stop codon are important at the nucleotide level as part of the *boxA* site for the termination of transcription in the absence of L-Trp, P24 and the UGA stop codon are also important for ribosome arrest in the presence of L-Trp. In species that possess a *tnaC* gene, P24 is highly conserved, and in *E.coli*, induction is reduced when changes are made to P24 (4,32,39). Accumulation of TnaC-tRNA^{Pro} is observed in response to L-Trp, consistent with the ribosome arrest occurring with P24 in the P-site and the stop codon in the A-site (29,40). This finding suggests that Trp acts to inhibit translation termination by preventing the cleavage of the peptidyl-tRNA by RF2. The identity of the *tnaC* stop codon is also crucial, and controls both the basal and induced levels of *tna* operon expression (41). The UGA stop codon is recognized by RF2, and in *E.coli* RF2 is less efficient at termination than RF1. The inefficiency of RF2 may be important for allowing L-Trp binding and/or action before RF2 can function to terminate translation. When the stop codon of *tnaC* is changed to UAA or UAG, both of which are recognized by RF1, translation terminates more efficiently and as a result both the basal and induced levels are impacted, resulting in less induction (41). While P24 and the UGA stop codon are individually important, the combination of Pro-stop may function synergistically to strengthen the arrest. The Pro-stop combination was found to be the most common cause of stalling in laboratory derived peptide sequences, and although the choice of the Pro codon was not important, UGA was the most highly represented stop codon(42). The Pro-stop combination may create a PTC conformation that is incompatible with RF2-mediated termination and in the case of TnaC, L-Trp may help to facilitate and/or prolong this conformation.

The formation of the arrest-site within the PTC by the P24-stop combination means that at the time of arrest the other crucial peptide residues W12, D16, and I19 are within the exit tunnel (43). W12 and D16 are the only two amino acids of TnaC that are absolutely conserved across all bacterial species that possess a *tnaC* gene; I19 along with P24 are the only two that are semi-conserved (39). Changes to each of these positions have been examined (30,31,36,39). TnaC has a single Trp codon at position 12, and its role in L-Trp induction of the *tna* operon was investigated due to the resemblance to the *trp* operon in regards to the components involved in regulation (36). Changing W12 to R, L, or a stop codon, abolishes induction (30,36). Addition of excess arginine to cultures of the W12R strain did not restore induction, suggesting that induction is not simply due to the accumulation of high levels of the free amino acid encoded by codon 12 (36). However, induction was partially restored to the strain in which W12 was replaced by a stop codon upon addition of a suppressor tRNA that inserts Trp at position 12 (36). Taken together, these results suggest that the translation of W12 by $tRNA^{Trp}$ is necessary for some aspect of L-Trp induction of reporter operon expression (36). The observation that the conservative change D16E eliminated L-Trp induction led to further analysis to determine if D16 functions to prevent L-Trp binding and/or action or by some other mechanism (31,39). Changes to D16 inhibited both the L-Trp-dependent accumulation of TnaC-$tRNA^{Pro}$ and the ability of L-Trp to block the transfer of the nascent TnaC peptide to puromycin (39). The results of these experiments suggest that D16 participates in the inhibition of peptidyl transferase activity resulting in translational arrest. The effect of changes to the only other semi-conserved residue besides P24, I19,

was also examined (31). The non-conservative I19N and I19T changes eliminate induction; however, how I19 participates in causing the L-Trp-mediated ribosome arrest is not understood (39). Structural analysis of the ribosome in the process of translating TnaC suggest that the critical residues implicated by the genetic and biochemical data may be interacting with residues in the ribosomal exit tunnel (43).

Stalling can be alleviated by mutations to specific 23S rRNA nucleotides and mutations altering r-proteins L4 and L22 within the exit tunnel, suggesting that interactions between exit tunnel components and specific amino acids of TnaC function to facilitate the arrest (44). The loop of r-protein L22 protruding into the exit tunnel and 23S rRNA nucleotides lining the wall of the exit tunnel on the same side as the L22 protrusion appear to be the main components of the exit tunnel involved in TnaC-mediated ribosome arrest. Changes to r-protein L22 residues K90 and G91 or to 23S rRNA nucleotides A752, U2609, or the insertion of an additional adenine residue in the A750-754 region, reduce or eliminate reporter operon induction (44). Many of these changes also inhibit TnaC-tRNA^{Pro} accumulation and allow puromycin release of TnaC in the presence of L-Trp, suggesting that these residues are important for hindering peptidyl-transferase activity in response to L-Trp (45). Residues within the loop of r-protein L4 that protrudes into the exit tunnel and/or residues of the 23S rRNA lining this side of the tunnel may play a minor role in L-Trp induction since changes to specific positions within these components slightly impact induction (44).

ERMCL

Erythromycin (Ery) and other macrolide antibiotics are bactericidal because their binding at the entrance of the ribosomal exit tunnel creates an obstruction leading to cell-wide translational arrest (46). The 2'-OH group of the deosamine sugar of Ery is responsible for binding within the exit tunnel through the formation of hydrogen bonds at three positions: N6 and N1 of A2058 and N6 of A2059 (46). The two most common ribosomal resistance mechanisms against macrolide binding are the A2058G mutation at the Ery binding site and the N6 dimethylation of A2058 by the Ery resistance family of methylases (46,47). In A2058G mutant ribosomes the presence of guanine instead of adenine at the Ery binding site affects the formation of the hydrogen bonds that are required for binding (48). In mitochondrial and cytoplasmic rRNAs of eukaryotes, the position corresponding to *E.coli* A2058 is a guanine instead of an adenine, which explains the selectivity of macrolides to bacterial ribosomes (49). The other mechanism of resistance, the dimethylation of N6 of A2058, would also prevent hydrogen bond formation, as well as cause a steric hindrance for binding due to the addition of the two bulky methyl groups (46).

The inducible *ermC* gene, which encodes a Ery resistance methylase, is preceded by the 19 amino acid long ORF that encodes the regulatory leader peptide ErmCL (7). The *ermCL*/*ermC* transcript adopts two different mRNA secondary structures, one in either the absence of *ermCL* translation or in the absence of Ery and the other conformation in the presence of subinhibitory concentrations of Ery (50). The mRNA secondary structure adopted by the transcript in the absence of Ery contains two stem-

loop structures, one containing the 3'-end of the *ermCL* coding sequence and the other containing the Shine Dalgarno (SD) sequence of *ermC* (50). Therefore, in the absence of Ery, the occlusion of the *ermC* SD sequence prevents translation (Figure 5A). In the presence of Ery, the ribosome stalls during translation of *ermCL*; the stalled ribosome prevents the first stem-loop from forming leading to the formation of an alternative stem-loop which does not occlude the *ermC* SD sequence (50). Therefore, Ery-mediated ribosome arrest leads to activation of *ermC* (7) (Figure 5B).

Since the binding of Ery within the ribosome exit tunnel causes cell-wide translational arrest, whether arrest during translation of *ermCL* was simply a consequence of the Ery-induced global translational arrest or if the ErmCL peptide itself has features that promote the arrest in response to Ery binding was analyzed (7,51). The effect of changes to the ErmCL amino acid sequence was first analyzed by ErmCL-mediated reporter gene induction in response to Ery and later by toeprinting assays (7,51). The results of both studies showed that the ^{6}IFVI^{9} sequence of ErmCL is required for ErmCL-mediated ribosome arrest in the response to Ery (7,51). By toeprinting, I9 of ErmCL was identified as the arrest-site with the I9 codon in the P-site and the S10 codon in the A-site at the time of the stall (7). The stalled ribosome was found to contain a 9 amino acid-long peptidyl-tRNA^{Ile} meaning that it was stalled after translocation and not trapped in the pre-translocation state, which would lead to the 10 amino acid-long peptidyl-tRNA^{Ser} (7). The location of the peptidyl-tRNA in the P-site suggests that the ErmCL peptide, in combination with Ery, functions to inhibit the

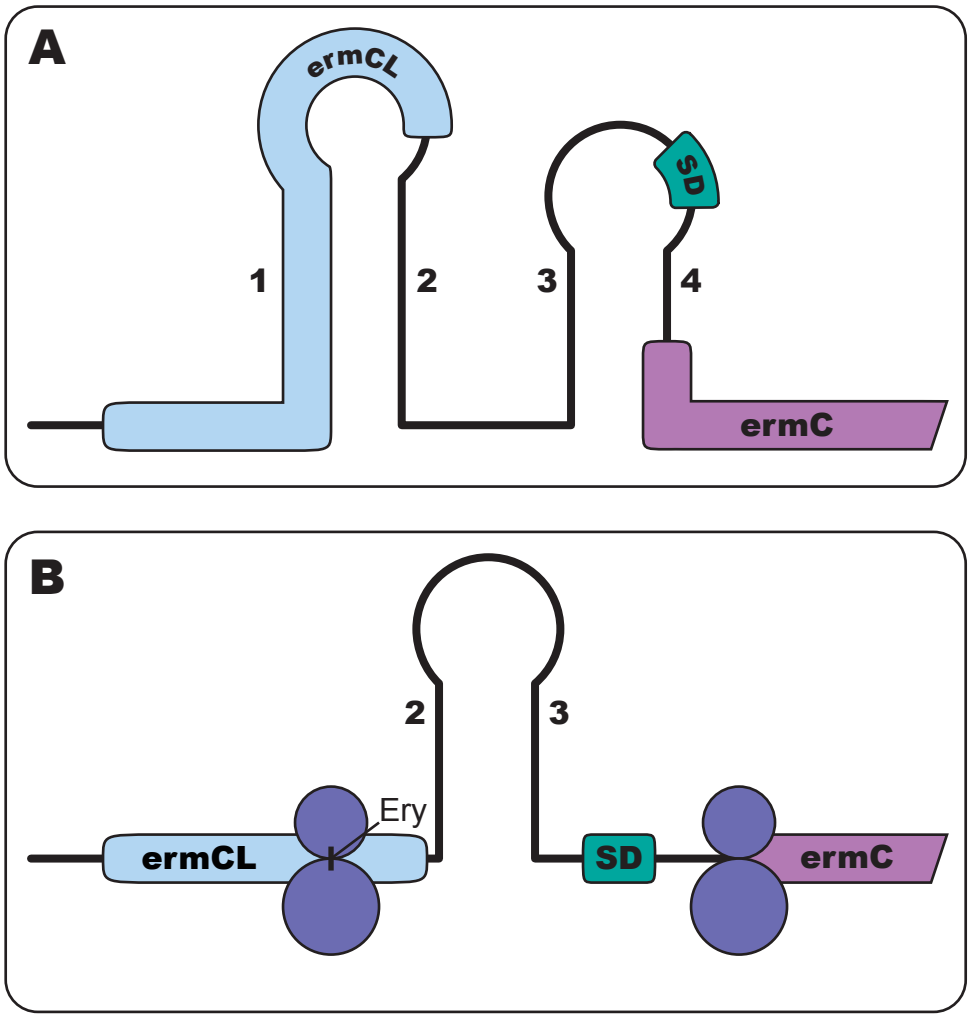

Figure 5. The adoption of an alternative mRNA secondary structure in response to Ery-mediated ribosome arrest in the *ermCL*/*ermC* transcript induces the expression of *ermC*. (**A**) In the absence of Ery, the *ermCL*/*ermC* transcript adopts a conformation with two stem-loop structures that is not conducive to *ermC* translation. One stem-loop contains the 3'-end of the *ermCL* coding sequence and the other stem-loop contains the SD sequence of *ermC*. The occlusion of the *ermC* SD sequence within the second stem-loop inhibits translation initiation. (**B**) In the presence of Ery, ribosome arrest occurs during translation of *ermCL*. The arrested ribosome prevents formation of the first stem-loop structure containing the 3'-end of *ermCL*, thus allowing an alternative stem-loop structure to form. This alternative stem-loop does not occlude the *ermC* SD sequence relieving the inhibition of translation initiation at *ermC*. SD = Shine-Dalgarno.

catalysis of peptide bond formation. This hypothesis was validated by the observation that Ery prevents the transfer of the stalled ErmCL peptide to puromycin (7). The observations that the stalled ErmCL peptide is much shorter than other RAPs and that the identity of residues 1-5 of ErmCL is not important for ribosome arrest, led to the questions of whether or not the length of the stalled peptide is important and if the length impacts the stall site. Insertion or deletion of one or more amino acid within the N-terminus resulted in less efficient stalling; however, the ribosome always arrested at the same site, with the I9 codon in the P-site (7). These results suggest that although the sequence of the N-terminus is not important, the length is important so that the peptide can reach a specific place within the exit tunnel to cause the ribosome arrest.

Mutations to ribosomal components within the exit tunnel decrease Ery-dependent stalling at the *ermCL* ORF, supporting the idea that ErmCL must reach a specific place in the exit tunnel to trigger ribosome arrest (5,7,52). Mutations to three 23S rRNA nucleotides close to the macrolide binding site drastically reduce both Ery-dependent ErmCL-driven reporter gene expression *in vivo* and ribosome stalling *in vitro* as assessed by toeprinting, without affecting Ery binding (5,7,52). 23S rRNA nucleotide A2062 extends into the exit tunnel opposite the Ery binding site (20). The narrowing of the exit tunnel entrance created by Ery binding and the A2062 protrusion is at an optimal location for interaction with the ErmCL IFVI stall sequence (7). Therefore, mutations of A2062 may prohibit recognition of the ErmCL stall sequence by the ribosome, preventing Ery-mediated ribosome arrest. Another 23S rRNA nucleotide located in the

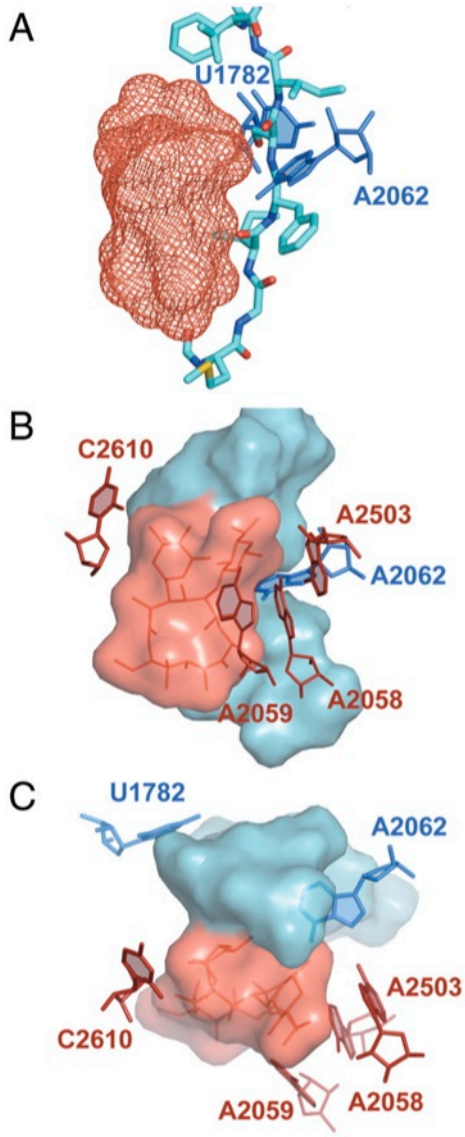

Figure 6. Dual function of the antibiotic cofactor in programmed ribosome stalling. (**A**) First, binding in the ribosome exit tunnel of a macrolide antibiotic (salmon mesh) ensures interaction of the *ermCL* stalling nascent peptide (cyan) with tunnel sensors, including U1782 and A2062 (blue). (**B and C**) Second, the antibiotic is recognized as a part of the composite stalling signal in the tunnel. Specific sensors (experimentally identified C2610 and A2503 as well as suspected A2058 and A2059) (red) are positioned to interact specifically with the drug molecule. The nascent peptide (cyan) and antibiotic (salmon) are shown in surface representation. (**B**) Side view of the peptide–antibiotic complex; (**C**) top view from the PTC down the tunnel. This figure was reprinted with permission from "Role of antibiotic ligand in nascent peptide-dependent ribosome stalling" by Nora Vázquez-Laslop, Dorota Klepacki, Debbie C. Mulhearn, Haripriya Ramu, Olga Krasnykh, Scott Franzblau, and Alexander S. Mankin. 2011.*Proceedings of the National Academy of Sciences of the United States of America*, 108, 10496-10501, Copyright [2011] by The National Academy of Sciences of the United States of America.

vicinity of the Ery binding site at the entrance of the exit tunnel is the post-transcriptionally modified nucleotide A2503 (5). A2503 is dimethylated at the C2 position by the RlmN methyltransferase (53). This modification as well as an adenine at this position are both required for Ery-dependent stalling at the *ermCL* ORF (5). The importance of the adenine at this position is likely due to the requirement for the dimethylation of this residue, while the addition of the two bulky methyl groups may facilitate the recognition of the ErmCL stall sequence by the ribosome, possibly through the positioning of ErmCL for interaction with A2062. The 23S rRNA nucleotide C2610 is also in close proximity to A2058, A2062, and A2503; and mutations to this residue affect Ery-induced ErmCL-mediated ribosome arrest (52). The cladinose sugar of Ery that is required for ErmCL-mediated ribosome stalling is 3.5 Å away from C2610 (52). This distance allows direct interaction between the 3" methyl group of the cladinose sugar and the hydrophobic face of C2610 (Figure 6) (52). The fact that the cladinose sugar of Ery is required for ErmCL-mediated ribosome arrest, the direct contact of the cladinose sugar with C2610, and the reduced stalling at the *ermCL* ORF in C2610 mutant ribosomes, implicates C2610 as the Ery sensor that specifically responds to the properly positioned macrolide contributing to stalling at the *ermCL* ORF. Besides 23S rRNA residues at the entrance of the exit tunnel, the loop of r-protein L22 at the constriction site may also be involved in ErmCL-mediated ribosome stalling in response to Ery (7). A deletion of three amino acids (M82-R84) in the β-loop of r-protein L22 reduced Ery-induced stalling at the *ermCL* ORF (7). The N-terminus of the 9 amino acid-long extended ErmCL peptide is in close proximity to this loop of r-protein L22 in

the exit tunnel (7). The requirement for the ErmCL peptide to reach a certain length for formation of the stalled complex and the proposed function of the constriction site as a discriminating gate are both consistent with the idea that r-protein L22 participates in ErmCL-mediated ribosome arrest.

SECM

The cytosolic ATPase SecA functions to target nascent peptides that possess a signal sequence to the SecYEG translocation machinery and assist in their translocation across the inner membrane (54). *secA* is translationally regulated by the leader peptide SecM, which is encoded upstream of *secA* in the same transcriptional unit (55). SecM monitors the protein export competency of the cell, and expression of *secA* is induced when protein export is compromised. SecM contains a signal sequence and a translational arrest domain, both of which are required for its regulatory activity (55).

The signal sequence of SecM and its recognition by SecA are required for translational repression of *secA* under conditions of excess secretion capacity (55,56). The cotranslational recognition of the SecM signal sequence by SecA results in the targeting of SecM to the SecYEG complex. The translocation of SecM via the SecYEG complex results in SecM being pulled from the ribosome (55). The 3'-end of *secM* is predicted to form a stem-loop structure with the region upstream of the *secA* coding sequence occluding the *secA* Shine-Dalgarno sequence (SD) when this region of *secM* is not translated (57,58). Therefore, when the levels of SecA are sufficient to support the protein secretion needs of the cell, SecM is continually pulled from the ribosome, and

the sequestration of the *secA* SD sequence is maintained, resulting in repression of *secA* (Figure 7A). When levels of SecA are insufficient to support protein translocation, the interaction of the SecM signal sequence with SecA is reduced, and translation of *secM* continues into the translational-arrest domain. Translational arrest disrupts the stem-loop structure, relieving the sequestration of the SD sequence of *secA*. Other ribosomes can bind to the available SD sequence and initiate translation resulting in the induction of *secA* (Figure 7B) (57).

The C-terminus of SecM contains the translational arrest domain. The stall site was identified by inserting a TAA stop codon into various positions near the 3'-end of the *secM* coding sequence (12). Insertion of a stop codon before or at the arrest site will result in translation termination at this position, relieving the ribosome arrest. However, the ribosome arrest will be maintained if a stop codon is inserted after the arrest site. Using this method, P166 was identified as the arrest point (12). Other amino acids in this region that are required for the arrest function were identified by alanine scanning mutagenesis (wild-type Ala residues were replaced by Ser) (12). Amino acids were designated as essential if the change to alanine (or serine) resulted in a decreased precipitation of peptidyl-tRNA by cetyltrimethylammonium bromide (CTABr) and an increase in the production of full-length product. CTABr precipitates nucleic acid, and is used to assess the accumulation of peptidyl-tRNA. Peptidyl-tRNA accumulates as a result of translational arrest. Also, insertions or deletions of one residue in the region severely compromised the arrest activity (12). The translational arrest sequence was identified as FXXXXWIXXXXGIRAGP (12). The residues that immediately precede

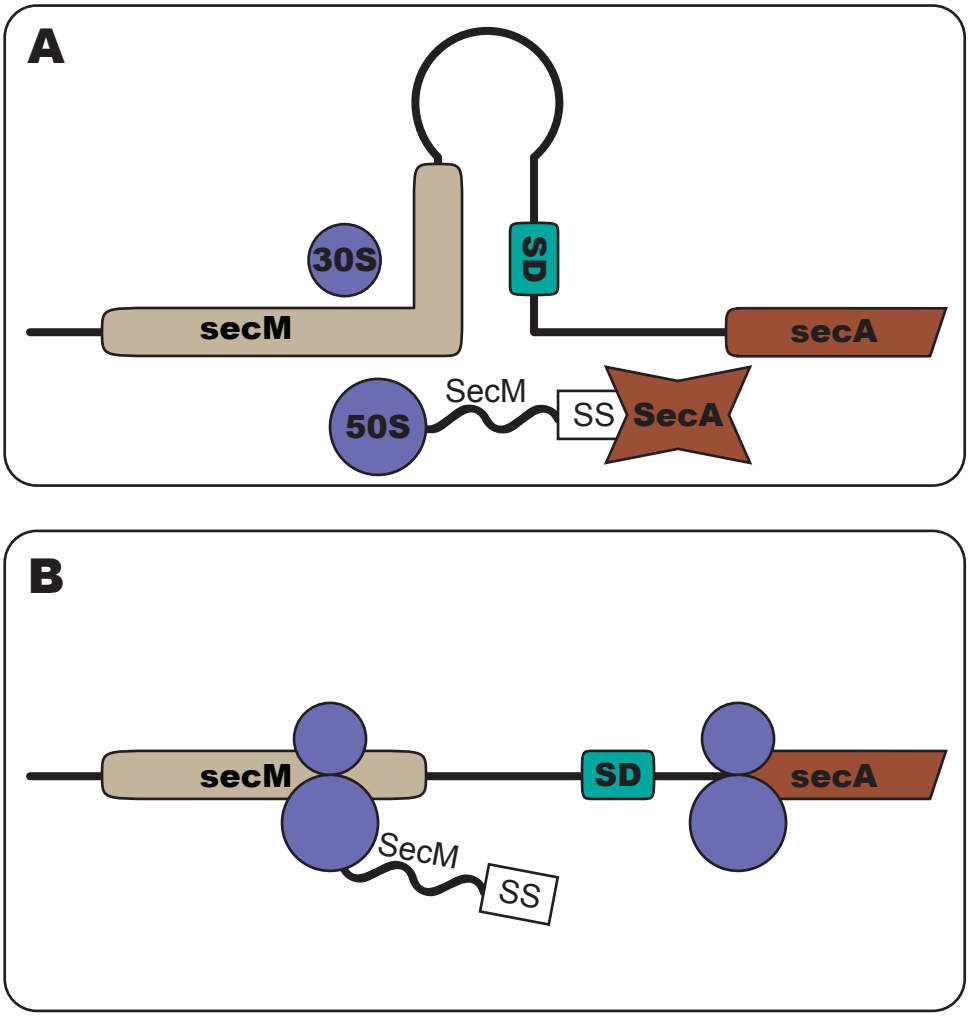

Figure 7. The leader peptide SecM contains an intrinsic ribosome arrest sequence, which regulates expression of the downstream gene, *secA*, based on whether the stall is alleviated or maintained. (**A**) The *secM*/*secA* transcript is predicted to form a secondary structure, which occludes the SD sequence of *secA*. When levels of SecA are sufficient to support the protein secretion needs of the cell, SecM, which contains a secretion signal sequence, is continually pulled from the ribosome, alleviating ribosomal arrest. Under these conditions the sequestration of the *secA* SD sequence within the stem-loop structure is maintained leading to repression of *secA* translation. (**B**) When the levels of SecA are not sufficient to support the protein secretion needs of the cell, the ribosome stall at the *secM* ribosome arrest sequence is maintained because SecM is not pulled from the ribosome by the secretion machinery. The stalled ribosome blocks the formation of the stem-loop structure, which results in induction of *secA* expression due to the availability of the SD for translation initiation. SD = Shine-Dalgarno, SS = Secretion signal.

the stall site residue, P166, likely interacts with components of the ribosome within the PTC, and these interactions may contribute to the inhibition of translation elongation. Other residues further away from the stall site, namely F150, W155, and I156, are within the ribosome exit tunnel at the time of the stall. Interactions between these residues and components of the ribosome exit tunnel may be necessary for translational arrest.

The SecM signal sequence is only required for regulated *secA* expression. The translational arrest domain [SecM(121-166)] is necessary and sufficient for the arrest function (59). SecM that does not contain the signal sequence produces a prolonged translational arrest that is independent of the protein translocation capacity of the cell (59). Since several of the critical residues of SecM would be within the ribosomal exit tunnel at the time of arrest, interactions between these residues of SecM and components of the ribosomal exit tunnel may play a role in the arrest. Therefore, just as mutations to specific positions of SecM relieve ribosome arrest, mutations to key positions within the ribosomal exit tunnel may also relieve the arrest. To test this possibility, the translational arrest domain fused to LacZα was used in a genetic screen for mutations in ribosomal components that relieve arrest (12). Due to translational arrest and incomplete LacZα production, cells with the SecM(140-166)-LacZα construct will produce white colonies on plates containing 5-bromo-4-chloro-3-indolyl-β-D-galactoside (X-gal). After mutagenesis cells can be screened on X-gal plates for production of blue colonies. Blue colonies result from translational read-through leading to production of LacZα.

Two amino acids of r-protein L22 and two positions within the 23S rRNA were identified through the genetic screen to be crucial for translational arrest. Changes to

G91 and A93 of r-protein L22 resulted in blue-colored colonies and increased production of full-length SecM(140-166)-LacZα (12). Both of these amino acids are in the region of r-protein L22 that forms the constriction site within the ribosomal exit tunnel. Changes to G91 and A93 would increase the size of the amino acid side chains leading to further constriction in this region, which may be responsible for the impairment of translational stalling. Two mutations within the 23S rRNA were also found to alleviate SecM-mediated ribosome arrest. The mutation A2058G and an insertion of an additional adenine in a region with five consecutive adenine residues (A749-A753 region) both result in blue-colored colonies and a substantial increase in the production of full-length SecM(140-166)-LacZα (12). A2058 is within the region of the 23S rRNA that lines the wall of the narrowest part of the exit tunnel. The A749-A753 region also occupies the narrowest part but on the opposite side of the exit tunnel (12). Since most of the ribosomal exit tunnel is composed of 23S rRNA, interactions between specific regions of the 23S rRNA and residues of SecM may play an important role in SecM-mediated ribosome arrest. The positioning of crucial residues of SecM within the exit tunnel at the time of the ribosome stall further supports this hypothesis.

MIFM

The YidC/Oxa1/Alb3 family of proteins function to insert proteins into the membrane and ensure assembly of many of these proteins within the membrane (60). YidC can either function in association with the Sec machinery or can function independently for insertion of proteins that lack large extracellular domains (61).

Bacillus subtilis encodes two YidC homologs, *spoIIIJ*/*yidC1*, which is constitutively expressed and *yqjG*/*yidC2*, which is only expressed under conditions where SpoIIIJ activity is limited (62). Although either SpoIIIJ or YidC2 alone can support viability, SpoIIIJ is the main contributor in the protein insertion pathway, while YidC2 functions as a backup system in the event that SpoIIIJ activity is compromised (8,62).

The observation that expression of *yidC2* is SpoIIIJ-dependent suggests that *B.subtilis* has a mechanism to monitor SpoIIIJ activity and increase YidC2 levels for maintenance of YidC activity (8). The *yidC2* gene is transcribed as an operon, with the upstream gene *yqz1*/*mifM*. The leader peptide MifM, encoded by the upstream gene regulates the expression of *yidC2* at the level of translation (8). MifM contains an N-terminal transmembrane domain, which is a substrate for SpoIIIJ, and the C-terminal translational arrest domain, both of which are required for the regulated expression of *yidC2* (8).

Interaction of MifM with SpoIIIJ is required to maintain the repression of *yidC2* (8). The interaction of the N-terminal transmembrane domain of ribosome-associated MifM with SpoIIIJ results in insertion of MifM into the membrane, and as a consequence the nascent peptide is pulled from the ribosome in a mechanism similar to SecM (12). The 3'-end of the *mifM* coding sequence is predicted to form a stem-loop structure with the SD sequence of *yidC2* (Figure 8A). The mechanical pulling of the nascent peptide disassociates the ribosome from the peptide and the mRNA, preventing the translation of the 3'-end of *mifM*. In the absence of *mifM* translation, the SD sequence of *yidC2* remains sequestered in the stem-loop and unavailable for ribosome

binding for translation initiation of *yidC2* (8). Therefore, adequate membrane insertion by SpoIIIJ results in the repression of *yidC2*. Under conditions in which membrane insertion is inhibited due to insufficient levels of SpoIIIJ, translation of *mifM* is attenuated resulting in induction of *yidC2* (8). When SpoIIIJ is unavailable to pull MifM from the ribosome, translation of MifM continues and ribosomal arrest disrupts the stem-loop structure making the *yidC2* SD sequence available for ribosome binding resulting in *yidC2* translation (Figure 8B) (8).

The mechanism of MifM-mediated ribosomal arrest is unique in that the ribosome stalls temporarily and consecutively at four or more codons (63). In most other RAPs studied to date, the functional stall happens at only one specific location. The multi-site stalling observed with MifM is hypothesized to be important for prolonging the stall so that sufficient levels of YidC2 can be produced to support membrane insertion in the absence of SpoIIIJ (63). The amino acid sequence, and not the nucleotide sequence of MifM, has been shown to be important for the stalling activity (8,63). Specifically, a stretch of four consecutive negatively charged amino acids (termed the DEED motif) immediately upstream of the first major arrest site is required for MifM-mediated ribosomal arrest and induction of reporter gene expression. Decreasing the net negative charge of the DEED motif results in decreased induction. However, only the net negative charge, and not the identity of the amino acids, is important (63). Besides the DEED motif, alanine-scanning mutagenesis was used to identify the minimal set of amino acids required for MifM-mediated ribosomal arrest.

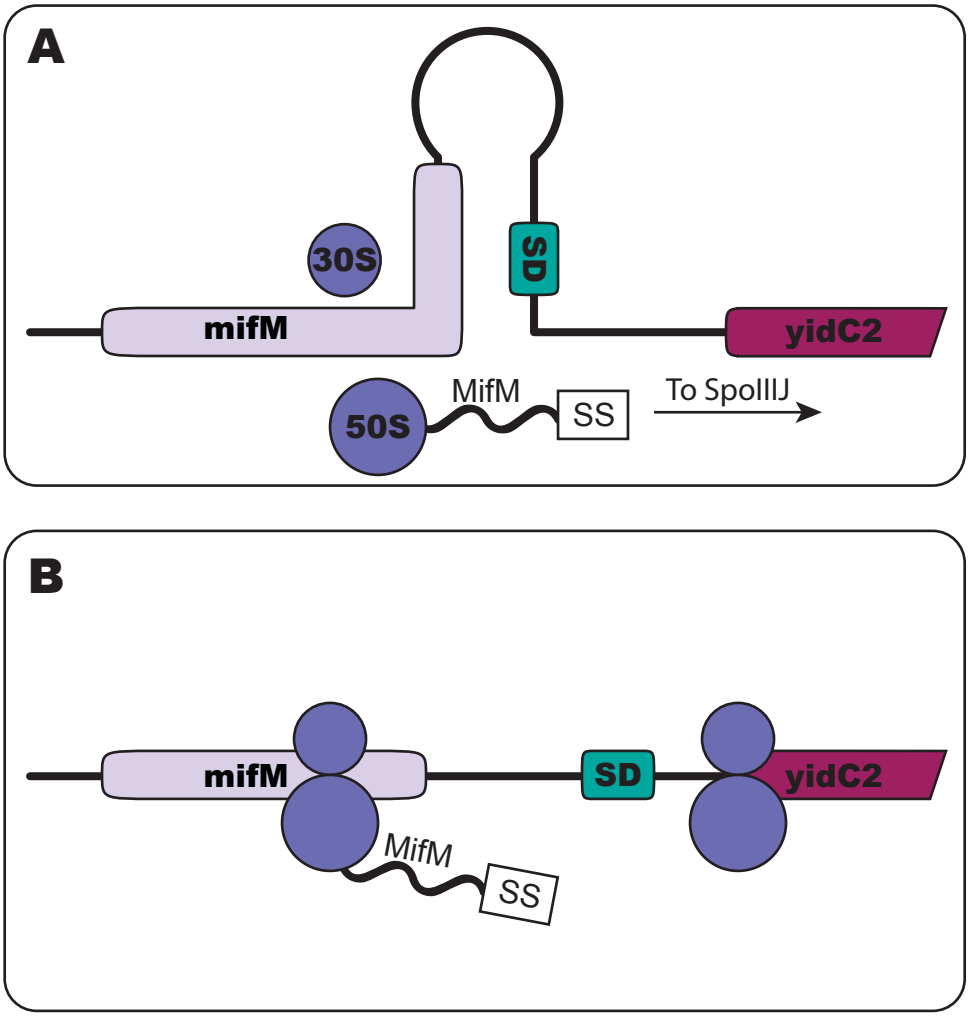

Figure 8. The MifM leader peptide, encoded upstream of *yidC2*, responds to the level of SpoIIIJ and regulates expression of the downstream *yidC2* gene. (**A**) The secondary structure of the *mifM*/*yidC2* transcript occludes the SD sequence of *yidC2* within a stem-loop structure, leading to the repression of *yidC2*. Under conditions where SpoIIIJ levels are sufficient to support the insertion of proteins into the membrane, the N-terminus of ribosomally-associated MifM interacts with SpoIIIJ, which results in MifM being pulled from the ribosome and inserted into the. The secondary structure of the mRNA is maintained and *yidC2* expression is repressed. (**B**) Under conditions where SpoIIIJ levels are limiting, ribosomally-associated MifM is not pulled from the ribosome and thus translation continues into the ribosome arrest domain of *mifM*. The arrested ribosome within the *mifM* coding sequence prevents the formation of the stem-loop structure; therefore, the SD sequence of *yidC2* is available for translation initiation and the repression of *yidC2* is relieved. SD = Shine-Dalgarno, SS = Secretion signal.

An amino acid was designated as essential if the change to alanine both increased production of full length MifMΔTM (MifM that lacks transmembrane domain) and reduced *yidC2* induction when SpoIIIJ is absent (8). Based on this analysis, R69, I70, W73, I74, M80, and N81 were determined to be essential. All of these amino acids are upstream of the translational arrest sites and are predicted to be within the ribosomal exit tunnel during arrest. Therefore, the identity of the amino acids within the ribosomal exit tunnel and not those at the arrest sites are critical for MifM-mediated ribosomal arrest (8).

During the time of translational arrest the amino acids of MifM that are critical for the arrest function reside within the ribosomal exit tunnel. Therefore, the interactions between these amino acids and components of the ribosomal exit tunnel may contribute to the arrest. A duplication of seven amino acids in r-protein L22 (^{94}SQINKRT^{100}) that confers erythromycin resistance compromises both MifM translational arrest and *yidC2* induction (8). This region of r-protein L22 forms part of the constriction site of the ribosomal exit tunnel, and mutations in this region are also know to affect SecM-, ErmCL-, and TnaC-mediated ribosomal arrest (7,12,44). The constriction site, which is made up of regions of r-proteins L4 and L22 that protrude into the exit tunnel, is approximately 30 Å from the PTC (7). The seven amino acid duplication within this region of r-protein L22 may disrupt an interaction between one or more of the critical MifM amino acids with specific residues of r-protein L22 that is required for the ribosomal arrest.

SUMMARY AND PURPOSE

The ribosome is tasked with the responsibility of synthesizing the entire array of proteins required by a cell. In most cases, the ribosome synthesizes proteins without evident discrimination of the peptide sequence being translated; however, in some cases the ribosome clearly responds to specific peptide sequences by arresting translation during their synthesis. The ribosome can either recognize intrinsic stall sequences within a RAP or respond to a stall site only in combination with a required small molecule. This nascent peptide-dependent translational arrest makes the ribosome an active participant in the regulation of the gene(s) whose expression is controlled by the regulatory leader peptide.

The fact that features of both the RAP and the ribosome are required for the nascent peptide-dependent arrest suggests that the ribosome must be recognizing some feature of the RAP likely through interactions between the ribosomal components and the nascent peptide. These interactions may be required for positioning the peptide such that other required interactions take place and/or for inducing conformational changes of the peptide, the ribosome, or both. The changes induced by these interactions lead to ribosome arrest by interfering with peptidyl transferase activity.

Studying nascent peptide-mediated stalling of the ribosome in *E.coli* has several advantages over studying it in a eukaryotic system. The mechanistic basis of fundamental translation processes is best understood in bacteria and thus tools are available in *E.coli* that facilitate the understanding of this mechanism of translational control. One available tool is the crystal structure of the prokaryotic ribosome, which

provides a high resolution structure of ribosomal components including the PTC and the ribosome exit tunnel (18). Also, cryo-EM structures of the *E.coli* ribosome in the process of translation (43). These structures provide insight into the interactions taking place between the nascent peptide and the ribosome and how these interactions lead to conformational changes that induce nascent peptide-dependent ribosome stalling. Other advantages to using *E.coli* as a model include the availability of rRNA mutations that have differential effects on different stall-inducing nascent peptides and the fact that nascent peptide-mediated stalling activity can be reliably assessed by *in vivo* studies (7,42,44,64,65).

The structural analysis of the ribosome in the process of translating TnaC has furthered our understanding of the relationship between essential residues of TnaC and exit tunnel components, predicting which interactions may be responsible for L-Trp-mediated ribosome arrest (43). However, biochemical data is still needed to assess the functionality of these interactions. The goal of this study was to combine data from the structural analysis with the biochemical data from my dissertation research to develop a model for the molecular mechanism of L-Trp-dependent ribosome arrest during the synthesis of TnaC. Mutational analyses of specific TnaC and 23S rRNA residues separately and in combination were used to confirm the interactions predicted by the structural analysis and understand the role of these interactions in ribosome arrest.

The cryo-EM model shows all four conserved residues of TnaC determined to be involved in L-Trp induction (W12, D16, I19, and P24) to be in close proximity to residues of the ribosome that are also important for L-Trp induction (43). W12 of TnaC

is adjacent to r-protein L22 residue R92 and 23S rRNA residue A751, which is consistent with the UV-crosslinking data showing that TnaC residue K11 can be cross-linked to 23S rRNA residue A750 (43,44). 23S rRNA nucleotides A752 and U2609 are predicted to form a base-pair interaction and the cryo-EM model shows D16 of TnaC contacting these two positions (43,66). The ribosomal contact partner of I19 is predicted to be A2058 and A2059 of the 23S rRNA; however, due to limited biochemical data on these residues, the role that this interaction may play on L-Trp induction is unknown (43). The PTC nucleotide U2585 is predicted to interact with P24 of TnaC and, in the presence of TnaC, U2585 and A2602 adopt conformations that are incompatible with release factor binding (43). Since the ribosome stalls as a result of the inhibition of peptidyl transferase activity, unexpectedly most of the crucial residues of TnaC and of ribosomal components are in the exit tunnel and not at the PTC. Therefore, understanding how nascent peptide-exit tunnel interactions, in combination with free L-Trp, contribute to translational arrest was crucial for developing a model of the molecular mechanism of TnaC-mediated L-Trp induction of ribosome arrest.

CHAPTER II

CRITICAL ELEMENTS THAT MAINTAIN THE INTERACTIONS BETWEEN THE REGULATORY TNAC PEPTIDE AND THE RIBOSOME EXIT TUNNEL RESPONSIBLE FOR TRP INHIBITION OF RIBOSOME FUNCTION*

INTRODUCTION

Expression of the *E. coli* tryptophanase operon, *tnaCAB*, is induced in response to L-tryptophan (L-Trp) by the action of the TnaC nascent peptide. TnaC stalls the ribosomes that have produced it in response to high L-Trp; the stalled ribosomes inhibit transcription attenuation, resulting in increased operon expression (1). The *tna* operon consists of a leader regulatory region, which includes *tnaC,* and two downstream structural genes, *tnaA* and *tnaB*. *tnaA* encodes tryptophanase, an enzyme involved in the degradation of L-Trp to obtain indole, energy and ammonia (21). In addition to its roles in biosynthetic pathways, the indole molecule is used in bacteria as a signal in regulating biofilm formation and quorum sensing (24). *tnaB* encodes a Trp permease for Trp transport into the cell (21). *tnaC* specifies the 24- residue TnaC regulatory leader peptide. Immediately downstream of *tnaC* there is a non-coding segment which contains Rho-dependent terminator sequences (21).

---

*Reprinted with permission from "Crucial elements that maintain the interactions between the regulatory TnaC and the ribosome exit tunnel responsible for Trp inhibition of ribosome function" by Allyson K. Martínez, Nitin H. Shirole, Shino Murakami, Michael J. Benedik, Matthew S. Sachs, and Luis R. Cruz-Vera, 2012. *Nucleic Acids Research*, 40(5), 2247-2257, Copyright [2012] by Oxford Journals

Transcription initiation of the *tna* operon is regulated by catabolite repression (67). Despite transcription activation by CAP/cAMP, transcription of the *tna* operon is terminated prematurely at the Rho-dependent termination sequences when low concentrations of L-Trp are present in the growth media (1). However, in the presence of high L-Trp, transcription of the *tna* operon is not attenuated at those sites and mRNA containing *tnaA* and *tnaB* is produced (1). Hydrolysis of the terminal TnaC-tRNA^{Pro} peptidyl-tRNA by the action of RF-2 protein during translation termination is inhibited by L-Trp, causing the translating ribosome to transiently stall at the *tnaC* stop codon (29,40). The stalled ribosome masks the binding sequences for the Rho termination-factor; the absence of interaction of Rho with the nascent mRNA allows transcription to continue into the *tnaA* and *tnaB* structural genes (32,40).

Analyses of the primary structure of the TnaC peptide from many bacterial species have revealed that the Trp residue at the 12th position (W12), an aspartic acid residue at the 16th position (D16), and a proline residue at the last position (P24) of *E. coli* TnaC are highly conserved (38,39). These conserved TnaC residues are essential for TnaC-mediated L-Trp-induction (39). Changing these amino acid residues abolishes L-Trp induction in vivo, the ability of L-Trp to inhibit the hydrolysis induced by RF-2, and L-Trp-inhibition of TnaC-tRNA^{Pro} cleavage induced by puromycin (36,39). The relative position of these conserved residues in the TnaC peptide is important as well: insertion or deletion of single amino acids between the W12 and the P24 residues abolishes L-Trp induction (68). These data indicate that the nature and positions of the

conserved TnaC residues are important for the nascent peptide's regulatory activity at the level of translation.

Nascent peptides mediating ribosome stalling are widespread in the microbial world (69). Some notable examples are SecM from the *secMA* operon of *E. coli*, MifM that regulates expression of the *yidC2* gene of *Bacillus subtilis*, ErmCL from the *erm* operon of erythromycin resistant bacteria, and the evolutionary conserved fungal arginine attenuator peptide (AAP) (7,8,12,70,71). As is the case for TnaC, these regulatory peptides contain amino acid residues whose nature and relative positions are essential for stalling activity (7,8,12,72).

Changes in the large subunit 23S rRNA sequence or in ribosomal protein L22 affect L-Trp induction. Insertion of an additional adenine nucleotide in the G745-A752 region (designated +A751ins), or the substitutions U2609C, A752C and A752U in the 23S rRNA, abolish the action of L-Trp to induce TnaC-mediated ribosome stalling (44). Replacements of the K90 residue of ribosomal protein L22 also affect L-Trp induction (44). These ribosomal components are located in the narrowest region of the ribosome exit tunnel (73). Cryo-EM structures of ribosomes containing TnaC-tRNA^{Pro} molecules suggest that W12 and D16 of TnaC are in close proximity to the K90 and R92 residues of ribosomal protein L22, and to 23S rRNA nucleotides A751-752 (43). Cross linking analysis confirms that the W12 residue of TnaC is in close proximity to the G745-A752 region of the 23S rRNA (44). The cryo-EM structure also indicates that the P24 residue of the TnaC peptide is close to the peptidyl transferase center (PTC) nucleotide U2585,

and adjacent to the nucleotides G2583 and U2584, mutations in the two latter positions are tolerated but affect L-Trp induction (43,64).

The evidence suggests that essential TnaC residues interact with components of the ribosomal exit tunnel, and that these interactions induce structural changes that are transferred from the TnaC-exit tunnel contact points to the PTC, resulting in inhibition of peptidyltransferase activity (68,74). The cryo-EM model suggests three possible routes where structural changes could be induced and transferred from the ribosomal exit tunnel to the PTC. In one possible route, the structural changes are transmitted through ribosomal protein L4 and the A2058-2059:2060-2062:2503:2451 23S rRNA nucleotides (43). However, changes at most of these positions do not affect L-Trp induction, although they affect the action of the SecM and ErmCL nascent peptides (5,44). A second possible route considers transmission of structural changes through the nascent TnaC peptide chain. Finally, in the third proposed route, transmission of structural changes occurs through the interactions observed between L22 and the A751-A752:U2609:U1781-U1782:U2586-U2585 23S rRNA nucleotides (43). This last route contains mostly those nucleotides in which changes are known from experimental data to affect L-Trp induction.

The fact that some elements of the ribosome exit tunnel are important for the function of the nascent TnaC peptide suggests that they may interact with this regulatory peptide. The proximity of these elements to the nascent peptide observed in the cryo-EM structure is also consistent with this idea (43). However, changes in these elements could also affect the structure of the ribosome exit tunnel in a manner that indirectly

affects interactions between the exit tunnel and TnaC. In this study, we show that the presence of the nascent TnaC peptide within the ribosome induces protection against chemical methylation of exit tunnel 23S rRNA nucleotide U2609. We observed that mutational changes in the nucleotides constituting the G745-A752 region of the 23S rRNA, and in conserved TnaC residues, that abolish TnaC-mediated regulation also reduced the methylation protection of U2609 conferred by wild type nascent TnaC. These results indicate that changes in the G745-A752 and U2609 regions greatly reduced the capacity of L-Trp and TnaC to inhibit ribosome function. The proximity of these regions of the ribosome to TnaC suggests that functional interactions are impaired by these mutational changes.

MATERIALS AND METHODS

Bacterial strains, plasmids and mutagenesis procedures

The *E. coli* K-12 strains, and plasmids containing selected genes used in this study, are listed in Table 1. Strains with replacements of the 23S rRNA gene were generated using plasmids pNK, and pK4-16 (Selwyn Quan and Catherine Squires, personal communication), which contain the *rrnB* operon (44). Replacements of *tnaC* sequences were generated in the pGF2500 plasmid that contains the *tna* promoter, a wild-type *tnaC* gene, the *tna* intercistronic region and a *rpoBC* terminator (29,44). Mutations in these genes were made using the QuikChange Lightning Site-Directed Mutagenesis kit (Agilent Technologies). Complementary primers were designed with the desired replacements flanked by ~10–15 nucleotides of the wild-type sequences on

each side of the change. The mutagenesis reactions were performed as recommended by the manufacturer in 50 μL final volume with 10-100 ng of plasmid and 10 pmol of each complementary primer. The plasmids that contained the desired replacements were confirmed by sequencing using the following primer: (5'-ACGGAATTCCTTGCCGAGTTTGACTC-3') which is complementary to the 3'-end of the *rpoBC* region.

Table 1. *E. coli* bacterial strains and plasmids used in this work.

Strains	Relevant genotype	Source
SR-14	*Δ7 rrn ΔlacZYA ΔrecA* λ tna_p tnaC(*tnaA'-'lacZYA*) (p*rrnC-sacB,* ptRNA67)	(44)
SQ351	MG1655 *Δ7 rrn Δ(lacZYA)* (pKK3535*,* ptRNA67)	(44)
AW122	Derived from SQ351 (p*rrnC-sacB*, ptRNA67)	This work
AW182	MG1655 *Δ7 rrn Δ(lacZYA) att7*::tna_p*tnaC(tnaA'-'lacZYA*) (p*rrnC-sacB,* ptRNA67)	This work
AW216	MG1655 *Δ7 rrn Δ(lacZYA) att7*::tna_p*tnaC(tnaA'-'lacZYA*) (pNK, ptRNA67)	This work
AW218	MG1655 *Δ7 rrn Δ(lacZYA) att7*::tna_p*tnaC(tnaA'-'lacZYA*) (pKKU2609C, ptRNA67)	This work
AW221	MG1655 *Δ7 rrn Δ(lacZYA) att7*::tna_p*tnaC(W12R)(tnaA'-'lacZYA*) (pNK, ptRNA67)	This work
AW227	MG1655 *Δ7 rrn Δ(lacZYA) att7*::tna_p*tnaC(tnaA'-'lacZYA*) (pNH153, ptRNA67)	This work
AW326	MG1655 *Δ7 rrn Δ(lacZYA) att7*::tna_p*tnaC(K18A)(tnaA'-'lacZYA*) (pNK, ptRNA67)	This work
AW600	MG1655 Δ7 *rrn* Δ(*lacZYA*) *att7*::tna_p*tnaC*(*D16A*)(*tnaA*'-'*lacZYA*) (pNK, ptRNA67)	This work

Table 1. Continued.

Plasmids	Description	Source
pNK	Wild-type *rrnB* operon; Amp^r, derived from ColE1.	(12)
pNH153	Derived from pNK; has an insertion at position 751 in the 23S rRNA gene	(12)
pKKU2609C	Derived from pNK; has a T-to-C replacement at position 2609 in the 23S rRNA gene	(75)
pNKA752C	Derived from pNK; has a A-to-C replacement at position 752 in the 23S rRNA gene	(45)
pK4-16	Wild-type *rrnB* operon; Km^r, derived from SC101.	Quan and Squires, personal communication
p*rrnC-sacB*	Wild type *rrnC* gene and a *sacB* gene, derived from SC101.	(76)
pKK3535	Wild type *rrnB* operon, derived from pBR322.	(77)
ptRNA67	tRNA encoding plasmid.	(76)
pGF2500	Wild type *tnaC* gene with the *rpoBC* terminator, derived from pUC18.	(29)
pAW137	Has the $tna_p tnaC$(ΔN2-H22) with BsaI-XhoI-BsaI linker-*tna*'-'*lacZYA* cloning reporter gene, derived from pACYC184.	This work

Creation of the *tnaA'-'lacZ* reporter gene at the *att7* site and *tnaA'-'lacZ* induction experiments

A DNA fragment containing the tna_p *tnaC*(*tnaA'-'lacZY*) reporter gene was amplified from the chromosome of the SVS1144 strain using the primers 5'-CTGGTCGACGCTTCTGTATTGGTAAGTAACCGCGC-3' and 5'-CTAGTCGACGCTTAAGCGACTTCATTCACCTGACG-3' (1). These primers amplify a DNA fragment containing 262 bp upstream of the start codon of *tnaC* through 2 bp downstream of the start codon of *lacY*. These elements are flanked by *SalI* sites on

both ends of the PCR product. This DNA fragment was cloned in the *SalI* site of pACYC184 plasmid. Inverse PCR products obtained with the primers 5'-CTGCTCGAGGGTCTCACGCCCTTGAATTGCCCTTCTGTAGC-3' and 5'-CTACTCGAGGGTCTCACATAATGCACTTATCCTCGCAAGAC-3' containing *XhoI* restriction sites, were digested with *XhoI* enzyme and ligated. This procedure eliminates the *tnaC* region that specifies the 2nd through the 22nd codons. The plasmid now contains a *tnaC* gene with an internal deletion marked with a *BsaI-XhoI-BsaI* cloning site, which allows direct insertion of synthetic oligonucleotides containing wild-type and mutated *tnaC* coding sequences [*tnaC*(ΔN2-H22) *Bsa*I-*Xho*I-*Bsa*I linker-*tnaA'*]. To avoid potential complications arising from the inverse PCR, the new cloning construct was moved into pRS552 plasmid as a *BamHI* fragment, to generate the *tnaC*(ΔN2-H22)-*tnaA'-'lacZYA* reporter gene that later was transfer back into pACYC184, generating plasmid pAW137 (1). Annealed oligonucleotides were used to insert either wild-type or mutant *tnaC* sequence into pAW137. 5 µl of each 100 mM complementary oligonucleotides were mixed in a microcentrifuge tube, incubated in boiling water for 2 min and allowed to cool to room temperature. Annealed oligonucleotides were ligated to BsaI digested pAW137, creating derivatives containing wild-type or mutant tnaC sequences. The *SalI* DNA fragments from these pAW137 derivatives were cloned into the *XhoI* site of pGRG36 plasmid (78). pGRG36 encodes the *Tn7* transposition machinery which allows site-specific transposition at the *att7* locus of *E. coli* (78). Two different orientations of the wild type or mutant *tnaC-tnaA'-'lacZYA* reporter genes result from this cloning method. Strains containing one of each orientation were

obtained for every construct. The plasmids derived from pGRG36 were transformed into chemical-competent AW122 cells. Transformants were selected on Luria-Bertani (LB) plates containing 100 μg/ml ampicillin at 32°C. The transposition protocol to move *tnaC-tnaA'-'*lacZYA reporters to the chromosomal *att7* site was carried out as described (78). Transposition was verified by replica plating colonies on LB plates containing, or lacking, 100 μg/ml ampicillin. The sequence of the region from tna_p through the *tnaA'-'lacZ* junction of the att7 integrants was confirmed by using PCR to amplify the *att7* locus using the primers 5'-GCGGCGACAACAGTTGCGACGGTGGTACG-3' and 5'-GCGGTTTTCTCCGGCGCGTAAAAATGCGCTCAGG-3' followed by sequencing of the resulting fragment. To analyze the expression of the *tnaA'-'lacZ* reporter gene we performed β-Gal assays as previously(79). β-Gal activity is reported in Miller units.

Puromycin assay

Stalled ribosome complexes were isolated using pGF2500 variants as previously indicated (44). 10 μL of isolated stalled complexes dissolved in buffer A (35 mM Tris-acetate, pH 8.0, 10 mM magnesium acetate, 175 mM potassium acetate, 10 mM ammonium acetate and 1 mM DTT) were mixed with 1 μl of water or 1 μl of 20 mM L-Trp. The mixtures then were mixed with 1 μl of water or 1 μl of 0.2 mM puromycin, and these mixtures were then incubated for 10 min at room temperature. The reactions were stopped by adding an equal volume of loading buffer (100 mM Tris-HCl, pH 6.8, 24% (v/v) glycerol, 8% sodium dodecyl sulfate, 4 % (v/v) β-mercaptoethanol and 0.4

mg/ mL bromophenol blue). The products of this reaction were resolved using 10% Tris-tricine polyacrylamide gels. The gels were dried by vacuum and then exposed to X-ray films.

Methylation protection and primer extension assays

50 μL of either 50S ribosomal subunits (40 A_{260}), obtained as previously indicated, or isolated stalled complexes dissolved in buffer A were mixed with either 2 μL of dimethyl sulfate (DMS, 1:6 dilution in ethanol) or 50 μL of 100mg/mL 1-cyclohexyl-(2-morpholinoethyl) carbodiimide metho-p-toluene sulfonate (CMCT) solution (44). Mixtures containing DMS or CMCT were incubated at room temperature for 10 min or 30 min, respectively. DMS reactions were stopped by adding 25 μL of a solution containing 1.4 M of β-mercaptoethanol and 1 M Tris-HCl (pH 8.0). The final mixtures were diluted by adding 10mM EDTA in DEPC treated water. The methylated rRNA was obtained by standard phenol chloroform extractions. Integrity of the extracted rRNAs was verified on 2% agarose gels. RNA was quantified using UV spectroscopy at A_{260}. Primer extension analysis was performed to detect the methylation of nucleotides in the 23S rRNA as indicated previously (44).

RESULTS

Nucleotide changes in the ribosome exit tunnel that affect TnaC/L-Trp inhibition of the ribosome function

Mutations in 23S rRNA nucleotides that constituted the ribosome exit tunnel reduce TnaC-mediated operon induction in response to L-Trp (44,64). We used bacterial strains in which the seven rRNA operons were deleted from their chromosomal locations to analyze how A752C, U2609C and +A751 insertion mutations in the 23S rRNA affected the inhibition of the ribosome function by L-Trp (44). These strains contained a homogeneous population of mutant ribosomes (Figure 9). To determine the effect of ribosomal mutations on TnaC-mediated regulation in response to L-Trp and L-Trp-analogs, we used bacteria that contained a *tnaC tnaA'-'lacZ* reporter gene (44). We tested the effects of these ribosomal mutations on the expression of the reporter gene in vivo using several concentrations of 1-methyl-L-Trp (1MT). This L-Trp analog induces operon expression but is not cleaved by tryptophanase, and thus is a more efficient inducer *in vivo* than L-Trp (80). The results are summarized in Figure 10 (primary data are shown in Table 2). Based on the induction curve, 40 μM of 1MT would be sufficient for maximal expression of the reporter gene in cells containing wild-type ribosomes (Figure 10, closed circles). For cells containing ribosomes with the +A751ins mutation, even at 100 μM 1MT operon induction was 12-fold lower than cells containing wild-type ribosomes (Figure 10, compare open squares with closed circles). Similar results were observed with cells containing A752C mutant ribosomes, in which 100 μM 1MT

induced 25-fold less operon expression than in wild type cells (Figure 10, compare open triangles with closed circles). These results indicated that +A751ins or A752C ribosomes allowed at most, slight induction of the *tna* reporter operon at high concentrations of 1MT (Figure 10, inset). Finally, we observed in cells containing ribosomes with the U2609C replacement that expression of the reporter gene was not induced by the addition of any amount of 1MT tested (Figure 10, open circles and data not shown). This result indicated that the U2609C replacement completely abolished TnaC-mediated regulation in response to 1MT. In summary, we observed differences in the way that the +A751ins, A752C and the U2609C mutations affected TnaC-mediated regulation.

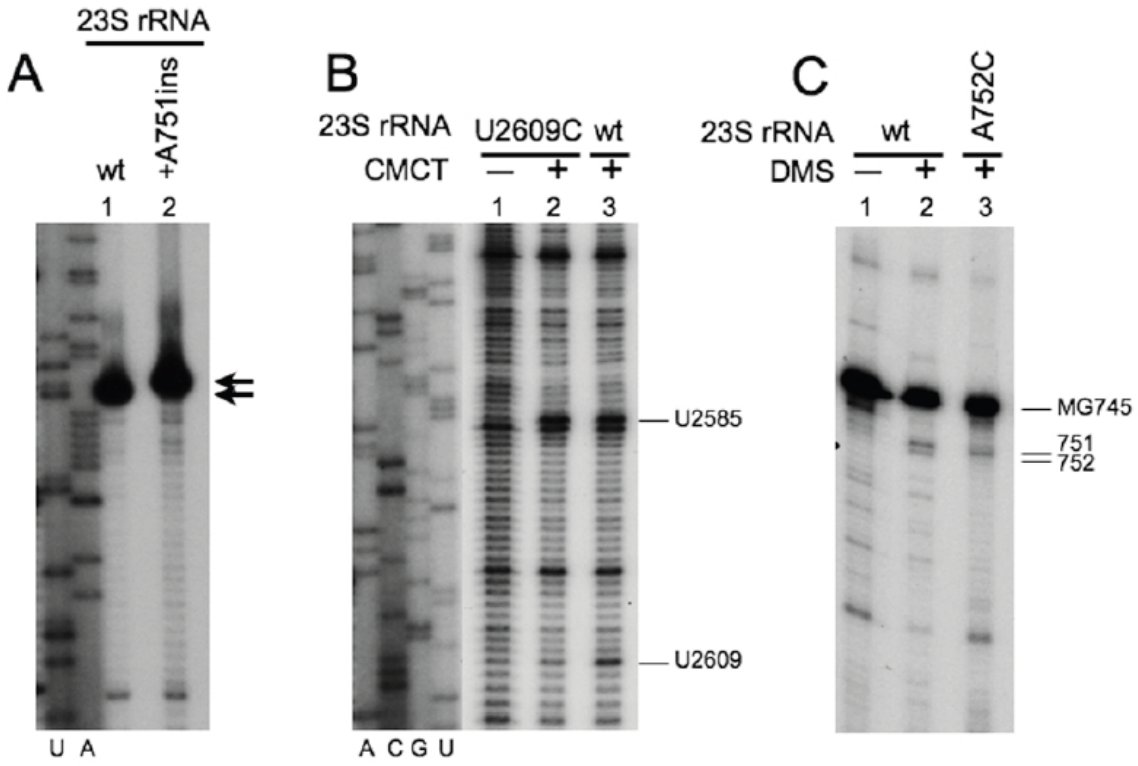

Figure 9. Ribosomes were isolated from bacterial cells containing plasmids expressing the indicated 23S rRNAs. (**A**) The presence of +A751ins 23S rRNA in the ribosomes could be detected using primer extension assays (Materials and Methods). cDNA synthesis on 23S rRNA template obtained from wild-type ribosomes is usually stopped by the natural methylated G745 nucleotide (MG745)(81). 23S rRNA were extracted from the isolated ribosomes and used to perform primer extension assays with [^{32}P]-labeled oligonucleotides complementary to nucleotides 821-838 of 23S rRNA. The final products of the reaction were resolved using 6% urea-polyacrylamide gels. The position of a significant stall of cDNA synthesis is indicated with arrows. (**B**) Isolated ribosomes were used to perform methylation protection assays (Materials and Methods). Ribosomes were exposed (+) or not (-) to the alkylating agent, CMCT, to methylate water-accessible uridines. 23S rRNAs were extracted and used to perform primer extension assays as indicated in part (**A**). Primer extension was performed using [^{32}P]-labeled oligonucleotides indicated in part (**A**). Nucleotides methylated in the presence of DMS are indicated.

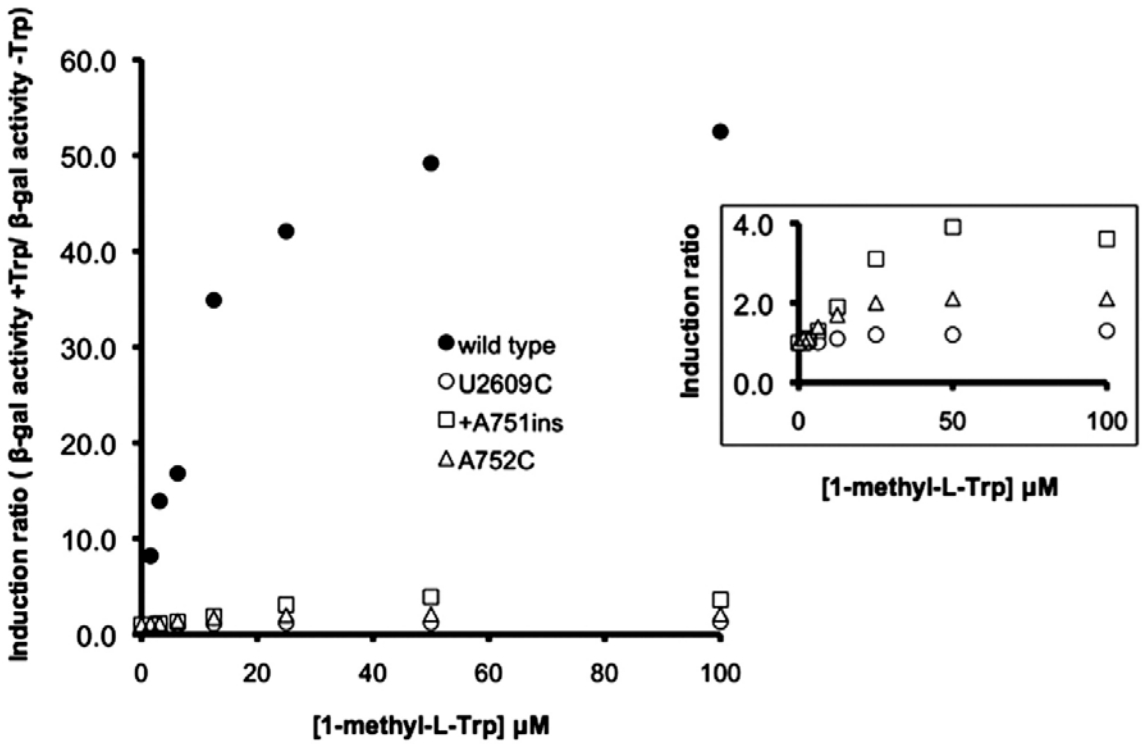

Figure 10. Mutations of 23S rRNA nucleotides that affect *tna* operon expression. Bacterial cells expressing the indicated 23S rRNA alleles in the Δ7 *rrn* strain were used to analyze expression of β-galactosidase from a *tnaC-tnaA'-'lacZ* protein fusion. Bacterial cultures were grown in minimal medium containing 0.2% glycerol, 0.05% acid-hydrolyzed casein, 0.01% vitamin B1, 100µg/ml ampicillin, and variable amounts of 1-methyl-L-Trp as an inducer. The figure on the right shows an amplification of the plots between the induction values 0 to 4.

Table 2. Primary data for results shown in **Figure 9**.

[1-L-M-Trp] µM	β-galactosidase activity (MU)[a]							
	wt 23S		U2609C 23S		+A751ins 23S		A752C 23S	
0	34	± 1	88	±1	29	±2	29	±1
1.56	281	±17	90	±1	30	±1	32	±1
3.13	475	±10	89	±2	31	±0	34	±1
6.25	575	± 5	88	±4	39	±1	40	±1
12.5	1196	±55	98	±4	56	±4	49	±1
25	1442	±26	103	±2	90	±3	58	±2
50	1684	±49	110	±7	115	±6	62	±5
100	1795	±29	115	±4	106	±1	62	±3

[a]Cultures of AW182 derived strains (Δ7 *rrn*) obtained by replacement of the p*rrnC-sacB* plasmid by pNK (AW216), pNH2609 (AW218), pNH153 (AW227), or pNK-A752C (AW839) were grown in minimal medium plus 0.2% glycerol, 0.05% acid-hydrolyzed casein, 0.01% vitamin B1 and 100µg/ml ampicillin and variable amounts of 1-methyl-L-Trp as an inducer. β-Galactosidase assays were performed in four independent experiments.

Nucleotide residues of the ribosome exit tunnel that are protected from methylation by the presence of nascent TnaC

The action of L-Trp on *tna* operon expression requires the presence of the TnaC nascent peptide within the ribosome (29). We performed methylation protection assays to determine if the nascent TnaC peptide protects 23S rRNA nucleotides A751, A752 and U2609 from chemical methylation (Materials and Methods). These nucleotide residues are water accessible in vacant ribosomes (ribosomes not engaged in polypeptide synthesis), and can therefore be methylated by alkylating agents (82). We also examine methylation of U2585, which forms part of the PTC (20). The alkylating agent CMCT induced methylation of U2585 and U2609 in vacant wild-type and +A751ins mutant ribosomes (Figure 11A compare lane 2 with lane 1, or lane 4 with lane 3). We observed that the U2585 methylation level was slightly less (30 ± 5%, n=4) in vacant +A751ins ribosomes than vacant wild-type ribosomes (Figure 11A, compare lane 4 with lane 2). We also observed than the methylation level of U2609 was slightly higher (25 ± 3%, n=4) in vacant +A751ins ribosomes than in wild-type ribosomes (Figure 11A, compare lane 4 with lane 2). The A752C mutant ribosomes, like the +A751ins ribosomes, differed from the wild-type. Vacant A752C ribosomes showed slightly reduced methylation (32 ± 5%, n=4) of U2585 and an increased methylation (50 ± 3%, n=4) of U2609 compared to wild-type ribosomes (Figure 10C, compare lanes 4 with lane 2). L-Trp did not affect methylation levels in vacant ribosomes (Figure 12). These observations suggested that there were differences in the architecture of the ribosome

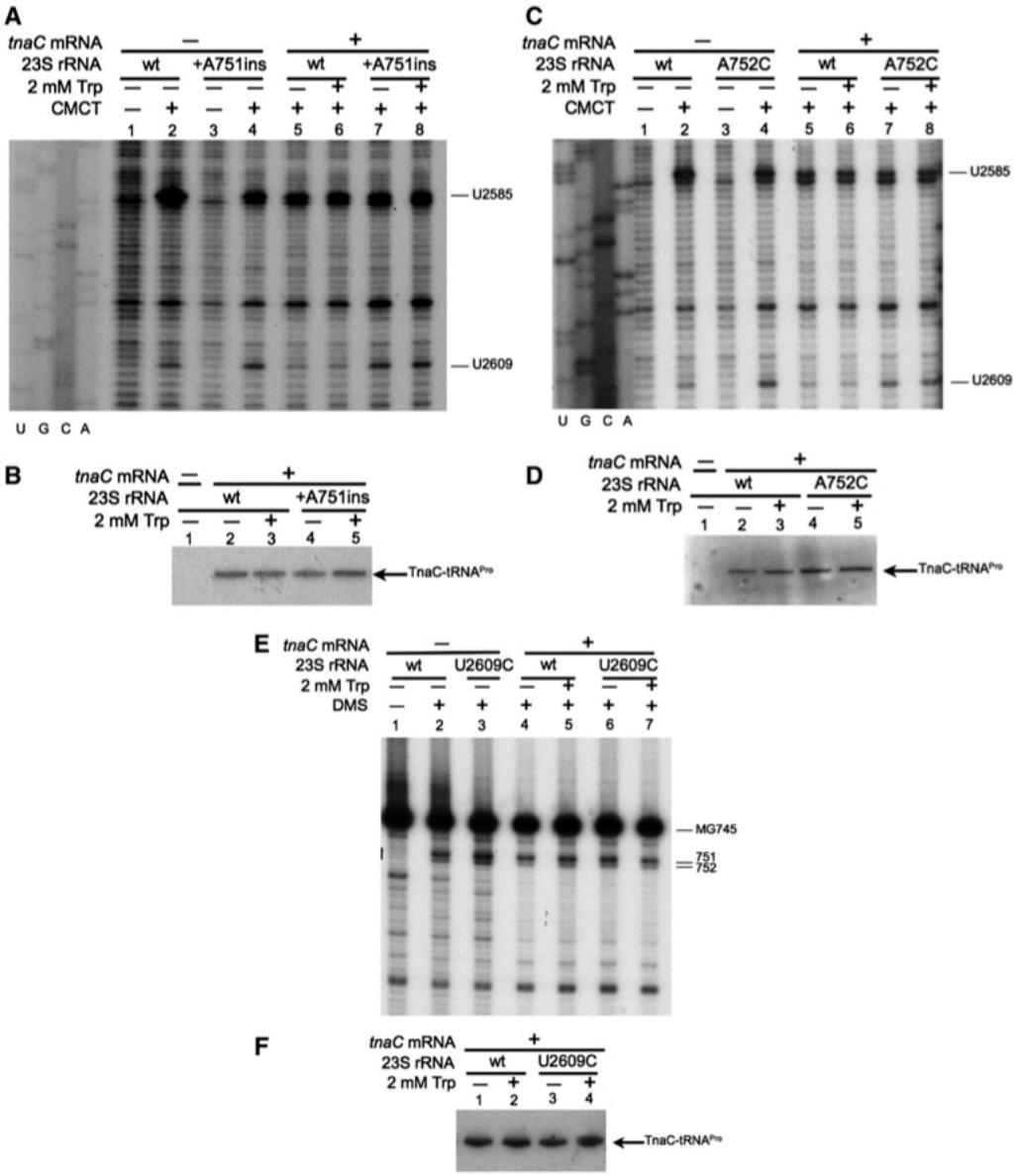

Figure 11. 23S rRNA nucleotides that are protected by the TnaC nascent peptide. (**A, C and E**) Methylation protection assays were performed with ribosomes containing the indicated 23S rRNA alleles. Ribosomes translating (+) or not (-) messengers containing the *tnaC* gene sequences were analyzed in a buffer containing (+) or not (-) Trp. The ribosomes were exposed (+) or not (-) to the indicated alkylating agents. These assays were performed with [^{32}P]-labeled oligonucleotides complementary to nucleotides 2654-2674 of 23S rRNA (**A and C**), and complementary to nucleotides 821-838 of 23S rRNA for (**E**). Nucleotides methylated are indicated. cDNA synthesis on 23S rRNA template obtained from wild-type ribosomes is usually stopped by the natural methylated G745 nucleotide (MG745) (**E**) (83). (**B, D and F**) Northern blot assays performed with the ribosomes indicated above. The ribosomal components were resolved in 10% denaturing tris-tricine polyacrylamide gels. The presence of the TnaC-tRNA^{Pro} in the complexes was determined using a [^{32}P]-labeled oligonucleotide complementary to the anti-codon region of the tRNA^{Pro1} (84).

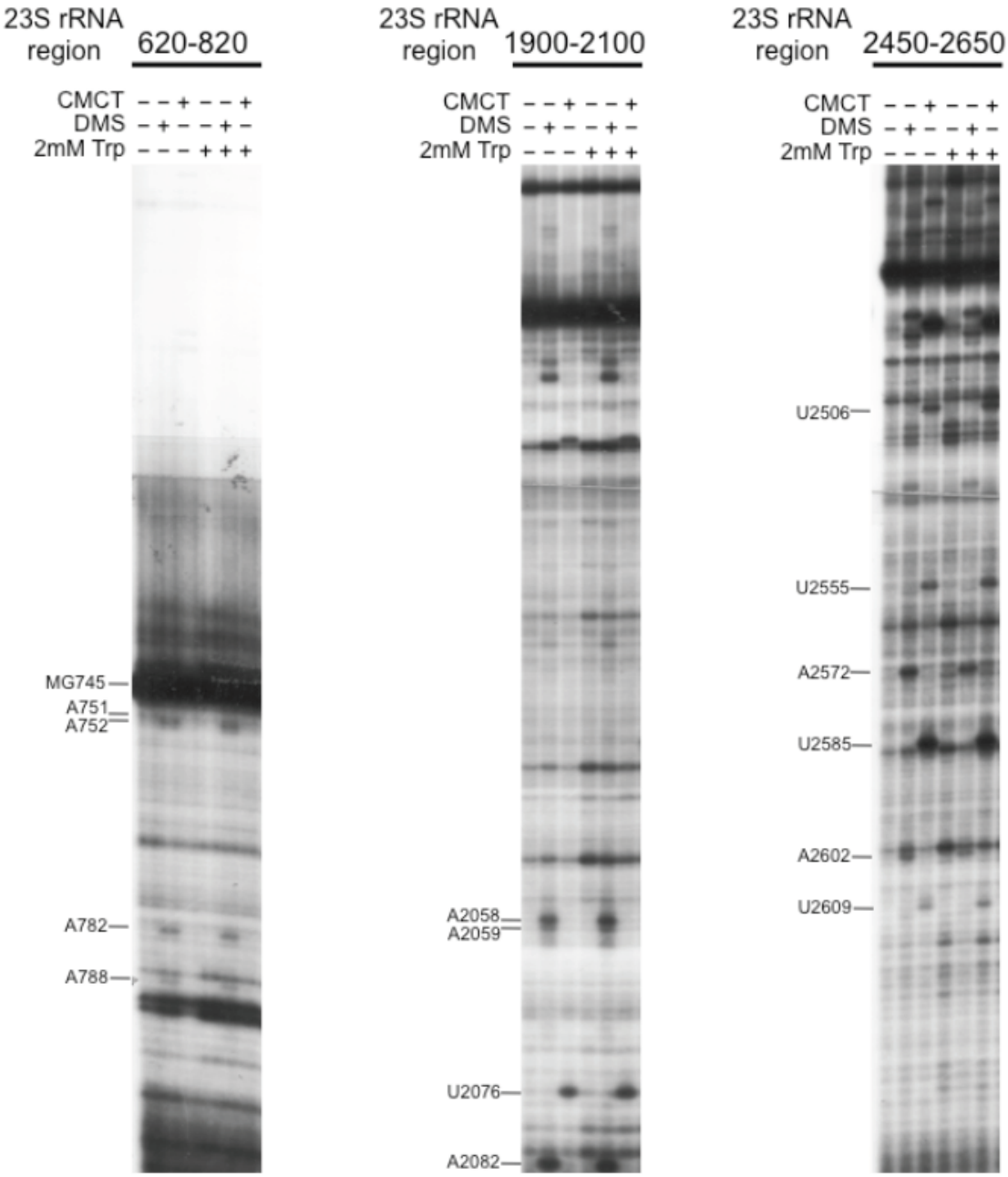

Figure 12. Methylation patterns of wild type ribosomes exposed to Trp. Wild type ribosomes not engaged in translation (vacant) were incubated in the presence (+) or absence (-) of Trp at 37°C for 10 minutes. The final mixes were exposed (+) or not (-) to alkylating agents either DMS or CMCT, the 23S rRNA was extracted and primer extensions were performed as indicated in the Materials and Methods. Primer extensions were performed using [^{32}P]-labeled oligodeoxynucleotides which reveal methylation of nucleotides corresponding to indicated regions. For 620-820 region we used the oligo 5'-GGCGCTACCTAAATAGCT-3' (44); for 1900-2100 region we used the oligo 5'-CTATCCTACACTCAAGGCTC-3'; and for 2450-2650 region we used the oligo 5'-TCCGGTCCTCTCGTACT-3' (84).

exit tunnel between vacant +A751ins or A752C mutant ribosomes and wild-type ribosomes.

The methylation levels of U2585 and U2609 were reduced when the wild-type ribosomes contained TnaC-tRNA^{Pro}. This reduction occurred independent of the presence of L-Trp (Figure 11A, compare lanes 5 or 6 with lane 2). The methylation of the U2609 nucleotide was substantially reduced (70 ± 3%, n=4) (Figure 11A, compare lanes 5 or 6 with lane 2) when TnaC-tRNA^{Pro} was in the ribosome. These results indicated that the presence of the TnaC-tRNA^{Pro} within the wild-type ribosome reduced the accessibility of the U2585 and U2609 nucleotides with a greater effect on U2609 accessibility. In contrast, we did not observe any change in the methylation level of U2585 or U2609 in +A751ins (Figure 11A, compare lanes 7 or 8 with lane 4) or A752C (Figure 11C, compare lanes 7 or 8 with lanes 5 or 6) mutant ribosomes containing TnaC-tRNA^{Pro}. These results indicate that TnaC-tRNA^{Pro} did not protect the U2585 and U2609 nucleotides in the +A751ins and A752C mutant ribosomes. These differences did not reflect changes in the capacity of mutant ribosomes to synthesize TnaC-tRNA^{Pro} as determined by Northern blots (Figure 11B and D).

Finally, we analyzed the U2609C mutant ribosomes. We focused our efforts on determining the DMS-accessibility of the A751 and A752 nucleotides because changes in these nucleotides affected the CMCT-accessibility of the U2609 nucleotide (see above). The water soluble alkylating agent DMS methylates A751 and A752 in vacant wild-type and U2609C mutant ribosomes (Figure 11E, compare lane 2 or lane 3 with lane 1) (82). The methylation levels of A751 and A752 nucleotides were not affected in

wild-type or U2609 mutant ribosomes containing a TnaC-tRNA^{Pro} molecule, in either the presence or absence of L-Trp (Figure 11E, compare lanes 4 and 5 with lane 2 or lanes 6 and 7 with lane 3). These results indicate that the presence of TnaC-tRNA^{Pro} did not affect the DMS-accessibility of these two nucleotides.

Exit tunnel nucleotide interactions that are important for TnaC-tRNA^{Pro} stalling activity

X-ray crystal structures of the *E. coli* 50S ribosomal subunits have shown that the 23S rRNA A752 and U2609 nucleotides form a base-pair interaction (66). To understand if this interaction is important for TnaC-mediated regulation we produced bacteria strains containing directed replacements at either or both positions in the 23S rRNA. These strains also contained the *tnaA'-'lacZ* L-Trp-inducible reporter gene (44). We determined the effects of these 23S rRNA mutations on the expression of this reporter gene by measuring β-galactosidase activity in cells grown with or without L-Trp (Table 3). Strain with wild-type ribosomes (A752/U2609) exhibited high expression levels of the *tnaA'-'lacZ* reporter gene in the presence but not the absence of L-Trp. Substitutions of A752 with uridine or cytosine substantially reduced induction of the reporter gene (Table 3, combinations A752U/U2609 and A752C/U2609). However, the A752G mutation did not affect the induction of the reporter (Table 3, nucleotide combination A752G/U2609). These results indicated that a purine nucleotide, A or G, was required at nucleotide 752 to enable TnaC function. Substitutions at position U2609 with A or C also abolished reporter gene induction by L-Trp in this analysis (Table 3,

nucleotide combinations A752/U2609C and A752/U2609A). Finally, while most combinations of nucleotide replacements at both positions gave uninducible phenotypes (Table 3, nucleotide combinations A752U/U2609A, A752U/U2609C, A752C/U2609A, A752C/U2609C), the combination A752G/U2609C in 23S rRNA conferred an inducible phenotype similar to the wild-type combination A752/U2609, whereas A752/U2609C did not (Table 3).

Table 3. A752 and U2609 nucleotide changes that affect *tnaA'-'lacZ* expression in the bacterial cell.

23S rRNAs	β-galactosidase activity[a]				Induction ratio (+Trp/-Trp)[b]
	-Trp		+Trp		
A752/U2609 (wt)	120	±10	4500	±20	37.5
A/U combination					
A752/U2609A	110	±12	100	±10	0.9
A752U/U2609	130	±15	140	±20	1.1
A752U/U2609A	90	±10	200	±13	2.2
G/C Combination					
A752/U2609C	75	±10	85	±6	1.1
A752G/U2609	150	±20	3500	±22	23.3
A752G/U2609C	120	±15	4200	±20	35.0
A752C/U2609	120	±10	160	±10	1.3
Other Combinations					
A752C/U2609A	130	±9	140	±8	1.1
A742C/U2609C	110	±12	140	±10	1.3
A752U/U2609C	90	±9	100	±8	1.1

[a]Cultures of SR-14 derived strains (Δ7 *rrn*) obtained by replacement of the p*rrnC-sacB* plasmid by pK4-16 variants were grown in minimal medium plus 0.2% glycerol, 0.05% acid-hydrolyzed casein, 0.01% vitamin B1 and 50μg/ml kanamycin with (+Trp) or without (-Trp) 100 μg/ml L-Trp. β-Galactosidase assays were performed in four independent experiments .
[b]Ratio of values for cultures grown with L-Trp (+Trp) and those grown without L-Trp (-Trp).

TnaC residues that protect the U2609 nucleotide

The presence of TnaC-tRNA^{Pro} within the wild-type ribosome reduced CMCT accessibility of the U2609 nucleotide (Figure 11A). These results suggested that either components of the TnaC peptide may be in close proximity to U2609, or interactions of TnaC-tRNA^{Pro} with other regions of the ribosome induced structural changes affecting this nucleotide. The model of TnaC-tRNA^{Pro} bound to a ribosome suggested by cryo-EM structures indicates that the TnaC residues W12, D16 and K18 are in the vicinity of the A751, A752 and U2609 (43). We determined expression levels *in vivo* of the *tnaA′-′lacZ* reporter construct containing either W12R, D16A or K18A substitutions in TnaC to establish their importance for TnaC-mediated regulation (Table 4). The replacements W12R and D16A substantially reduced induction of the reporter gene in response to L-Trp (Table 4) (39). In contrast, the TnaC K18A mutation retained regulatory capacity (Table 4). A K18E mutation also did not interfere with regulatory function (data not shown). These results indicated that residues W12 and D16, but not K18, were important for L-Trp induction.

We examined the impact of L-Trp on the function of ribosome complexes containing wild-type, W12R, D16A and K18A TnaC nascent peptides using puromycin, an aminoacyl-tRNA analog that is an A-site substrate at the PTC. Puromycin was added to wild-type ribosomes containing wild-type or mutated TnaC peptides (Figure 13A). The addition of L-Trp inhibited puromycin activity on ribosomes containing either wild-type or K18A nascent TnaC peptides (Figure 13A, compare lane 4 with lane 2; or lane 8 with lane 6). However, the addition of L-Trp did not inhibit puromycin activity on

Table 4. TnaC residue changes that affect *tnaA'-'lacZ* expression in bacterial cell.

TnaC peptide	β-galactosidase activity (MU)				Induction ratio (+Trp/-Trp)
	-Trp		+Trp		
TnaC	30	±1	717	±85	23.9
TnaC(W12R)	51	±3	42	± 2	0.8
TnaC(K18A)	23	±1	985	±20	42.8
TnaC(D16A)	30	±1	29	± 0	1.0

[a]Cultures of *rrn*+ E. *coli* bacterial strains AW216 (Wt), AW221 (W12R), AW326 (K18A) and AW600 (D16A) were grown in minimal medium plus 0.2% glycerol, 0.05% acid-hydrolyzed casein, 0.01% vitamin B1 and 100μg/ml ampicillin with (+Trp) or without (-Trp) 100 μg/ml L-Trp. β-Galactosidase assays were performed in three independent experiments .
[b]Ratio of values for cultures grown with L-Trp (+Trp) and those grown without L-Trp (-Trp).

ribosomes containing either the W12R or D16A mutant TnaC peptides (Figure 13A, compare lane 12 with lane 10; or lane 16 with lane 14). These results indicated that the replacements W12R and D16A, but not K18A, affected the capacity of TnaC to inhibit peptidyltransferase activity in response to L-Trp, consistent with their regulatory phenotypes *in vivo*.

Finally, we analyzed the effects of W12R, D16A and K18A TnaC peptides on the protection of the U2609 nucleotide from methylation by CMCT (Figure 13B). The presence of wild-type TnaC-tRNA^{Pro} substantially reduced the methylation level of the U2609 nucleotide that was observed in vacant wild-type ribosomes (Figure 13B, compare lanes 3 and 4 with lane 2), as also observed in the experiments shown in Figure 11. In contrast, in ribosomes complexes containing W12R or D16A TnaC-tRNA^{Pro} the methylation level of U2609 was not affected (Figure 13B, compare lanes 5 and 6 or lanes 7 and 8 with lane 2). These results indicated that W12R and D16A mutations

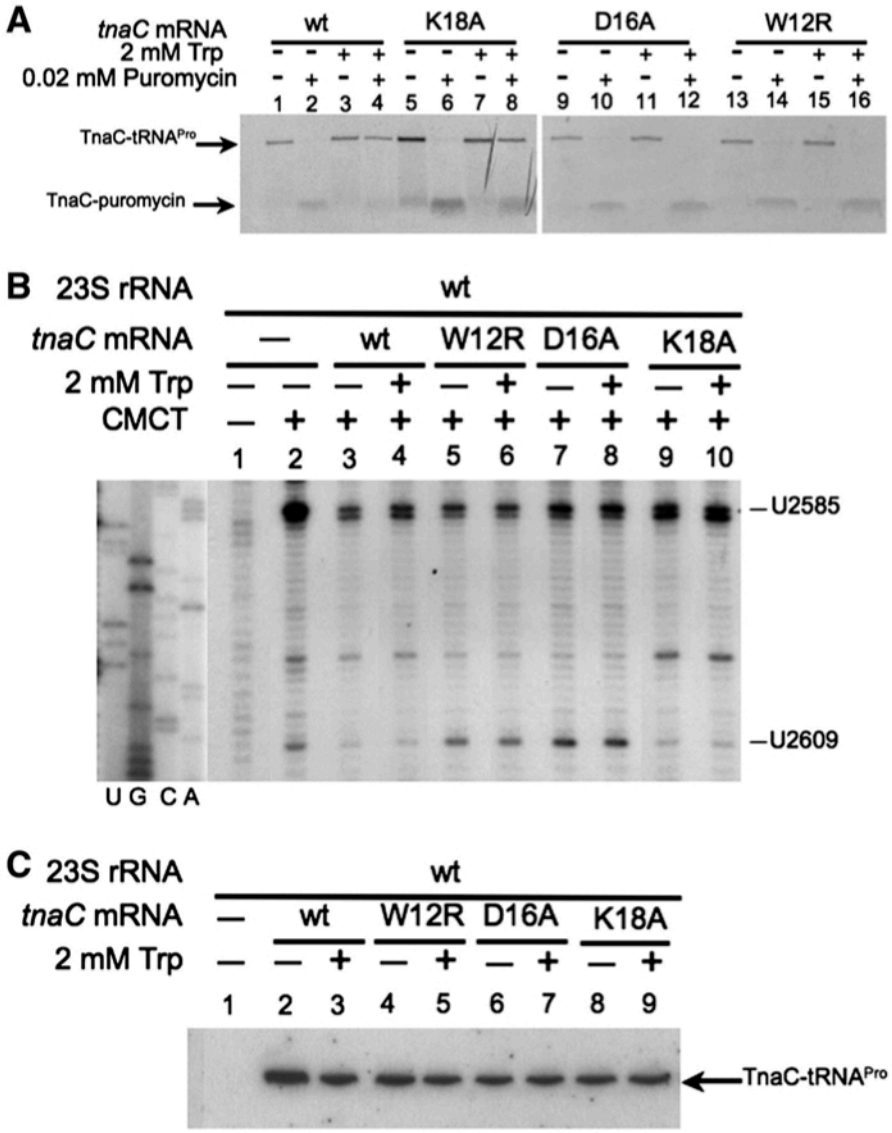

Figure 13. Nascent TnaC peptide residues involved in the protection of the U2609 nucleotide. (**A**) Isolated ribosome complexes containing the indicated *tnaC* mRNAs were tested with (+) or without (-) puromycin in the presence (+) or absence (-) of Trp. The final products of each reaction were resolved on 10% tris – tricine polyacrylamide gels. The TnaC-tRNA^{Pro} and TnaC-puromycin molecules position are indicated with arrows. (**B**) Methylation protection assays performed with wild type ribosomes containing the indicated *tnaC* mRNAs. The experiments were carried out as indicated in Figure 2 using the alkylating agent CMCT. Nucleotides methylated by the presence of CMCT are indicated. (**C**) Northern blot assays performed with the ribosome complexes indicated above. The TnaC-tRNA^{Pro} in the ribosome complexes was detected as indicated in Figure 11.

reduced the protection of U2609 conferred by the presence of the wild-type TnaC-tRNA^{Pro} within the ribosome. However, the methylation of U2609 within ribosomes containing K18A TnaC-tRNA^{Pro} was similar to that observed with ribosomes containing wild-type TnaC-tRNA^{Pro} (Figure 13B, compare lanes 9 and 10 with lane 2 or lanes 3 and 4). These effects on U2609 methylation were independent of the presence of Trp (Figure 12B, compare - lanes with + lanes). These results indicated that the K18A replacement did not affect TnaC-tRNA^{Pro}-mediated protection of U2609 from methylation.

DISCUSSION

The data presented here show that, in ribosomes that can respond to functional TnaC, functional TnaC-tRNA^{Pro} in the ribosome exit tunnel protects U2609 of the 23S rRNA from methylation by CMCT (Figure 13). These results are consistent with the structural model obtained from cryo-EM data, where it has been observed that U2609 conformation is affected by the presence of the TnaC peptide (43). The cryo-EM model suggests that the changes in the conformation of U2609 are not the result of major structural changes in the exit tunnel (43). These data suggest that interaction between U2609 and TnaC residues is a major reason for the difference in methylation-sensitivity of U2609 when comparing ribosomes containing either no peptide or nonfunctional TnaC peptide to ribosomes containing functional TnaC peptide. The cryo-EM model further suggests that the K18 residue of TnaC might be involved in positioning U2609 (43). However, our mutagenesis analyses did not support this view. Replacing the K18

residue by alanine, a small non-charged amino acid, did not affect either Trp induction in *vivo* (Table 4) or inhibition of TnaC-tRNA^{Pro} cleavage by puromycin (Figure 13A). Also, the protection of U2609 was not affected by the K18A TnaC mutation (Figure 13B). The TnaC mutations W12R and D16A, which eliminate Trp-mediated ribosome stalling (Table 4 and Figure 13A), abolished the protection from methylation of U2609 (Figure 13B). Therefore, these essential residues of the TnaC peptide may interact with U2609 directly. Alternatively, W12 and D16 interactions with other elements of the ribosome may relay structural changes through the TnaC peptide to establish a position for U2609 that protects this nucleotide from methylation (43,65). Cryo-EM structures of eukaryotic ribosomes containing either of the regulatory peptides CMV or AAP suggest that amino acids that are important for stalling interact with the A751 and U2609 nucleotides (85). The essential residues for stalling Ser-12 of CMV and the Asp-12 of AAP seem to be in the proximity of A751 (10,72,85). Meanwhile, the important residues Lys-18 of CMV and Trp-19 of AAP are close to U2609 (10,72,85). These positions correspond with the conserved residues W12 and Ile-19 of TnaC (39). Furthermore, comparison of the cryo-EM structures of ribosomes containing each of these regulatory peptides reveal that they interact in similar manner with the A751-752 and U2609 region (81). These observations suggest that the interactions between the region constituted by A751-A752 and U2609 and residues of regulatory peptides are essential for stalling in prokaryotic and eukaryotic systems. This region of the ribosomal exit tunnel might be a common anchor-place for regulatory peptides (Figure 14). The ErmCL peptide seems to be the exception as the action of this regulatory peptide is not

affected by mutations in the A751 and U2609 nucleotides (5). The ErmCL peptide is shorter and might not reach these nucleotides, in fact ErmCL is anchored to the A2058 nucleotide by erythromycin (Figure 14) (7).

X-ray structures of the *E. coli* 50S ribosomal subunit have shown that the A751 and A752 help form the exit tunnel. The exit tunnel structure is presumably stabilized by base-pairing, base-stacking interactions, and by the presence of the extended loop of ribosomal protein L22 (73,86). Furthermore, A752 has base-pairing interactions with U2609 (66). A752-U2609 base pairing interaction is also important for antibiotic binding (66). Changes in either A752 or U2609 resulted in reduced regulation by TnaC in response to Trp (Table 3). These changes could eliminate base-pairing interactions between nucleotides at these two positions. In this regard, the A752G single substitution and the A752G/U2609C double substitution allowed TnaC-mediated regulation (Table 3), suggesting that the G replacement at the 752 position might generate G:U base pairing interaction with the U2609 or G:C interaction with C2609 nucleotide retaining the contacts between these two nucleotide positions. Therefore, it seems that the base pairing between the 752 and the 2609 nucleotide positions are required for TnaC function (Figure 14).

In vacant ribosomes lacking a nascent peptide in the exit tunnel, the +A751ins and the A752C mutations affected the conformation of the U2609 nucleotide as well as that of the U2585 nucleotide, a residue located in the PTC, as assessed by their sensitivity to chemical methylation (Figure 11A and 11B). The +A751ins mutation also affects the function of other regulatory peptides such as SecM (12). These results

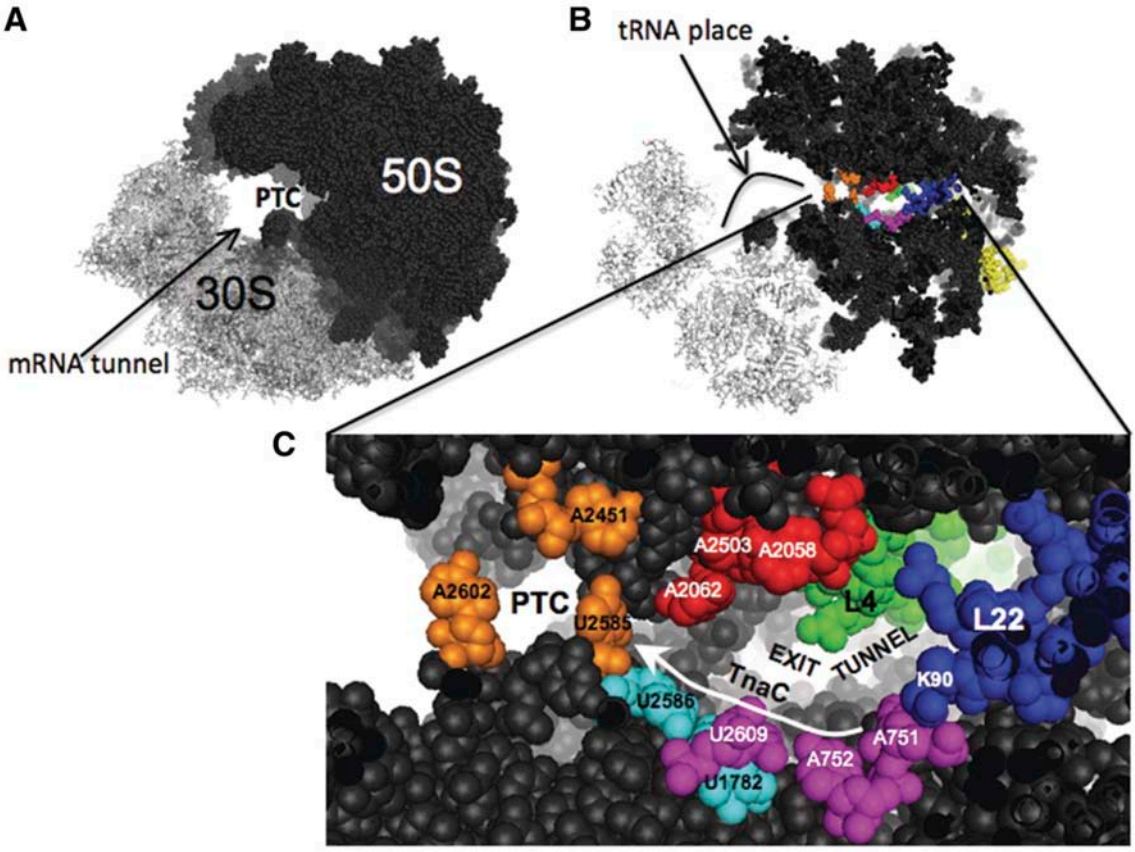

Figure 14. Regions of the ribosomal exit tunnel essential for stalling. (**A**) Lateral vision of the 70S ribosome of *E. coli* (73). (**B**) Sagittal plane section of the 70S ribosome (73). (**C**) Visual amplification of the PTC and the first part of the exit tunnel. Nucleotides in orange constitute the PTC region, these nucleotides are involved in the peptidyl transferase and hydrolysis of peptidyl-tRNAs during translation (87). Nucleotides in red are essential for stalling induced by the nascent peptides ErmCL and SecM (5,12). Nucleotides in pink and the amino acid residue K90 of the ribosomal protein L22 are essential for stalling induced by SecM and TnaC (12,44). Nucleotides in cyan connect the nucleotides U2585 and U2609. White arrow indicates possible structural relay from the exit tunnel to the PTC produced by the TnaC nascent peptide.

indicate that these mutations generate perturbations in the structure of the exit tunnel. These perturbations might be transferred from U2609 to U2585 through the nucleotides U1782 and U2586 (Figure 14, cyan nucleotides). Similar results have been observed in erythromycin-resistant ribosomes containing mutations in the extended loop of the ribosomal protein L22 (88). Also, mutations in the loop of L22 affect the function of the

regulatory nascent ErmCL peptide as well as the nascent TnaC peptide (7,44). Therefore, perturbations in the shape of the exit tunnel induced by changes in the G745-A752 nucleotide region, as well as the loop of L22, may affect the way that nascent peptides interact with the ribosome. This is consistent with the idea that the shape of the exit tunnel is a determining factor for the function of regulatory nascent peptides (89,90).

CHAPTER III

INTERACTIONS OF THE TNAC NASCENT PEPTIDE WITH RRNA IN THE EXIT TUNNEL ENABLE THE RIBOSOME TO RESPOND TO FREE TRYPTOPHAN

INTRODUCTION

Ribosomes are cellular molecular complexes whose primary function is carrying out protein synthesis, in all organisms. Prokaryote ribosomes are composed of two subunits: the small, 30S subunit, which facilitates the decoding of genetic information from mRNA templates, and the large, 50S subunit, which performs the polymerization of amino acids into polypeptides. Polypeptide assembly takes place in the peptidyl transferase center (PTC), which catalyzes peptide bond formation. Nascent polypeptides exit the ribosome through the peptide exit tunnel, a structure that begins at the PTC and spans the body of the large subunit.

Translation, and ultimately gene expression, can be regulated at many different levels. One of them is by direct interaction of small molecules with specific sites in the large ribosomal subunit. For instance, several antibiotics, which interfere with protein synthesis, inhibit ribosome function by binding to either the PTC or the peptide exit tunnel. Nascent peptides can also regulate the activities of the large subunit, modulating gene expression. These regulatory nascent peptides, termed ribosome arrest peptides (RAPs), induce translational arrest; the resulting arrested ribosomes control either transcription or translation of the downstream genes in the same operon (69,91,92).

RAPs contain specific domains, predominantly near their carboxyl termini, that are required for inducing ribosome stalling (65,69,91-93). Genetic analyses have shown that components of the ribosomal PTC and exit tunnel are required for the action of RAPs. Furthermore, structural analyses of arrested ribosomes containing RAPs show that their stalling domains form specific interactions with the PTC and the peptide exit tunnel (81). However, the exact roles of the observed interactions in inhibiting ribosome function remain obscure.

Tryptophanase is an enzyme involved in the metabolic degradation of L-tryptophan (L-Trp) (23). Tryptophanase catalyzes the breakdown of L-Trp into indole, pyruvate, and ammonia. Pyruvate and ammonia are used as carbon and nitrogen sources, respectively and indole is involved in establishing several bacterial phenotypes (26,94). In *Escherichia coli* and *Proteus vulgaris*, for example, the tryptophanase coding gene is within the tightly regulated *tnaCAB* operon. This operon contains a regulatory leader region including a small open reading frame, designated *tnaC*, which encodes the RAP TnaC, followed in the operon by two major structural genes, *tnaA,* encoding tryptophanase, and *tnaB*, encoding an L-Trp specific transporter (21,95). Both the catabolite activator protein (CAP) and free L-Trp are required to induce expression of *tnaCAB* (67,96). While initiation of transcription of the *tnaCAB* operon is under catabolite repression control, continuation of transcription into the *tnaA* and *tnaB* structural genes is regulated by the available concentration of free L-Trp. After synthesizing the *tnaC* mRNA segment, the transcribing RNA polymerase pauses in the *tnaC-tnaA* intergenic spacer region before it can reach the *tnaA* and *tnaB* structural

genes. When the cellular L-Trp levels are low, TnaC synthesis is completed, releasing TnaC and the translating ribosome at the *tnaC* stop codon. Dissociation of the ribosome allows the interaction of the Rho-termination factor with the RNA polymerase that is paused in the *tnaC-tnaA* intergenic region. This promotes premature Rho-dependent transcription termination to occur before the polymerase reaches the structural genes of the operon (1,29,32,96). Conversely, when cellular L-Trp levels are high, L-Trp is bound to the ribosome, and the ribosome translating *tnaC* mRNA stalls at either the *tnaC* stop codon in *E. coli* or the *tnaC* Lys-33 codon in *P. vulgaris* (40,97). The presence of the stalled ribosome in the mRNA 5'-leader prevents the interaction of the Rho-termination factor with RNA polymerase. Therefore, transcription of the *tna* mRNA operon continues, and *tnaA* and *tnaB* are transcribed and expressed (32,40,96,98).

In bacteria that possess the *tnaCAB* operon, the specified TnaC peptides range in length from 24 to 36 amino acid residues. TnaC peptides of *E. coli* and *P. vulgaris* contain two highly conserved and one semi-conserved functional residues: a unique tryptophan residue (W12 in *E. coli* and W20 in *P. vulgaris*), a unique aspartic acid residue (D16 in *E. coli* and D24 in *P. vulgaris*) and a proline residue (P24 in *E. coli* and P32 in *P. vulgaris*) whose mutations prevent translational arrest and L-Trp-dependent *tnaCAB* operon induction (38,39). These TnaC peptides also contains a semi-conserved residue, I19 in *E. coli* and L27 in *P. vulgaris*, which importance for TnaC function is unknown (39). It has been suggested that interactions between these TnaC residues and the ribosome promote the formation of a L-Trp binding site, at which bound L-Trp inhibits ribosome function (39). The binding of L-Trp to the TnaC-peptidyl-$tRNA^{Pro}$-

ribosome complex has been shown to block either release factor 2 (RF2)-catalyzed hydrolysis of TnaC-tRNA^{Pro} at P24 (in *E. coli*), or the transfer of the TnaC peptide from TnaC-tRNA^{Pro} to Lysyl-tRNA^{Lys} at K33 (in *P. vulgaris*) (40,97). It has been proposed that free L-Trp binds either at or near the PTC A-site, but the exact location of the L-Trp binding site, unfortunately, remains unknown (68,84). It is also unclear how bound L-Trp inhibits ribosome function and what role(s) the TnaC peptide plays in the formation of the L-Trp binding site.

Genetic, biochemical, and computational analyses have revealed possible points of interaction between the TnaC peptide and the stalled ribosome (38,43,44,84,99). The available data suggest that TnaC residues W12 and D16 might be involved in interactions with amino acid residues R92 and K90 of r-protein L22, and 23S rRNA nucleotides A752 and U2609 (38,43,99). Molecular dynamics simulations also suggest that TnaC amino acid residue I19 might in be contact with 23S rRNA nucleotides A2058, A2059 and U2609 (38). Cryo-EM reconstructions of the TnaC-stalled ribosome complex suggest that the stalling signal may be transmitted by a relay of TnaC-ribosome interactions from the exit tunnel to the PTC either via the TnaC peptide chain or through the ribosome, causing conformational arrangements in the PTC that impede its activity (43). Unfortunately, the cryo-EM analyses did not reveal the binding site for L-Trp (43).

In this study, we analyze the contribution of specific 23S rRNA nucleotides and TnaC residues in the ability of the ribosome to respond to varying concentrations of free L-Trp or the L-Trp analog, 1-methyl-L-Trp (1MT). Our genetic and biochemical analyses demonstrate that 23S rRNA nucleotide A2058 and TnaC residue I19 are

important in promoting the sensing of L-Trp by the ribosome. Our data also indicate that Trp-tRNA^{Trp}, unlike free L-Trp, does not induce either ribosome stalling or expression of the *tnaCAB* operon. We conclude from our analyses that TnaC-ribosome interactions induce the formation of a critical L-Trp binding site within the ribosome.

MATERIALS AND METHODS

Bacteria strains and plasmids

The *E. coli* K-12 strains and plasmids containing selected genes used in this study are listed in Table 5. For *in vitro* assays, replacements of *tnaC* and 23S rRNA sequences were generated in the pGF2500 and pNK plasmids respectively using the QuikChange Lightning Site-Directed Mutagenesis Kit (Agilent Technologies). S30 cell free extracts used in *in vitro* assays were prepared from bacterial strains with replacements of the 23S rRNA variants made as previously indicated (44). For *in vivo* assays, reporter gene mutants were obtained as follows: the *tna$_p$tnaC-tnaA'*- region from 281 nucleotides upstream of the *tnaC* translation start through the *BamHI* site at the *tnaA'-'lacZ* junction were amplified from pAW137 derivatives using the primers AW217 and AW218. The PCR products were digested with *BamHI* and ligated to *BamHI* digested pUC18. Site-directed mutagenesis to change the start codon of *tnaC* to a TGA stop codon or insert codons at *tnaC* position 25 were carried out on pUC18 derivatives using Phusion DNA polymerase and the manufacturer's instructions (ThermoScientific). Complementary primers were designed with the desired replacements flanked by ~10–15 nucleotides of the wild-type sequences on each side of

the change. The pUC18 plasmid derivatives that contained the desired replacements were confirmed by sequencing. *BamHI* fragments from pUC18 derivatives were ligated to *BamHI* digested pRS552, which creates an in-frame translational fusion of *tnaA* and *lacZ*. *SalI* fragments from pRS552 derivatives containing tna_p*tnaC-tnaA'-'lacZYA* with desired *tnaC* changes were ligated to *SalI* digested pACYC184. Finally, SalI fragments from pACYC184 derivatives were ligated to *XhoI* digested pGRG36. Site-specific transposition into the *att7* locus of *E.coli* was carried out and confirmed as previously described (78,99).

Bacterial strains containing mutant variants of the *tnaA'-'lacZ* reporter genes and mutant variants of the 23S RNA gene were made as follows: pNK plasmids with desired 23S rRNA mutations were transformed into AW122 derivatives. Plating onto LB containing 100 μg/ml Amp was used to select for transformants. Transformants were picked into 2 ml LB containing 100 μg/ml Amp and incubated overnight at 37°C. 10^{-6} dilutions of the overnight cultures were plated on LB plates containing 5% sucrose, selecting against the prrnC-sacB plasmid, and incubated overnight at 37°C (76). Colonies from LB-5% sucrose plates were replica plated onto LB plates containing either 100 μg/ml Amp or 25 μg/ml Kan. Successful replacements of p*rrnC-sacB* with pNK derivatives were confirmed by the Amp^R/Kan^S phenotype. After plasmid replacements, the 23S rRNA A2058 and A2059 mutations were verified in the strains by first amplification of 23S rRNA 1350-2902 region, followed by sequencing of the resulting PCR products.

Table 5. *E. coli* bacterial plasmids and strains used in this work.

Plasmid	**Description**	**Source**
ptRNA67	tRNA encoding plasmid	(76)
prrnC-sacB	Wild-type *rrnC* operon; Km^r, and a *sacB* gene, derived from pCS101	(76)
pNK	Wild-type *rrnB* operon; Amp^r, derived from ColE1	(12)
pNKA2058G	Derived from pNK has a A-to-G replacement at position 2058 in the 23S rRNA	This study
pNKA2058T	Derived from pNK has a A-to-T replacement at position 2058 in the 23S rRNA	This study
pNKA2059C	Derived from pNK has a A-to-C replacement at position 2059 in the 23S rRNA	This study
pNKA2059G	Derived from pNK has a A-to-G replacement at position 2059 in the 23S rRNA	This study
pNKA2059T	Derived from pNK has a A-to-T replacement at position 2059 in the 23S rRNA	This study
pKKU2609C	Derived from pNK has a T-to-C replacement at position 2609 in the 23S rRNA	(75)
pAW137	Has the *tna$_p$tnaC*(*ΔN2-H22*) with BsaI-XhoI-BsaI linker-*tnaA*'-'*lacZYA* cloning reporter gene derived from pACYC184	(99)
Strain	**Description**	**Source**
SQ351	MG1655 *Δ7 rrn Δ(lacZYA)* (pKK3535, ptRNA67)	(44)
AW122	Derived from SQ351 (p*rrnC-sacB*, ptRNA67)	(99)
AW153	MG1655 Δ(*lacZYA*) *att7*::*tna$_p$tnaC*(*tnaA*'-'*lacZYA*)	(99)
AW154	MG1655 Δ(*lacZYA*) *att7*::*tna$_p$tnaC*(*W12R)*(*tnaA*'-'*lacZYA*)	(99)
AW516	MG1655 Δ(*lacZYA*) *att7*::*tna$_p$tnaC*(*I19A*)(*tnaA*'-'*lacZYA*)	This study
AW517	MG1655 Δ(*lacZYA*) *att7*::*tna$_p$tnaC*(*I19W*)(*tnaA*'-'*lacZYA*)	This study
AW607	MG1655 Δ(*lacZYA*) *att7*::*tna$_p$tnaC*(*I19M*)(*tnaA*'-'*lacZYA*)	This study

Table 5. Continued.

Strain	Description	Source
AW608	MG1655 Δ(*lacZYA*) *att7*::tna_p*tnaC*(*I19L*)(*tnaA*'-'*lacZYA*)	This study
AW609	MG1655 Δ(*lacZYA*) *att7*::tna_p*tnaC*(*I19V)*(*tnaA*'-'*lacZYA*)	This study
AW643	MG1655 Δ(*lacZYA*) *att7*::tna_p*tnaC(ΔAUG)*(*tnaA*'-'*lacZYA*)	This study
AW747	MG1655 Δ(*lacZYA*) *att7*::tna_p*tnaC*(*W12R)(ΔAUG)*(*tnaA*'-'*lacZYA*)	This study
AW221	MG1655 Δ7 *rrn* Δ(*lacZYA*) *att7*::tna_p*tnaC*(*W12R)*(*tnaA*'-'*lacZYA*) (pNK, ptRNA67)	(99)
AW216	MG1655 Δ7 *rrn* Δ(*lacZYA*) *att7*::tna_p*tnaC*(*tnaA*'-'*lacZYA*) (pNK, ptRNA67)	(99)
AW677	MG1655 Δ7 *rrn* Δ(*lacZYA*) *att7*::tna_p*tnaC*(*tnaA*'-'*lacZYA*) (pNKA2059C, ptRNA67)	This study
AW676	MG1655 Δ7 *rrn* Δ(*lacZYA*) *att7*::tna_p*tnaC*(*tnaA*'-'*lacZYA*) (pNKA2059G, ptRNA67)	This study
AW675	MG1655 Δ7 *rrn* Δ(*lacZYA*) *att7*::tna_p*tnaC*(*tnaA*'-'*lacZYA*) (pNKA2059T, ptRNA67)	This study
AW680	MG1655 Δ7 *rrn* Δ(*lacZYA*) *att7*::tna_p*tnaC*(*tnaA*'-'*lacZYA*) (pNKA2058G, ptRNA67)	This study
AW673	MG1655 Δ7 *rrn* Δ(*lacZYA*) *att7*::tna_p*tnaC*(*tnaA*'-'*lacZYA*) (pNKA2058T, ptRNA67)	This study
AW701	MG1655 Δ7 *rrn* Δ(*lacZYA*) *att7*::tna_p*tnaC*(*I19A*)(*tnaA*'-'*lacZYA*) (pNK, ptRNA67)	This study
AW684	MG1655 Δ7 *rrn* Δ(*lacZYA*) *att7*::tna_p*tnaC(I19A)*(*tnaA*'-'*lacZYA*) (pNKA2059C, ptRNA67)	This study
AW681	MG1655 Δ7 *rrn* Δ(*lacZYA*) *att7*::tna_p*tnaC(I19A)*(*tnaA*'-'*lacZYA*) (pNKA2059G, ptRNA67)	This study

Table 5. Continued.

Strain	Description	Source
AW683	MG1655 Δ7 *rrn* Δ(*lacZYA*) *att7*::*tna*$_p$*tnaC*(*I19A)*(*tnaA*'-'*lacZYA*) (pNKA2059T, ptRNA67)	This study
AW682	MG1655 Δ7 *rrn* Δ(*lacZYA*) *att7*::*tna*$_p$*tnaC(I19A*)(*tnaA*'-'*lacZYA*) (pNKA2058G, ptRNA67)	This study
AW685	MG1655 Δ7 *rrn* Δ(*lacZYA*) *att7*::*tna*$_p$*tnaC*(*I19A*)(*tnaA*'-'*lacZYA*) (pNKA2058T, ptRNA67)	This study
AW691	MG1655 Δ7 *rrn* Δ(*lacZYA*) *att7*::*tna*$_p$*tnaC*(*I19M*)(*tnaA*'-'*lacZYA*) (pNK, ptRNA67)	This study
AW692	MG1655 Δ7 *rrn* Δ(*lacZYA*) *att7*::*tna*$_p$*tnaC*(*I19M)*(*tnaA*'-'*lacZYA*) (pNKA2059C, ptRNA67)	This study
AW694	MG1655 Δ7 *rrn* Δ(*lacZYA*) *att7*::*tna*$_p$*tnaC*(*I19M)*(*tnaA*'-'*lacZYA*) (pNKA2059G, ptRNA67)	This study
AW693	MG1655 Δ7 *rrn* Δ(*lacZYA*) *att7*::*tna*$_p$*tnaC*(*I19M)*(*tnaA*'-'*lacZYA*) (pNKA2059T, ptRNA67)	This study
AW700	MG1655 Δ7 *rrn* Δ(*lacZYA*) *att7*::*tna*$_p$*tnaC*(*I19M)*(*tnaA*'-'*lacZYA*) (pNKA2058G, ptRNA67)	This study
AW695	MG1655 Δ7 *rrn* Δ(*lacZYA*) *att7*::*tna*$_p$*tnaC*(*I19M)*(*tnaA*'-'*lacZYA*) (pNKA2058T, ptRNA67)	This study
AW704	MG1655 Δ7 *rrn* Δ(*lacZYA*) *att7*::*tna*$_p$*tnaC*(*I19V*)(*tnaA*'-'*lacZYA*) (pNK, ptRNA67)	This study
AW705	MG1655 Δ7 *rrn* Δ(*lacZYA*) *att7*::*tna*$_p$*tnaC*(*I19V*)(*tnaA*'-'*lacZYA*) (pNKA2059C, ptRNA67)	This study
AW706	MG1655 Δ7 *rrn* Δ(*lacZYA*) *att7*::*tna*$_p$*tnaC*(*I19V*)(*tnaA*'-'*lacZYA*) (pNKA2059G, ptRNA67)	This study
AW707	MG1655 Δ7 *rrn* Δ(*lacZYA*) *att7*::*tna*$_p$*tnaC*(*I19V*)(*tnaA*'-'*lacZYA*) (pNKA2059T, ptRNA67)	This study

Table 5. Continued.

Strain	Description	Source
AW708	MG1655 Δ7 *rrn* Δ(*lacZYA*) *att7*::*tna*$_p$*tnaC*(*I19V*)(*tnaA*'-'*lacZYA*) (pNKA2058G, ptRNA67)	This study
AW709	MG1655 Δ7 *rrn* Δ(*lacZYA*) *att7*::*tna*$_p$*tnaC*(*I19V*)(*tnaA*'-'*lacZYA*) (pNKA2058T, ptRNA67)	This study
AW711	MG1655 Δ7 *rrn* Δ(*lacZYA*) *att7*::*tna*$_p$*tnaC*(*I19L*)(*tnaA*'-'*lacZYA*) (pNK, ptRNA67)	This study
AW712	MG1655 Δ7 *rrn* Δ(*lacZYA*) *att7*::*tna*$_p$*tnaC*(*I19L*)(*tnaA*'-'*lacZYA*) (pNKA2059C, ptRNA67)	This study
AW713	MG1655 Δ7 *rrn* Δ(*lacZYA*) *att7*::*tna*$_p$*tnaC*(*I19L*)(*tnaA*'-'*lacZYA*) (pNKA2059G, ptRNA67)	This study
AW714	MG1655 Δ7 *rrn* Δ(*lacZYA*) *att7*::*tna*$_p$*tnaC*(*I19L*)(*tnaA*'-'*lacZYA*) (pNKA2059T, ptRNA67)	This study
AW715	MG1655 Δ7 *rrn* Δ(*lacZYA*) *att7*::*tna*$_p$*tnaC*(*I19L*)(*tnaA*'-'*lacZYA*) (pNKA2058G, ptRNA67)	This study
AW724	MG1655 Δ7 *rrn* Δ(*lacZYA*) *att7*::*tna*$_p$*tnaC*(*I19L*)(*tnaA*'-'*lacZYA*) (pNKA2058T, ptRNA67)	This study
AW218	MG1655 Δ7 *rrn* Δ(*lacZYA*) *att7*::*tna*$_p$*tnaC*(*tnaA*'-'*lacZYA*) (pNH2609, ptRNA67)	(99)
AW814	MG1655 Δ7 *rrn* Δ(*lacZYA*) *att7*::*tna*$_p$*tnaC*(*I19L*)(*tnaA*'-'*lacZYA*) (pNH2609, ptRNA67)	This study
AW671	MG1655 Δ(*lacZYA*) *att7*::*tna*$_p$*tnaC*(*+W25*)(*tnaA*'-'*lacZYA*)	This study
AW672	MG1655 Δ(*lacZYA*) *att7*::*tna*$_p$*tnaC*(*+W25*)*(ΔAUG)*(*tnaA*'-'*lacZYA*)	This study
AW772	MG1655 Δ(*lacZYA*) *att7*::*tna*$_p$*tnaC*(*W12R*)(*+W25*)(*tnaA*'-'*lacZYA*)	This study

Table 5. Continued.

Strain	Description	Source
AW752	MG1655 Δ(*lacZYA*) *att7*::*tna*$_p$*tnaC*(*W12R*)(+*W25*)(*ΔAUG*)(*tnaA*'-'*lacZYA*)	This study
AW778	MG1655 Δ(*lacZYA*) *att7*::*tna*$_p$*tnaC*(+*I25-AUU*)(*tnaA*'-'*lacZYA*)	This study
AW755	MG1655 Δ(*lacZYA*) *att7*::*tna*$_p$*tnaC*(+*I25-AUU*)(*ΔAUG*)(*tnaA*'-'*lacZYA*)	This study
AW750	MG1655 Δ(*lacZYA*) *att7*::*tna*$_p$*tnaC*(+*I25-AUA*)(*tnaA*'-'*lacZYA*)	This study
AW801	MG1655 Δ(*lacZYA*) *att7*::*tna*$_p$*tnaC*(+*I25-AUA*)(*ΔAUG*)(*tnaA*'-'*lacZYA*)	This study
AW826	MG1655 Δ(*lacZYA*) *att7*::*tna*$_p$*tnaC*(+*stop25*)(*tnaA*'-'*lacZYA*)	This study

Analysis of the effect of the A2058G mutation on protein expression in *E. coli*

The wild type pKK3535 and the mutant pNKA2058G plasmids were introduced into *E. coli* strain SQ171 (100). After plasmid exchange, the purity of the population of the mutant ribosomes in the cells carrying the pNKA2058G plasmid was verified by primer extension (76,101). For the protein analysis, cells logarithmically growing in LB medium at 37°C were harvested by centrifugation and rapidly frozen. Protein isolation and 2D-DIGE analysis was performed by Dr. Lewis M. Brown at Comparative Proteomics Center, Columbia University as previously described (102). Proteins were extracted from the gel and identified by mass-spectrometry of the tryptic digests.

tnaA'-'lacZ reporter gene expression analysis

To analyze the expression of the *tnaA'-'lacZ* reporter gene we performed β-Gal assays as previously described (79). β-gal activity is reported in Miller units.

In vitro accumulation of TnaC-tRNA^{Pro} and puromycin protection assays

In vitro reactions testing the effect of increasing concentrations of L-Trp on the accumulation of TnaC-tRNA^{Pro} were carried out as described previously (44). The reaction mixtures were performed with S30 cell free extracts (wild type or 23S rRNA mutants) and [^{35}S]-labeled methionine. After incubation at 25°C for 5 minutes, 4 mg of wild type or *tnaC* mutant mRNAs were added to the reaction mixtures. Equal aliquots of reaction mixture were added to tubes containing equal volume of L-Trp in increasing concentrations. The reaction tubes were then incubated at 37°C for 10 minutes, and precipitated using acetone. Dried pellets were resuspended with 25 μL of 1X loading buffer (10X Tricine loading buffer: 4% SDS, 12% glycerol, 50 mM Tris pH 6.8, 2% 2-mercaptoethanol, 0.005% bromophenol blue) and loaded for electrophoresis on to 10% tris-tricine polyacrylamide gels . [^{35}S]-labeled methionine resolved molecules were detected using autoradiography and their intensity determined with the ImageJ software. Puromycin protection assays were performed with isolated TnaC-tRNA-ribosome complexes obtained as previously indicated (44). Solutions containing [^{35}S]-methionine labeled complexes were mixed with several concentrations of L-Trp before being mixed with a puromycin solution. The final products of each reaction were resolved and analyzed as indicate above.

Toeprinting analysis

Toe-printing assays were performed essentially as described, following performing cell free transcription-translation reactions using a PURExpress system kit version (New England Biolabs) where ribosomes were added separately and amino acid concentrations could be adjusted (Δ ribosomes, Δ amino acids) (7). Ribosomes were isolated from the corresponding *E. coli* SQ171 described above. Importantly, to avoid different levels of free L-Trp background in the ribosome preparations, wild type and mutant ribosomes were isolated in parallel using same batches of media and buffers. The DNA templates used to direct translation contained the entire *tnaC* ORF and were PCR-amplified from wt plasmid pGF2500 or its mutant versions (described above) using forward primer T7-tnaC-2, 5'-TAATACGACTCACTATAGGGAGTTTTATAAGGAGGAAAACATATGAATATCTTACATATATGTG-3', to add the T7 promoter sequence and an optimized translation initiation region, and reverse primer tnaC-toe-2, 5'-AGCAAACAAATAGATCACATTG-3', which was also used as the toe-printing primer. Translation reactions were performed for 15 min at 37°C with a mixture containing every amino acid at 0.3 mM except for L-tryptophan whose concentration was adjusted, from stock solutions in water, from zero through the range 12.5 μM to 25 mM.

RESULTS

23S rRNA nucleotides A2058 and A2059 are important for ribosome stalling induced by TnaC and L-Trp

The 23S rRNA nucleotides A2058 and A2059 are located at the surface of the exit tunnel, which makes them susceptible to interactions with nascent peptides and other ligands. These nucleotides form a hydrophobic crevice, which constitutes the binding site for antibiotic ligands involved in ribosome stalling regulated by the ErmCL RAP (5,78,99,103). The A2058 nucleotide also participates in translation arrest induced by the SecM RAP (5,12). In a search for other cellular proteins whose expression might depend on the nascent peptide recognition in the tunnel, we used 2D-differential gel electrophoresis (2D-DIGE) to compare global expression of proteins in wild type *E. coli* cells with those carrying the 23S rRNA A2058G mutation. When cells were grown in rich (LB) medium, the most dramatic effect revealed by this analysis was the decreased expression of tryptophanase whose steady state level in the mutant was reduced 7.5 fold compared to the wild type cells (Figure 15). This result suggested that nucleotide A2058 plays an important role in the regulation of expression of the *tnaCAB* operon.

To further investigate the role of A2058 and its neighboring residue A2059 in *tna* operon regulation, we prepared a library of plasmids containing mutant 23S rRNA genes with nucleotide replacements at either A2058 or A2059 (Table 5). These plasmids were introduced into bacterial cells lacking chromosomal *rrn* alleles and containing a *tnaC tnaA'-'lacZ* reporter construct (see Experimental Procedures), and the *in vivo* expression of the *tnaA'-'lacZ* reporter in response to Trp was analyzed (44,99). The cells were

grown in minimal media supplemented with 100 mg/ml L-Trp as inducer (see Experimental Procedures). While in minimal media most of the A2058 and A2059 changes did not significantly affect the expression of the reporter in the presence of 100 mg/ml L-Trp (Table 6), we observed a 2.6-fold reduced expression of *tnaA'-'lacZ* in cells with the A2058U substitution. Importantly, the previously reported U2609C transition had a much more profound effect on the reporter expression and essentially

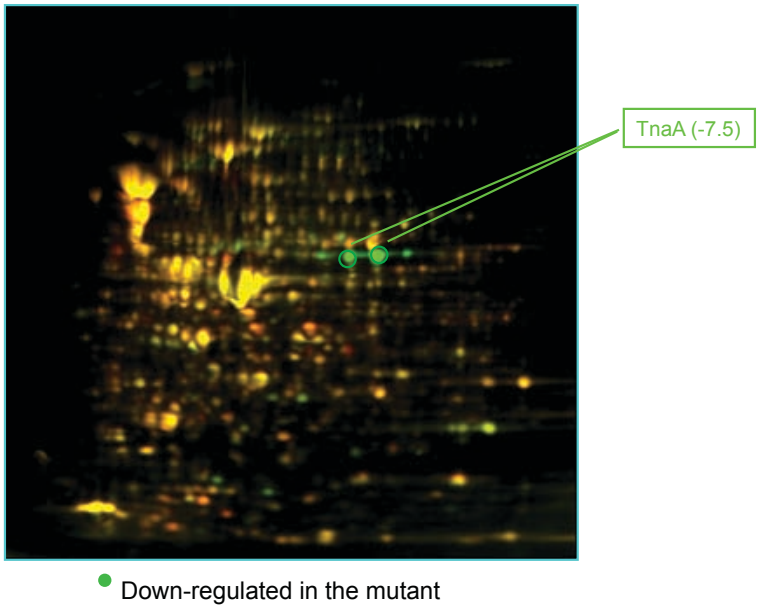

Figure 15. *In vivo* expression of the tryptophanase enzyme. A representative image of a 2D-DIGE experiment performed with total protein obtained from *E. coli* bacteria cells expressing the 23S rRNA wild type (protein labeled with Cy3; green) and the 23S rRNA A2058 mutant (protein labeled with Cy5; red) genes is shown. Green-lines indicate the position of the protein bands corresponding to the tryptophanase enzyme (TnaA). The differential value in TnaA concentration between protein samples is indicated between parentheses.

abolished its induction in the presence of 100 mg/ml L-Trp (Table 6). In order to eliminate the possible influence of L-Trp degradation and utilization, we verified these

results using a range of 1-methyl-L-Trp (1MT) concentrations (Figure 16A). 1MT is an L-Trp analog that functions as an inducer of the *tna* operon but unlike L-Trp, is not degraded or incorporated into proteins and thus is maintained at a stable concentration within the cell (80,99). Some of the A2059 and A2058 mutations affected the dependence of the reporter induction on 1MT concentration. Thus, in the minimal

Table 6. Expression of the *tnaA'-'lacZ* protein fusion in different A2058-A2059 mutant backgrounds.

23S rRNA	β-galactosidase activity[a]				Induction ratio (+Trp/-Trp)[b]
	-Trp		+Trp		
wild-type	18	±2	665	±22	36.9
U2609C	29	±3	47	± 2	1.6
A2058G	21	±1	882	±25	42.0
A2058U	17	±1	252	± 6	14.8
A2058C	ND[c]		ND		ND
A2059G	16	±0	659	±24	41.2
A2059U	27	±2	1077	± 9	39.9
A2059C	20	±0	858	±33	42.9

[a]Cultures of Δ7 *rrn* E. *coli* bacterial strains were grown in minimal medium plus 0.2% glycerol, 0.05% acid-hydrolyzed casein, 0.01 % vitamin B1 and 100μg/ml ampicillin with (+Trp) or without (-Trp) 100 μg/ml L-Trp. β-Galactosidase assays were performed in three independent experiments.
[b]Ratio of values for cultures grown with L-Trp (+Trp) and those grown without L-Trp (-Trp).
[c] Not enough bacterial cells were obtained to perform the experiments because cells expressing the 23S rRNA A2058C replacement grew poorly. Cells containing only A2058C ribosomes are not viable.

Figure 16. Sensibility of mutant ribosomes for L-Trp. (**A**) β-galactosidase activity (given in Miller Units) was measured on cultures of bacterial cells (Δ7 *rrn*) carrying the *tnaC-tnaA'-'lacZ* reporter gene and the indicated 23S rRNA alleles. Cultures were grown in minimal medium containing the indicated concentrations of 1-methyl-L-Trp (1MT). The 1MT concentration required for 50% of induction was calculated using the data from these curves and the LMMpro nonlinear regression software program version 1.06 (http://www.alfisol.com/IFS/IFS-003/LMMpro-Downloads.php). (**B**) Autoradiograms showing toeprinting assays performed with *in vitro* translation reactions. Translation reactions were performed with cell-free extracts reconstituted with ribosomes containing the indicated 23S rRNAs variants and with wild type *tnaC* mRNAs. The TnaC peptide sequence and the *tnaC* codon sequence are shown on the left side of the figure. The positions of stalled ribosomes are shown with boxes in the *tnaC* codon sequence and with arrows in the right side of the autoradiograms. (**C**) A plot showing the induction values with respect to L-Trp concentrations is also shown on the right side of the figure. Induction values were calculated by using the following formula: intensity of the band corresponding to the proline codon position obtained for each sample/ intensity of the band corresponding to the proline codon position obtained in the sample without L-Trp. (**D**) Autoradiograms showing L-Trp-protection assays performed with stalled ribosomes complexes containing the indicated 23S rRNAs and wild type *tnaC* mRNAs. Puromycin-cleavage of the TnaC-$tRNA^{Pro}$ molecules was challenged with the indicated L-Trp concentrations. TnaC-$tRNA^{Pro}$ and TnaC band positions are indicated with arrows. The % of TnaC-$tRNA^{Pro}$ that remained in each experiment was calculated using the following formula: % of TnaC-$tRNA^{Pro}$ = [amount of remained TnaC-$tRNA^{Pro}$/ (amount of remained TnaC-$tRNA^{Pro}$ + amount of TnaC)]. The L-Trp concentration required for 50% protection was calculated as indicted above using the % value of TnaC-$tRNA^{Pro}$ that remained after puromycin treatment.

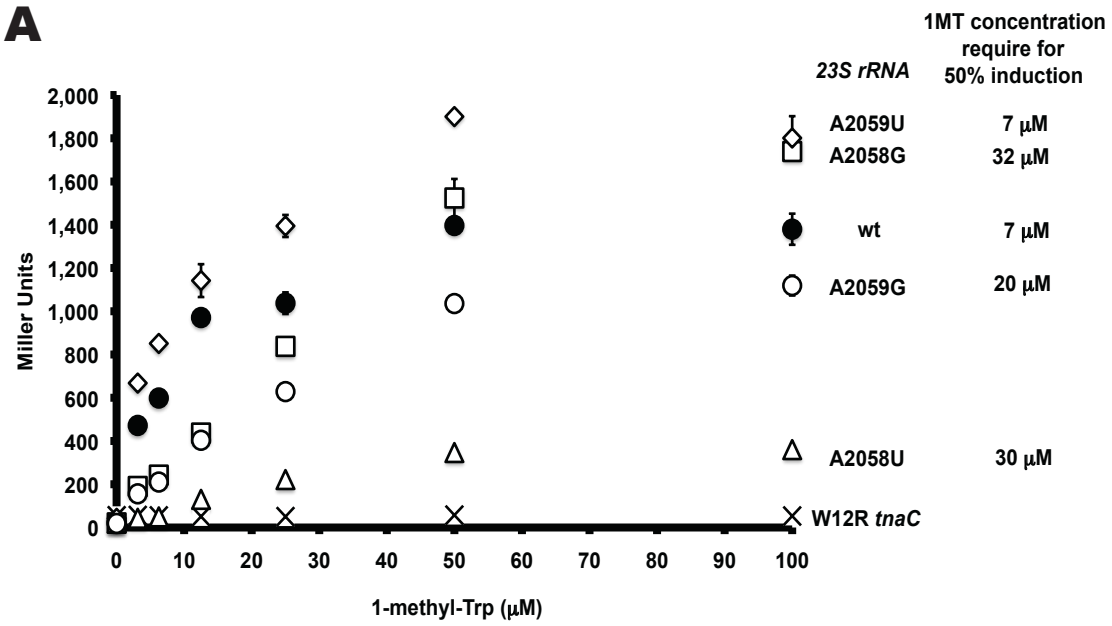
A
1MT concentration require for 50% induction
23S rRNA
A2059U
A2058G
7 μM
32 μM
wt
7 μM
A2059G
20 μM
A2058U
30 μM
W12R tnaC
Miller Units
2,000
1,800
1,600
1,400
1,200
1,000
800
600
400
200
0
0 10 20 30 40 50 60 70 80 90 100
1-methyl-Trp (μM)

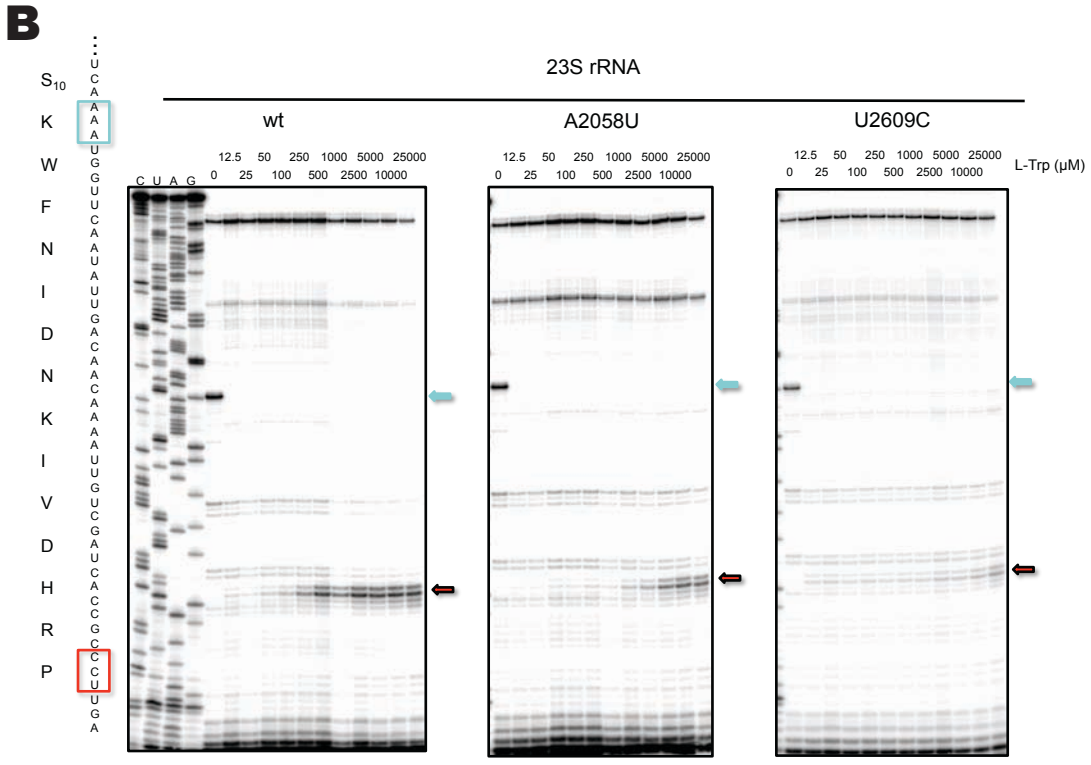
B
23S rRNA
wt
A2058U
U2609C
L-Trp (μM)
0 12.5 25 50 100 250 500 1000 2500 5000 10000 25000
C U A G
S10
K
W
F
N
I
D
N
K
I
V
D
H
R
P

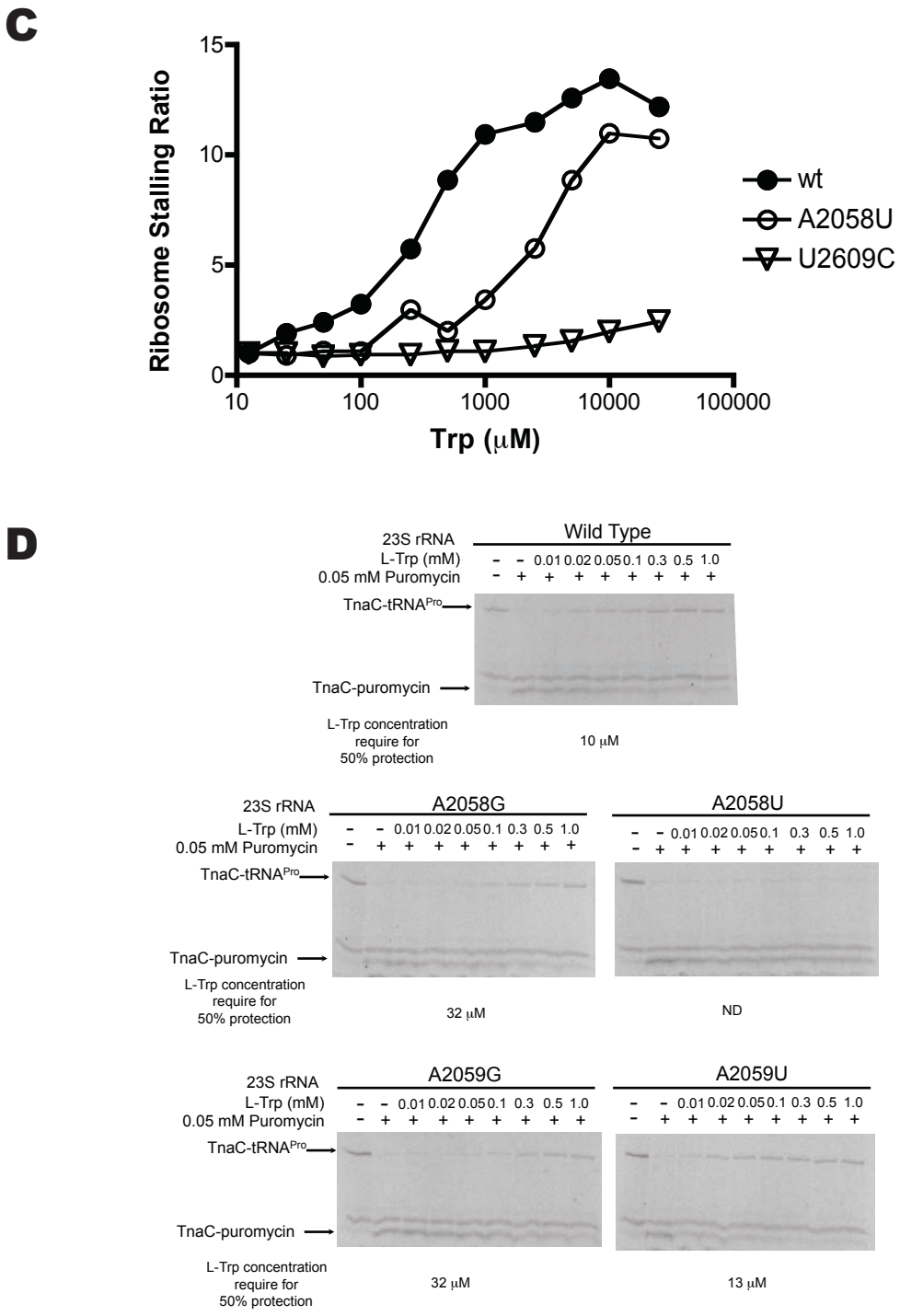

Figure 16. Continued.

medium at lower concentrations of 1MT, the reporter was poorly induced in the A2058G mutant, but induction reached the wild type level at high concentrations of 1MT. The expression of the reporter in the A2059G mutant was slightly lower compared to the strain containing wild-type ribosomes. More importantly however, the expression of the reporter in the A2058U mutant remained low compared to the wild-type control at all 1MT concentrations. Remarkably, however, higher concentrations of 1MT were required to reach 50% maximal induction in the A2058G, A2058U and A2059G mutants compared to the control (Figure 16A). These data indicated that changes of A2058 and A2059 nucleotides affected the sensitivity of the reporter gene to Trp inducer.

To verify the observed *in vivo* effects in a better-defined system, we analyzed L-Trp-dependent stalling of wild type or A2058U or U2609C ribosomes in an *in vitro* cell-free translation system. Translation of *tnaC* mRNA was performed in the transcription-translation system assembled from purified components where the concentrations of L-Trp could be accurately adjusted (104). Ribosome stalling at the P24 codon of *tnaC* (Figure 16B, red arrow) was monitored by toeprinting analysis (see Experimental Procedures) over a wide range of concentrations of L-Trp. In the absence of L-Trp, translation was arrested at the W12 codon, because of the lack of Trp-tRNA^{Trp}. Increasing the concentration of free L-Trp in the reaction to 12.5 μM eliminated the arrest at the Trp codon, yet only negligible ribosome stalling at the Pro24 codon was observed because the concentration of free L-Trp was insufficient for efficient formation of the TnaC-dependent stalled complex. Significant ribosome stalling occurred at the Pro24 codon when translation reactions were performed at higher concentrations of L-

Trp. Most importantly, the concentration dependence of TnaC-mediated translation arrest was shifted towards higher concentrations for the A2058U mutant compared to wild type (Figure 16C, compare closed circles with open circles). In contrast, U2609C mutant ribosomes completely lost their ability to stall at the Pro24 codon of *tnaC*, regardless of the L-Trp concentration (Figure 16C). These results indicated that U2609C the mutation affected the general mechanism of TnaC-assisted stalling, whereas the A2058U mutation decreased the affinity of the ribosome for free L-Trp.

We also tested the ability of L-Trp to inhibit PTC functions in the isolated ribosome/TnaC-tRNA^{Pro} stalled complexes containing changes in nucleotides A2058 or A2059. Transfer of the nascent TnaC peptide from TnaC-tRNA^{Pro} to puromycin was monitored to determine if L-Trp was still capable of preventing this transfer in the stalled complexes containing mutant ribosomes. Isolated complexes were reacted with puromycin in the presence of increasing concentrations of L-Trp (Figure 16D). An approximately 3-fold higher concentration of L-Trp was required to achieve 50% of the maximum PTC inhibition in the A2058G or A2059G mutants compared to wild type ribosome (Figure 15D). No inhibition of the TnaC-tRNA^{Pro} reactivity with puromycin was observed in the complex containing A2058U ribosomes up to 1 mM of L-Trp (the highest concentration of inducer tested in these experiments). These results corroborated that changes in nucleotides A2058 and A2059 affect the concentration dependence of L-Trp -mediated inhibition of the ribosome activity that underlies programmed translation arrest at the *tnaC* gene.

Features of TnaC residue I19 important for ribosome stalling induced by L-Trp

Molecular dynamic simulations that were based on the 5.8 Å cryo-EM map of the 70S-TnaC complex placed TnaC residue I19 in close proximity to 23S rRNA nucleotides A2058 and A2059 (38,43). Furthermore, this TnaC residue is highly conserved among several bacterial species, suggesting a role in Trp-dependent *tnaC* translation arrest (39). To test whether the I19 residue of TnaC is involved in sensing the presence of the inducer, we replaced it with hydrophobic residues of variable sizes and tested the mutants *in vitro* and *in vivo*. *In vitro* formation of stalled ribosome complexes was assessed by detecting the accumulation of the TnaC-tRNA^{Pro} in a cell-free translation system in the presence of high concentration of L-Trp (Figure 17A) (29). No TnaC-tRNA^{Pro} was observed in the wild type complex at low concentration of L-Trp, but when the concentration of the inducer was raised to 4 mM, TnaC-tRNA^{Pro} accumulated, indicating that the wild type TnaC peptide in the ribosomal exit tunnel makes the ribosome sensitive to L-Trp. Substitution I19L produced similar amounts of accumulated TnaC-tRNA^{Pro} as the wild type mRNA (Figure 17A, compare lane 4 with lane 10). However, translation of mRNAs containing the codon changes I19V, I19M or I19F resulted in diminished accumulation of TnaC-tRNA^{Pro} compared to the wild type mRNA, whereas the I19A or I19W mutations abolished completely any TnaC-tRNA^{Pro} accumulation upon the addition of 4 mM L-Trp (Figure 17A, compare lane 4 with lane 16). These results indicated that the nature of the residue at position 19 of the TnaC peptide is important for its ribosome arrest function in response to L-Trp.

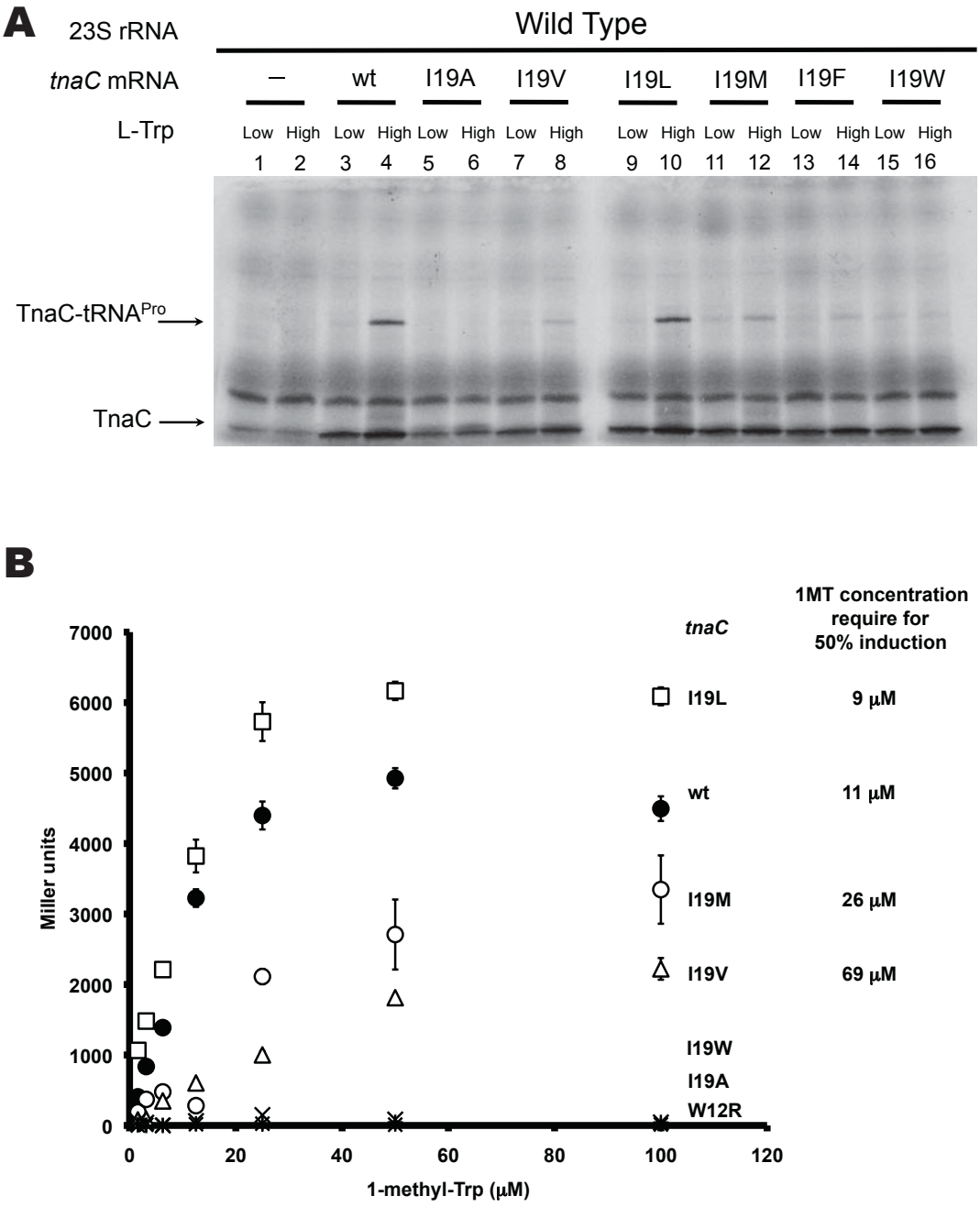

Figure 17. Effects of mutant TnaC peptides on the sensibility of ribosomes for L-Trp. (**A**) Autoradiograms showing *in vitro* accumulation of TnaC-tRNA^{Pro} performed with wild type cell-free extracts and the indicated *tnaC* mRNAs variants. The reactions were performed adding (High) or not (Low) and extra 4 mM L-Trp. TnaC-tRNA^{Pro} and TnaC band positions are indicated with arrows. (**B**) β-galactosidase activity obtained from cultures of bacterial cells (*rrn*+) carrying a *tnaC-tnaA'-'lacZ* reporter gene containing the indicated *tnaC* alleles. The plot and the 1MT concentration required for 50% induction were obtained as indicated in Figure 16A.

We tested the expression of *tnaC tnaA'-'lacZ* constructs containing *tnaC* genes with I19 codon replacements *in vivo* (Figure 17B). The expression of these constructs was analyzed at different concentrations of 1MT to determine the effects of the mutations on the sensitivity of the ribosome to inducer concentration (64,99). As expected, wild-type TnaC and the I19L replacement showed very similar inducer dependence (Figure 17B). The I19A and I19W replacements, like the previously examined substitution W12R, completely abolished the expression of the reporter gene (Figure 17B). The I19V and I19M replacements reduced the level of induction of the reporter construct (Figure 17B). However, the most remarkable observation was that the I19M and I19V mutations changed the sensitivity for the system to the concentration of the inducer: these mutants required 2.4 times and 6.3 times more 1MT, respectively, compared to the wild type construct to obtain 50% of maximum induction. These results were confirmed *in vitro* (Figure 18). These data indicated that, similar to the effect of the 23S rRNA A2058 and A2059 mutations, changes in the nature of residue I19 of TnaC peptide alter the Trp concentration dependence of the translation arrest at *tna*C mRNA.

Figure 18. (**A**) L-Trp protection analyses using isolated stalled ribosomes. Stalled ribosome complexes were isolated from *in vitro* translation reactions performed with RF2 depleted cell free extracts and biotinylated *tnaC* mRNAs indicated in the figure. The isolated complexes were mixed or not (-) with the indicated concentrations of L-Trp prior the addition (+) of 0.05 mM puromycin. Products of the reactions were resolved in 10% tris-tricine polyacrylamide gels. TnaC-tRNA^{Pro} and TnaC-puromycin molecule positions are shown by arrows. (**B**) Plot % of TnaC-tRNA^{Pro} protected vs tryptophan concentration. The values of % of TnaC-tRNA^{Pro} protected were obtained from the figures in (**A**) and the following formula: intensity of the band corresponding to TnaC-tRNA^{Pro} obtained for each sample/(intensity of the band corresponding to TnaC-tRNA^{Pro} + intensity of the band corresponding to TnaC).

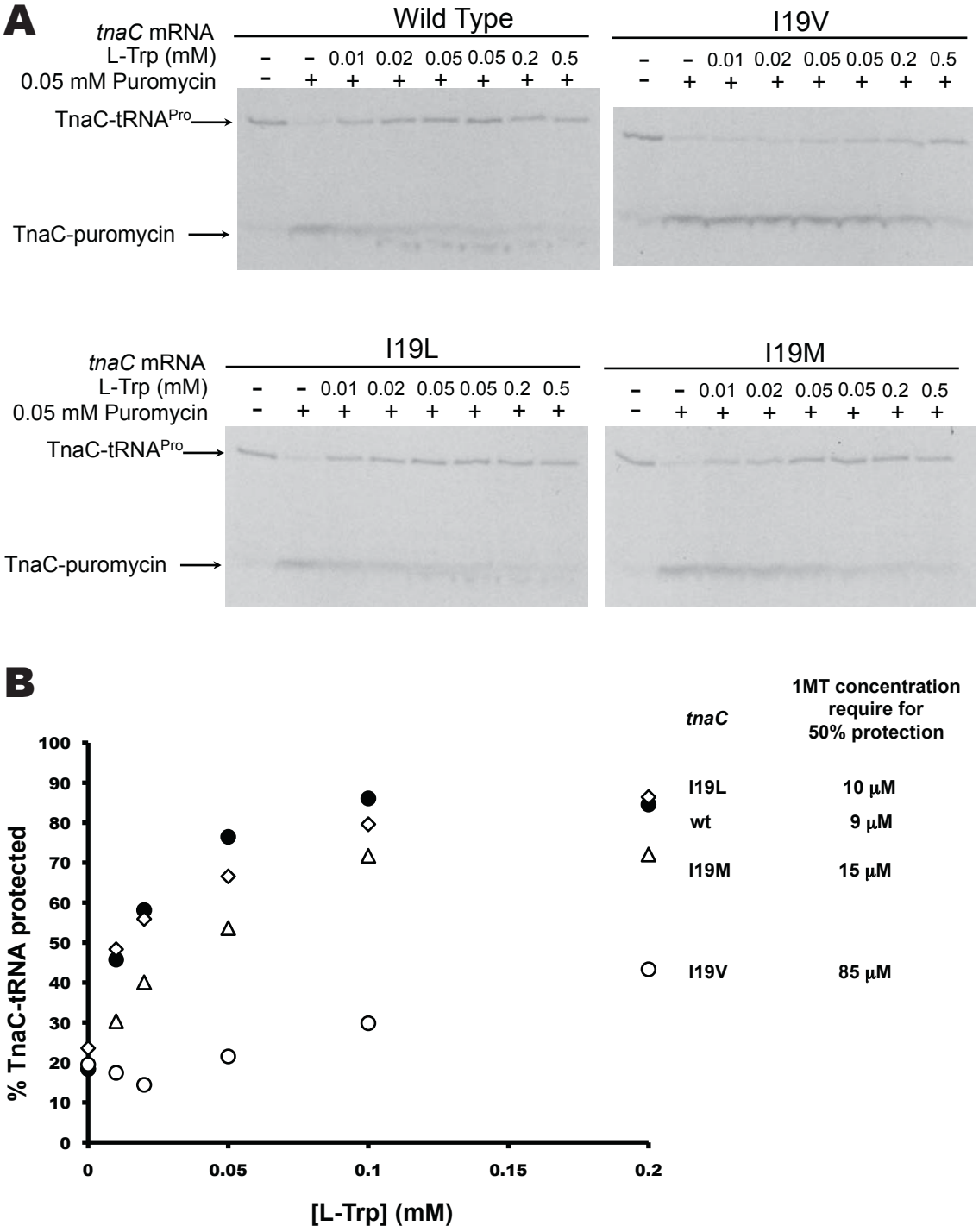
A
tnaC mRNA
L-Trp (mM)
0.05 mM Puromycin
Wild Type
I19V
I19L
I19M
- - 0.01 0.02 0.05 0.05 0.2 0.5
- + + + + + + +
TnaC-tRNAPro
TnaC-puromycin
B
% TnaC-tRNA protected
[L-Trp] (mM)
0 10 20 30 40 50 60 70 80 90 100
0 0.05 0.1 0.15 0.2
tnaC
1MT concentration require for 50% protection
I19L 10 μM
wt 9 μM
I19M 15 μM
I19V 85 μM

Functional relationship between TnaC residue I19 and 23S rRNA nucleotide A2058

We have shown that changes to the 23S rRNA nucleotide A2058 (Figure 16) and to the TnaC residue I19 (Figure 17) affect the sensitivity of the ribosome to L-Trp. To determine whether there is a genetic interaction between these two sensory elements, we tested whether the nascent peptide mutation could compensate for the negative effect on stalling of the A2058U mutation. Results obtained by *in vitro* toeprinting assays using wild type or I19L *tnaC* mRNAs in combination with the wild type ribosomes were in a good agreement with the results of *in vivo* and *in vitro* experiments shown in Figure 17; the I19L mutation had little effect on Trp-concentration dependence of the translation arrest induced in wild type ribosomes. Strikingly, however, the I19L mutation partly restored the reduced Trp sensitivity of stalling of the A2058U mutant ribosomes (Figure 19A and B). This compensatory effect of the nascent peptide mutation was specific for the A2058U mutant ribosomes, because the same I19L mutation was unable to compensate for the negative effect on stalling of the ribosomes carrying the U2609C mutation (Figure 20).

The compensatory effect of the I19L TnaC mutation on the A2058U ribosomes was even more pronounced *in vivo*. We tested the expression of wild type or *tnaC*(I19L) *tnaA*`-`*lacZ* constructs in cells containing wild type or A2058U ribosomes (Figure 19C; Figure 21), As we showed above (Figure 16), expression of the wild type reporter was substantially reduced in the cells containing A2058U ribosomes. Strikingly,

Figure 19. Effects of the TnaC I19L mutant peptide in the sensibility of the A2058U mutant ribosome for L-Trp. (**A**) Toeprinting assays performed as indicated in Figure 15C. Cell-free extracts were reconstituted with either wild type ribosomes or ribosomes containing 23S rRNAs with the replacement A2058U. *In vitro* translation was performed with wild type and I19L mutant *tnaC* mRNAs. (**B**) Plots showing the induction levels obtained using several concentrations of L-Trp. The data was obtained from the gels shown in Figure 18A and Figure 19. Induction of stalled ribosomes was determined from *in vitro* reactions containing either wild-type or I19L mutant *tnaC* mRNAs and cell-free extracts reconstituted with the ribosomes indicated for each plot. The induction levels were obtained as indicated in Figure 15C. (**C**) β-galactosidase activity obtained from cultures of bacterial cells (Δ7 *rrn*) carrying a *tnaC-tnaA'-'lacZ* reporter gene containing the indicated *tnaC* alleles and expressing the indicated 23S rRNA variants. The plot and the 1MT concentration required for 50% induction were obtained as indicated in Figure 16A.

A

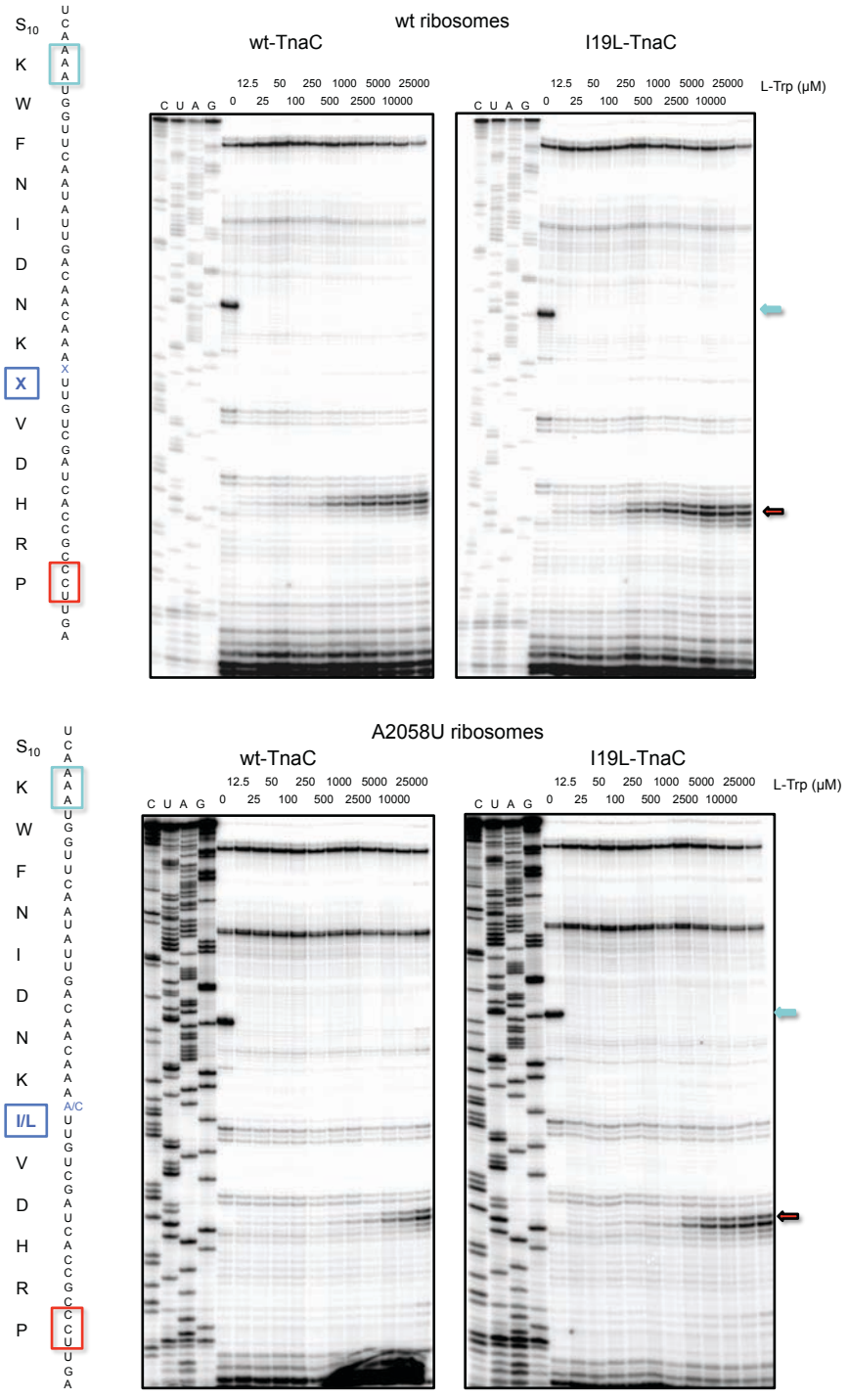
wt ribosomes
wt-TnaC
I19L-TnaC
12.5 50 250 1000 5000 25000
0 25 100 500 2500 10000
C U A G
L-Trp (μM)
S10
K
W
F
N
I
D
N
K
X
V
D
H
R
P
A2058U ribosomes
I/L

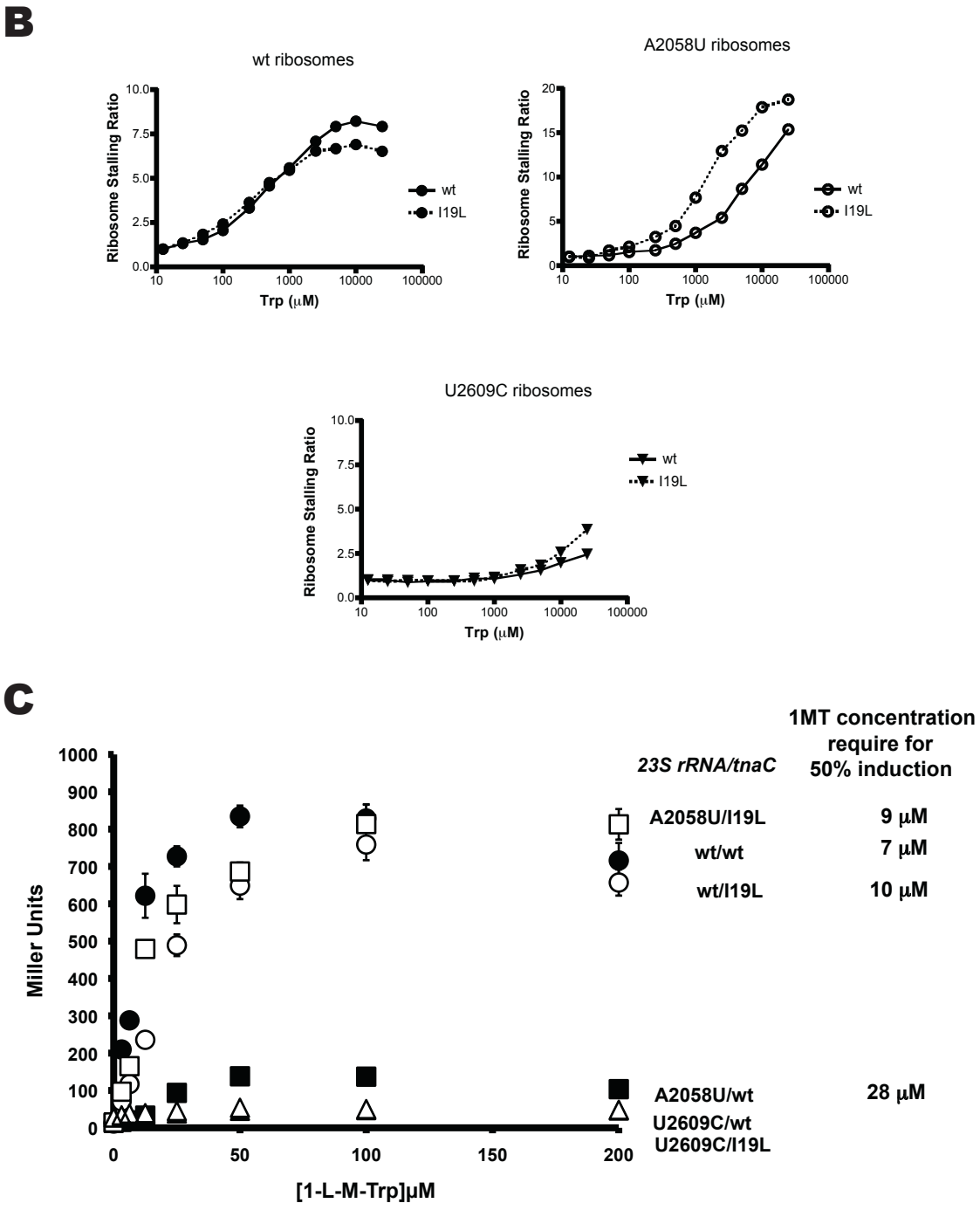

Figure 19. Continued

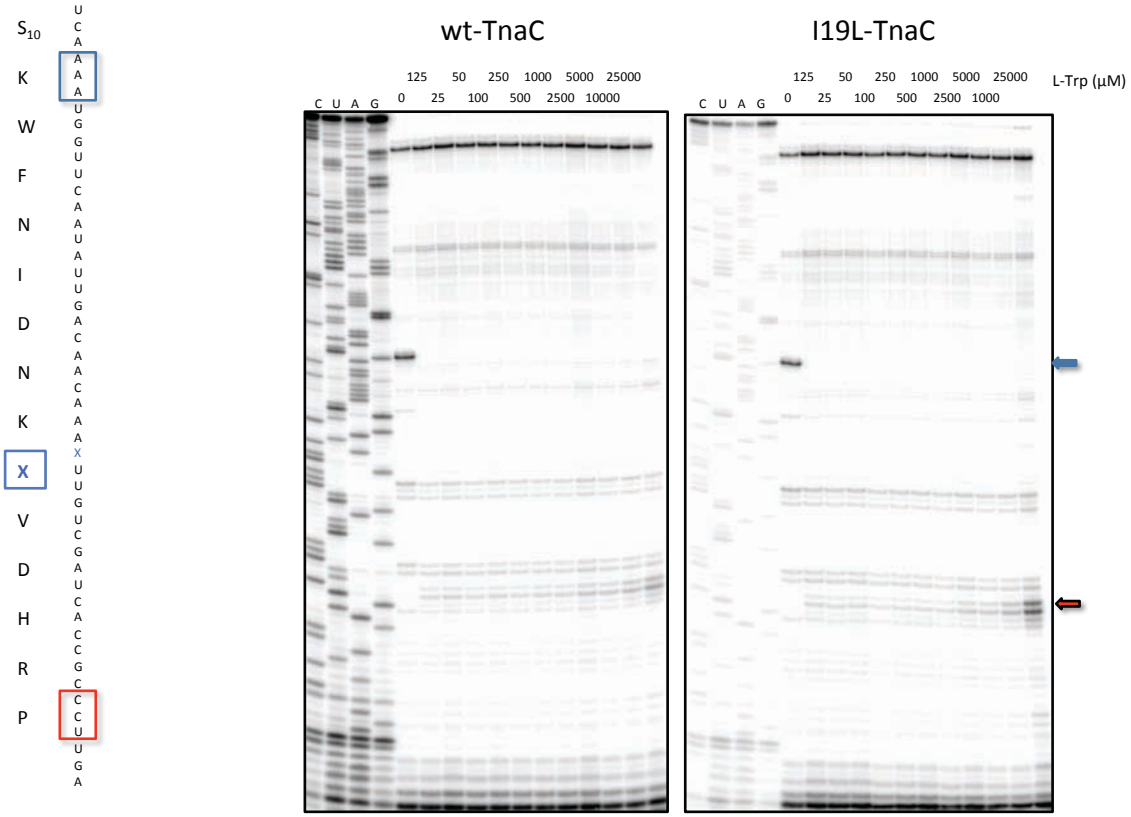

Figure 20. Toeprinting analysis with extracts containing 23S U2609C rRNA and wild-type or I19L *tnaC* mRNAs. Toeprinting analysis performed as indicated in supplementary Figure 17.

however, the I19L mutation in TnaC restored the sensitivity of A2058U ribosomes to the concentration of free L-Trp. Corroborating the *in vitro* results, this compensatory effect of the TnaC mutation remained specific to the A2058U mutation *in vivo*, because expression of the mutant reporter remained at very low levels in the cells with U2609C ribosomes. Altogether, these data indicate that the I19L mutation in the TnaC nascent peptide is able to suppress the loss of Trp sensitivity of A2058U mutant ribosomes, revealing that the ribosome and the nascent peptide cooperate to optimize the affinity of the system to free L-Trp.

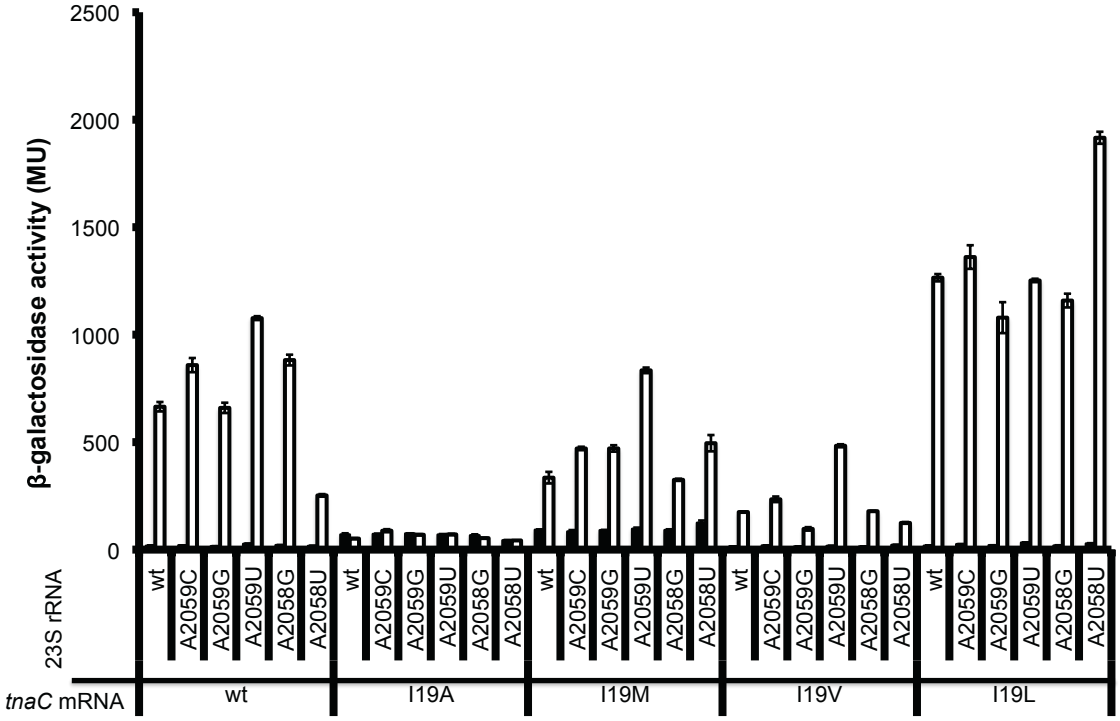

Figure 21. Effects of A2058 and A2059 23S rRNA mutations on I19 mutant TnaC peptides. Bacterial cells (Δ7 *rrn*) expressing the indicated 23S rRNAs and *tnaC* alleles were used to analyze expression of β-galactosidase from a *tnaC-tnaA'-'lacZ* protein fusion. The tested cultures were grown in minimal medium containing 0.2% glycerol, 0.05% acid-hydrolyzed casein, 0.01 % vitamin B1 in the presence of several concentrations of 1MT.

The A-site bound Trp-tRNA^{Trp} is unable to substitute the function of free L-Trp in translation arrest

Our data show that the 23S rRNA nucleotide A2058 and the TnaC residue I19 are both involved in modulating the affinity of L-Trp to the ribosome and that there might be a functional interaction between these two elements. These data are compatible with the possibility that the binding site for free L-Trp might be in the ribosomal nascent peptide exit tunnel. However, this hypothesis seemingly contradicts the previous proposal that the L-Trp binding site is located at the ribosomal A-site

because in previously reported experiments, tryptophanyl-tRNA^{Trp} could replace free L-Trp as an inducer of ribosome stalling *in vitro* (68). Therefore, we revisited whether tryptophanyl-tRNA^{Trp} in the ribosomal A-site could substitute for the free L-Trp requirement as the stalling cofactor at the end of the *tna*C open reading frame (ORF). We performed *in vitro* translation assays by programming extracts with T7 transcribed wild type mRNA or a mutant *tnaC* mRNA (tnaC W25) containing a Trp codon inserted between the Pro24 codon and the stop codon. Our cell free extracts were made from a strain containing the tryptophanase gene and RNAseI activity. These experiments differ from those previously described by Gong and Yanofsky in which transcription and translation were coupled *in vitro* using circular DNA containing the *tnaC* gene and cell free extracts lacking of both the tryptophanase activity and the RNAseI activity (29,68). In contrast to the previous study, our *in vitro* conditions would not maintain high concentrations of either L-Trp or mRNAs during the reactions, making the assay more sensitive to small changes in both L-Trp and mRNA concentrations. In contrast to the previous observations, no accumulation of peptidyl-tRNA was significantly detected when *tnaC* W25 mRNA was translated irrespective of the presence of absence of exogenously added L-Trp (Figure 22A). This result argued against the idea that tryptophanyl-tRNA^{Trp} in the A-site substituted for free L-Trp bound at a specific ribosomal site required for translation arrest.

Figure 22. Tryptophanyl-tRNA^{Trp} as an inducer. (**A**) Autoradiogram showing *in vitro* accumulation of TnaC-tRNA^{Pro} performed with cell-free extracts containing ribosomes with the indicated 23S rRNAs. The indicated *tnaC* mRNAs variants were translated adding (High) or not (Low) an extra 4 mM L-Trp to the reactions. TnaC-tRNA^{Pro} and TnaC band positions are indicated with arrows. (**B**) Toeprinting assays performed with *in vitro* translation reactions. The indicated *tnaC* mRNAs variants were translated using wild type cell-free extracts and variable concentrations of L-Trp. The TnaC peptide sequence and the *tnaC* codon sequence for both mRNA variants are shown on the left side of each figure. The positions of stalled ribosomes are shown with boxes in the *tnaC* codon sequence and with arrows in the right side of the autoradiograms. (**C**) β-galactosidase activity obtained from cultures of bacterial cells (*rrn*+) carrying a *tnaC-tnaA'-'lacZ* reporter gene containing the indicated *tnaC* variants. The cultures were grown in the presence (+Trp) or in absence (-Trp) of 100 μg/ml L-Trp.

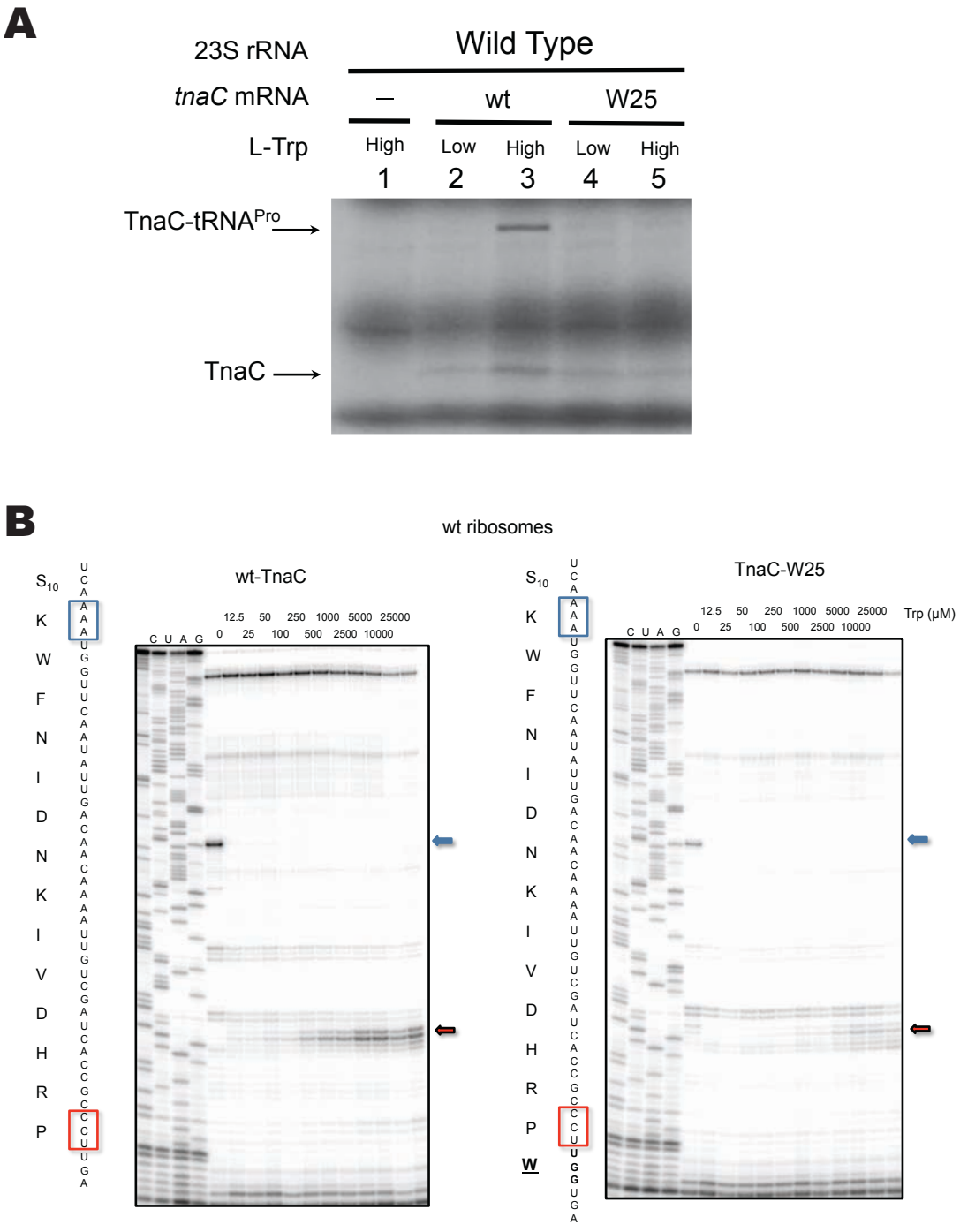
A
23S rRNA
Wild Type
tnaC mRNA
–
wt
W25
L-Trp
High
Low
High
Low
High
1
2
3
4
5
TnaC-tRNAPro
TnaC
B
wt ribosomes
wt-TnaC
TnaC-W25
S10
K
W
F
N
I
D
N
K
I
V
D
H
R
P
W
C U A G
12.5 50 250 1000 5000 25000
0 25 100 500 2500 10000
Trp (μM)

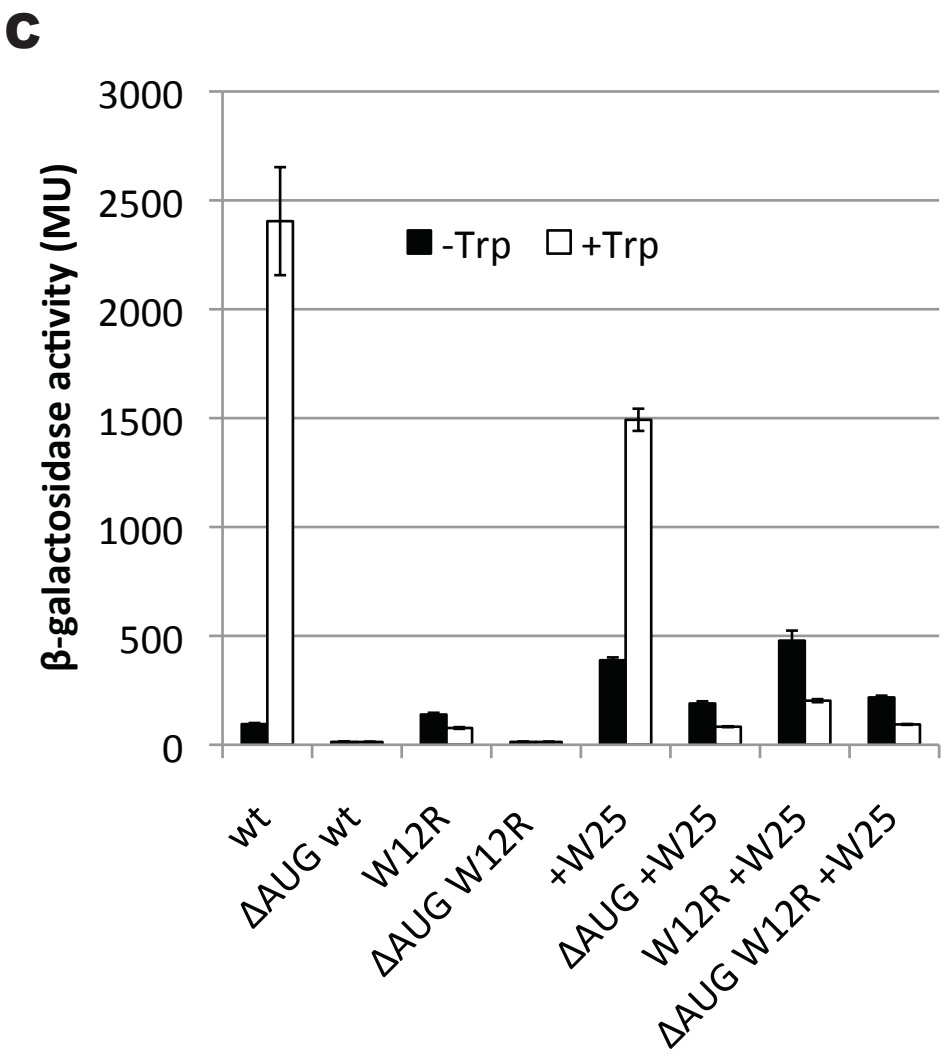

Figure 22. Continued.

To further verify this negative result we used *in vitro* toe-printing as an alternative independent approach (Figure 22B). If tryptophanyl-tRNA^{Trp} in the A-site can substitute for the role of free L-Trp in stalling, then even at the minimal L-Trp concentrations sufficient to bypass the W12 codon, ribosomes translating W25 mRNAs would stall at the Pro24 codon. Strikingly, however, ribosomes stalled at Pro24 of *tnaC*

W25 mRNA were nearly undetectable at low concentrations of Trp. This result indicates that binding of tryptophanyl-tRNA^{Trp} in the A-site of the ribosome that carries TnaC-tRNA^{Pro} in the P-site does not induce translation arrest. Furthermore, even at high concentrations of L-Trp, ribosomes translating *tna*C W25 mRNA stalled less efficiently than those translating wild type *tna*C ORF, confirming that addition of an extra Trp codon at the end of the *tnaC* ORF, not only fails to rescue Trp-independent stalling, but is even detrimental for Trp-induced translation arrest.

We further verified the *in vitro* results indicating that TnaC W25 does not induce ribosome arrest in the absence of L-Trp by following the *in vivo* Trp-mediated expression of *tnaA* in bacteria containing *tnaC tnaA'-'lacZ* reporter constructs with several changes in its *tnaC* sequence. As seen in Figure 22C, the *tnaC* W25 construct retained the L-Trp dependence confirming that the A-site bound tryptophanyl-tRNA^{Trp} does not substitute for binding of free L-Trp to the ribosome as a stalling cofactor. Elimination of the *tna*C start codon (ΔAUG) or the W12R replacement in the TnaC sequences eliminated the L-Trp-dependent induction in the expression of both the wild type and the W25 reporter genes. Combined, the results of *in vitro* and *in vivo* experiments argue that the A-site bound Trp-tRNA^{Trp} does not substitute for binding of free L-Trp to the ribosome suggesting that free L-Trp binding site does not coincide with the position of the Trp moiety of aminoacyl-tRNA in the PTC A-site. Accordingly, the possibility that the L-Trp binding site is not in the PTC, but in the exit tunnel is consistent with our data in which Trp placed at the PTC does not induce stalling.

DISCUSSION

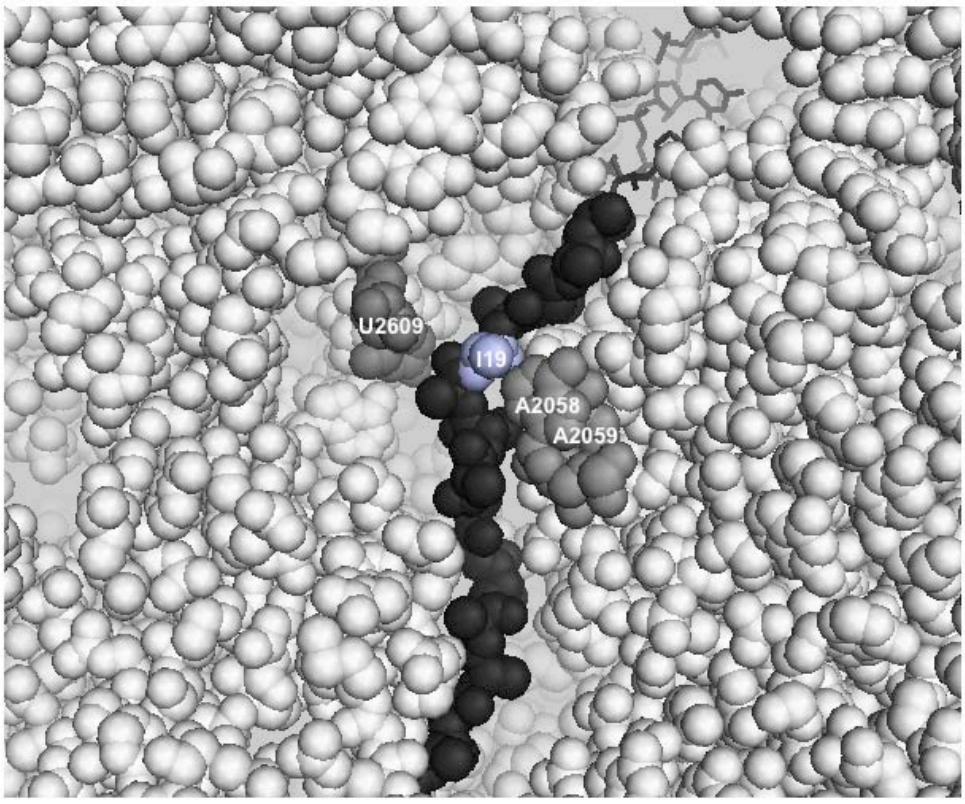

Figure 23. Model of the 50S ribosomal subunit bound to a TnaC-tRNA^{Pro} molecule. This model, obtained by Seidelt *et al*., shows the TnaC nascent peptide (dark-gray balls) within the peptide exit tunnel (43). The 23S rRNA nucleotides (light-gray balls), proposed by Trabuco *et al.*, that could contact the TnaC residue I19 (light blue balls) are shown as well. The 3'end segment of the tRNA^{Pro} (dark-gray sticks) is shown at the PTC P-site (38).

In this study we present genetic and biochemical evidence for a functional interaction between the regulatory nascent TnaC peptide and the ribosome in modulating the affinity of the ribosome for free L-Trp, the crucial cofactor in TnaC-mediated translational arrest. Mutations of either the 23S rRNA nucleotides A2058 or A2059, or

the TnaC residue I19, affect the response of translational arrest to the L-Trp concentration. Importantly, however, the TnaC I19L substitution specifically suppresses the effect of the 23S rRNA A2058U mutation that reduces the affinity of the TnaC-$tRNA^{Pro}$-ribosome complex for free L-Trp, arguing that the ribosome and the RAP cooperate in controlling properties of the L-Trp binding site. Indeed, both cryo-EM and molecular dynamics analyses suggested that the 23S rRNA residues A2058 and A2059 are in close proximity to TnaC residue I19 and thus may serve as interacting partners in modulating L-Trp binding or retention in the ribosome (Figure 23) (38,43).

Although previous data suggested that the free L-Trp binding site could coincide with the placement of the tryptophanyl moiety of Trp-$tRNA^{Trp}$ bound in the ribosomal A-site, re-evaluating the previous experiments using more natural conditions and alternative approaches suggest that Trp-$tRNA^{Trp}$ cannot substitute for free L-Trp (68). This, by no means, excludes the formal possibility of binding of free L-Trp in the PTC, but raises the possibility of other interpretations. One possibility is that the L-Trp binding site is formed at the site of interaction of the 23S rRNA nucleotides A2058 and A2059 with TnaC, once the I19 residue reaches these two nucleotides (Figure 23). This model, however, would presume that L-Trp binding at this site is extremely short-lived, because its lifespan would be limited by the addition of P24 at the C-terminus of the nascent peptide, and peptide release upon binding of the release factor RF2. An alternative, more attractive possibility is that the L-Trp binding site is formed by the residues A2058 and A2059, whereas the nascent peptide modulates the retention (dissociation rate) of L-Trp at this site. The A2058 and A2059 nucleotides form a

hydrophobic crevice in the exit tunnel where a number of ribosome-targeting antibiotics bind, including macrolides that also serve as cofactors of translational arrest mediated by leader peptides of various *erm* genes (91,103,105). Perhaps the hydrophobic planar side chain of L-Trp could be drawn into the crevice, possibly intercalating between the two adenine bases. We should note, however, that we did not observe any significant changes in reactivity of the A2058 and A2059 residues of the vacant *E. coli* ribosome to the modifying reagent dimethylsufate, even at high (5 mM) concentration of L-Trp (Klepacki and Vázquez-Laslop, unpublished results).

Alternatively, specific interactions between 23S rRNA nucleotides A2058 and A2059 and TnaC residue I19 may allosterically induce the formation of the L-Trp binding site at the PTC or another ribosomal location. Biophysical analyses suggest that residues of nascent peptides within the exit tunnel region constituted by the nucleotides A2058 and A2059 are constricted to their possible spatial conformations, inducing specific interactions between nascent peptides and the exit tunnel (106). Once specific contacts between I19 of TnaC and tunnel adenines are established, the stalling signal may be relayed to the L-Trp binding site via the nascent peptide, the ribosome, or both. Relaying the conformational change from the tunnel to the PTC has been proposed for other cases of peptide-mediated translational arrest (7,12,43,107). Such a possibility would be compatible with the observation that L-Trp competes with the PTC-targeting antibiotic sparsomycin for binding to the ribosome (84). In fact, another hydrophobic crevice, formed by A2451 and C2452 in the PTC is used as a binding site by a number of antibiotic molecules (103). The properties of this crevice and its putative affinity for

L-Trp could be affected by events occurring in the exit tunnel, involving the interactions between the 23S rRNA nucleotides A2058 and A2059 and the TnaC residue I19.

Regardless of the actual location of the ribosomal binding site for free L-Trp, our results clearly establish that direct interactions between the regulatory nascent TnaC peptide and the elements of the exit tunnel modulate the affinity of the ribosome for L-Trp.

CHAPTER IV

A COMBINED SELECTION AND SCREENING APPROACH FOR IDENTIFYING MUTATIONS THAT CAN RESTORE THE L-TRP DEPENDENT RIBOSOME ARREST FUNCTION TO THE LOSS-OF-FUNCTION TNAC(D16E) MUTANT

INTRODUCTION

The *tnaCAB* operon of *Escherichia coli* encodes the genes required for the catabolism of L-Trp (23). The two structural genes of the operon *tnaA* and *tnaB* encode tryptophanase and an L-Trp-specific permease, respectively (21,96). Tryptophanase catalyzes the breakdown of L-Trp into pyruvate, ammonia, and indole (23). Pyruvate and ammonia are used by the cell as carbon and nitrogen sources, respectively, while indole is a volatile signaling molecule that can function in quorum sensing and biofilm formation (24,25). The expression of *tnaA* and *tnaB* is regulated by elements within the 5'-leader region of the operon that includes *tnaC*, which encodes the 24 amino acid ribosome arrest peptide (RAP) TnaC. In combination with the other regulatory elements of the 5'-leader region, TnaC regulates read-through transcription into the structural genes by an attenuation of transcription mechanism (21,96). Transcription initiation of *tnaCAB* is controlled by catabolite repression, occurring upon cAMP/CAP binding at the promoter (27). Continuation of transcription into the structural genes is regulated by TnaC-mediated ribosome arrest in response to free L-Trp (1).

In the absence of inducing levels of L-Trp, translating ribosomes terminate after synthesis of TnaC, releasing the nascent peptide and ribosomal subunits from the

mRNA. The absence of ribosomes at the end of *tnaC* allows binding of the transcription termination factor Rho to its *rut*-binding site, which is immediately downstream of the *tnaC* coding sequence. Rho can then interact with paused RNA polymerase, promoting premature transcription termination before *tnaA* and *tnaB* are transcribed (1,29,32,96). In the presence of inducing levels of L-Trp, translation termination is inhibited after synthesis of TnaC, causing the ribosome to stall at the *tnaC* stop codon. The stalled ribosome blocks Rho's access to its *rut*-binding site; therefore, transcription is able to continue into the structural genes of the operon (1,29,32,96).

TnaC-mediated stalling requires elements of both the nascent peptide and of the ribosome. Changes at specific positions of the TnaC peptide or of specific elements of the large ribosomal subunit, the 23S rRNA or ribosomal proteins L4 and L22, abolish TnaC-mediated stalling in response to L-Trp. The TnaC peptide has three highly conserved residues: W12, D16, and P24, each of which has a functional role in ribosome arrest induced by TnaC (30,31,36,68,96). Structural analyses have revealed possible interactions between these functional residues of TnaC and elements constituting the peptidyl transferase center (PTC) or exit tunnel of the ribosome (38,43). The specific ribosomal elements that are predicted to interact with the crucial TnaC residues also have a functional role in TnaC-mediated arrest (44,45,64,99). However, due to a lack of genetic and biochemical analyses on the functionality of the interactions between the TnaC peptide and ribosomal components, how the TnaC peptide, ribosomal components, and L-Trp work in concert to facilitate the stalling of the ribosome is still unclear. Identifying either *cis*-acting mutations to the TnaC peptide or *trans*-acting mutations to

ribosomal components that restore the ability of loss-of-function TnaC mutants to induce ribosome arrest in response to L-Trp may provide the missing details of the interplay between the ribosome and the TnaC peptide that leads to ribosome stalling.

To this end, we used a combined forward genetic selection and screening approach to isolate and identify mutations that suppress the inability of a specific amino acid substitution in TnaC, D16E, to induce ribosome arrest. A screen had been previously developed by Nakatogawa and Ito using a translational *lacZ* fusion to the stalling sequence of the RAP SecM, that after mutagenesis allowed screening for mutations that alleviated SecM-mediated stalling (12). However, this method could not be used for TnaC due to the requirements for other regulatory elements outside of the *tnaC* coding sequence within the 5'-leader region of the *tnaCAB* transcript. Therefore, to maintain all of the required regulatory elements within the *tnaCAB* 5'-leader region a translational fusion was created between *tnaA* and *lacZ* for our studies. Also, while Nakatogawa and Ito were able to see a dramatic difference in the color of colonies grown on plates containing the chromogenic substrate, 5-bromo-4-chloro-3-indolyl-β-D-galactopyranoside (X-gal), such that white colonies were produced by strains in which the ribosome was capable of stalling at the SecM stalling sequence and blue colonies were produced by strains in which ribosome arrest at the SecM stalling sequence was alleviated, such a drastic difference in colony color on X-gal containing plates was not observed with our *tnaC-tnaA'-'lacZ* constructs (12). Instead of using a color screening approach, we took advantage of the *tnaA'-'lacZ* translational fusion as well as the presence of the other genes of the *lac* operon, *lacY* and *lacA*, in our constructs to create a

combined forward genetic selection and screening approach for the identification of mutations that restore Trp-inducibility to loss-of-function TnaC mutants. Using this method we isolated both *cis*-acting and *trans*-acting mutations (in addition to true revertants) that restored Trp-inducibility to the nonfunctional TnaC(D16E) mutant and characterized the *cis*-acting second-site mutations for their effects on *tnaC-tnaA*'-'*lacZ* reporter expression.

MATERIALS AND METHODS

Bacteria strains and plasmids

The *E. coli* K-12 strains and plasmids containing selected genes used in this study are listed in Table 7. Bacteria strains containing mutant variants of the *tnaA'-'lacZ* reporter genes and mutant variants of the 23S RNA gene were made as previously described (99).

Table 7. *E.coli* bacterial plasmids and strains used in this work.

Strains	Relevant genotype	Source
MB4091	DH10B *E.coli* cells containing pKD46	(108)
AW122	Derived from SQ351 (p*rrnC-sacB*, ptRNA67)	(99)
AW153	MG1655 Δ(*lacZYA*) *att7*::*tna*$_p$*tnaC*(*tnaA*'-'*lacZYA*)	(99)
AW154	MG1655 Δ(*lacZYA*) *att7*::*tna*$_p$*tnaC*(*W12R*)(*tnaA*'-'*lacZYA*)	(99)

Table 7. Continued

Strains	Relevant genotype	Source
AW182	MG1655 Δ7 *rrn* Δ(*lacZYA*) *att7*::*tna*$_p$*tnaC*(*tnaA*'-'*lacZYA*) (p*rrnC-sacB*, ptRNA67)	(99)
AW216	MG1655 Δ7 *rrn* Δ(*lacZYA*) *att7*::*tna*$_p$*tnaC*(*tnaA*'-'*lacZYA*) (pNK, ptRNA67)	(99)
AW218	MG1655 Δ7 *rrn* Δ(*lacZYA*) *att7*::*tna*$_p$*tnaC*(*tnaA*'-'*lacZYA*) (pNH2609, ptRNA67)	(99)
AW227	MG1655 Δ7 *rrn* Δ(*lacZYA*) *att7*::*tna*$_p$*tnaC*(*tnaA*'-'*lacZYA*) (pNH153, ptRNA67)	(99)
AW513	MG1655 Δ(*lacZYA*) *att7*::*tna*$_p$*tnaC*(*D16A*)(*tnaA*'-'*lacZYA*)	(99)
AW643	MG1655 Δ(*lacZYA*) *att7*::*tna*$_p$*tnaC*(*ΔAUG*)(*tnaA*'-'*lacZYA*)	This study
AW673	MG1655 Δ7 *rrn* Δ(*lacZYA*) *att7*::*tna*$_p$*tnaC*(*tnaA*'-'*lacZYA*) (pNK-A2058U, ptRNA67)	This study
AW675	MG1655 Δ7 *rrn* Δ(*lacZYA*) *att7*::*tna*$_p$*tnaC*(*tnaA*'-'*lacZYA*) (pNK-A2059U, ptRNA67)	This study
AW676	MG1655 Δ7 *rrn* Δ(*lacZYA*) *att7*::*tna*$_p$*tnaC*(*tnaA*'-'*lacZYA*) (pNK-A2059G, ptRNA67)	This study
AW677	MG1655 Δ7 *rrn* Δ(*lacZYA*) *att7*::*tna*$_p$*tnaC*(*tnaA*'-'*lacZYA*) (pNK-A2059C, ptRNA67)	This study
AW680	MG1655 Δ7 *rrn* Δ(*lacZYA*) *att7*::*tna*$_p$*tnaC*(*tnaA*'-'*lacZYA*) (pNK-A2058G, ptRNA67)	This study
AW741	Derived from MB4091 with *tna* operon:::Cam^R	(99)
AW797	MG1655 Δ(*lacZYA*) *att7*::*tna*$_p$*tnaC*(*D16K*)(*tnaA*'-'*lacZYA*)	This study
AW819	MG1655 Δ7 *rrn* Δ(*lacZYA*) Δ(*tnaCAB*) *att7*::*tna*$_p$*tnaC*(*tnaA*'-'*lacZYA*) (*prrnC-sacB*, ptRNA67)	This study
AW821	MG1655 Δ(*lacZYA*) *att7*::*tna*$_p$*tnaC*(*D16E*)(*tnaA*'-'*lacZYA*)	This study
AW822	MG1655 Δ7 *rrn* Δ(*lacZYA*) *att7*::*tna*$_p$*tnaC*(*D16E*)(*tnaA*'-'*lacZYA*) (p*rrnC-sacB*, ptRNA67)	This study
AW834	MG1655 Δ7 *rrn* Δ(*lacZYA*) *att7*::*tna*$_p$*tnaC*(*D16E*)(*tnaA*'-'*lacZYA*) (pNK, ptRNA67)	This study
AW839	MG1655 Δ7 *rrn* Δ(*lacZYA*) *att7*::*tna*$_p$*tnaC*(*tnaA*'-'*lacZYA*) (pNK-A752C, ptRNA67)	(99)

Table 7. Continued

Strains	Relevant genotype	Source
AW845	MG1655 Δ7 *rrn* Δ(*lacZYA*) Δ(*tnaCAB*) *att7*::*tna*$_p$*tnaC*(*D16E*)(*tnaA*'-'*lacZYA*) (p*rrnC-sacB*, ptRNA67)	This study
AW854	Derived from AW845 *att7*::*tna*$_p$*tnaC*(*D16E*)(*tnaA*'-'*lacZYA*) (*prrnC-sacB*, ptRNA67)	This study
AW855	Derived from AW845 *att7*::*tna*$_p$*tnaC*(*D16E/R23S*)(*tnaA*'-'*lacZYA*) (p*rrnC-sacB*, ptRNA67)	This study
AW856	Derived from AW845 *att7*::*tna*$_p$*tnaC*(*D16E/R23S*)(*tnaA*'-'*lacZYA*) (p*rrnC-sacB*, ptRNA67)	This study
AW857	Derived from AW845 *att7*::*tna*$_p$*tnaC*(*D16E*)(*tnaA*'-'*lacZYA*) (p*rrnC-sacB*, ptRNA67)	This study
AW858	Derived from AW845 *att7*::*tna*$_p$*tnaC*(*tnaA*'-'*lacZYA*) (p*rrnC-sacB*, ptRNA67)	This study
AW859	Derived from AW845 *att7*::*tna*$_p$*tnaC*(*S10P/D16E*)(*tnaA*'-'*lacZYA*) (p*rrnC-sacB*, ptRNA67)	This study
AW860	Derived from AW845 *att7*::*tna*$_p$*tnaC*(*tnaA*'-'*lacZYA*) (p*rrnC-sacB*, ptRNA67)	This study
AW861	Derived from AW845 *att7*::*tna*$_p$*tnaC*(*S10P/D16E*)(*tnaA*'-'*lacZYA*) (*prrnC-sacB*, ptRNA67)	This study
AW862	Derived from AW845 att7::*tna*$_p$*tnaC*(*tnaA*'-'*lacZYA*) (*prrnC-sacB*, ptRNA67)	This study
AW863	Derived from AW845 *att7*::*tna*$_p$*tnaC*(*tnaA*'-'*lacZYA*) (p*rrnC-sacB*, ptRNA67)	This study
AW864	Derived from AW845 *att7*::*tna*$_p$*tnaC*(*tnaA*'-'*lacZYA*) (p*rrnC-sacB*, ptRNA67)	This study
AW865	Derived from AW845 *att7*::*tna*$_p$*tnaC*(*tnaA*'-'*lacZYA*) (p*rrnC-sacB*, ptRNA67)	This study
AW869	Derived from AW845 *att7*::*tna*$_p$*tnaC*(*D16E/R23H*)(*tnaA*'-'*lacZYA*) (p*rrnC-sacB*, ptRNA67)	This study
AW888	MG1655 Δ(*lacZYA*) *att7*::*tna*$_p$*tnaC*(*S10P*)(*tnaA*'-'*lacZYA*)	This study
AW909	MG1655 Δ(*lacZYA*) *att7*::*tna*$_p$*tnaC*(*S10P/D16E*)(*tnaA*'-'*lacZYA*)	This study

Table 7. Continued

Strains	Relevant genotype	Source
AW922	MG1655 Δ(*lacZYA*) *att7*::*tna*$_p$*tnaC*(*R23H*)(*tnaA*'-'*lacZYA*)	This study
AW925	MG1655 Δ(*lacZYA*) *att7*::*tna*$_p$*tnaC*(*D16E/R23H*)(*tnaA*'-'*lacZYA*)	This study
AW930	MG1655 Δ(*lacZYA*) *att7*::*tna*$_p$*tnaC*(*S10P/D16K*)(*tnaA*'-'*lacZYA*)	This study
AW933	MG1655 Δ(*lacZYA*) *att7*::*tna*$_p$*tnaC*(*S10P/W12R*)(*tnaA*'-'*lacZYA*)	This study
AW940	MG1655 Δ(*lacZYA*) *att7*::*tna*$_p$*tnaC*(*S10PΔAUG*)(*tnaA*'-'*lacZYA*)	This study
AW946	MG1655 Δ(*lacZYA*) *att7*::*tna*$_p$*tnaC*(*D16EΔAUG*)(*tnaA*'-'*lacZYA*)	This study
AW949	MG1655 Δ(*lacZYA*) *att7*::*tna*$_p$*tnaC*(*S10P/D16EΔAUG*)(*tnaA*'-'*lacZYA*)	This study
AW952	MG1655 Δ(*lacZYA*) *att7*::*tna*$_p$*tnaC*(*S10P/D16A*)(*tnaA*'-'*lacZYA*)	This study
AW955	MG1655 Δ(*lacZYA*) *att7*::*tna*$_p$*tnaC*(*D16K/R23H*)(*tnaA*'-'*lacZYA*)	This study
AW958	MG1655 Δ(*lacZYA*) *att7*::*tna*$_p$*tnaC*(*W12R/R23H*)(*tnaA*'-'*lacZYA*)	This study
AW961	MG1655 Δ(*lacZYA*) *att7*::*tna*$_p$*tnaC*(*R23HΔAUG*)(*tnaA*'-'*lacZYA*)	This study
AW965	MG1655 Δ(*lacZYA*) *att7*::*tna*$_p$*tnaC*(*D16A/R23H*)(*tnaA*'-'*lacZYA*)	This study
AW967	MG1655 Δ7 *rrn* Δ(*lacZYA*) *att7*::*tna*$_p$*tnaC*(*S10P*)(*tnaA*'-'*lacZYA*) (pNK-A752, ptRNA67)	This study
AW968	MG1655 Δ7 *rrn* Δ(*lacZYA*) *att7*::*tna*$_p$*tnaC*(*S10P*)(*tnaA*'-'*lacZYA*) (pNH153, ptRNA67)	This study
AW969	MG1655 Δ7 *rrn* Δ(*lacZYA*) *att7*::*tna*$_p$*tnaC*(*S10P*)(*tnaA*'-'*lacZYA*) (pNH2609, ptRNA67)	This study
AW970	MG1655 Δ7 *rrn* Δ(*lacZYA*) *att7*::*tna*$_p$*tnaC*(*S10P)*(*tnaA*'-'*lacZYA*) (pNK-A2059C, ptRNA67)	This study
AW973	MG1655 Δ(*lacZYA*) *att7*::*tna*$_p$*tnaC*(*D16E/R23HΔAUG*)(*tnaA*'-'*lacZYA*)	This study

Table 7. Continued

Strains	Relevant genotype	Source
AW974	MG1655 Δ7 *rrn* Δ(*lacZYA*) *att7*::*tna*$_p$*tnaC*(*S10P*)(*tnaA*'-'*lacZYA*) (pNK-A2059G, ptRNA67)	This study
AW975	MG1655 Δ7 *rrn* Δ(*lacZYA*) *att7*::*tna*$_p$*tnaC*(*S10P*)(*tnaA*'-'*lacZYA*) (pNK-A2059U, ptRNA67)	This study
AW976	MG1655 Δ7 *rrn* Δ(*lacZYA*) *att7*::*tna*$_p$*tnaC*(*S10P*)(*tnaA*'-'*lacZYA*) (pNK-A2058U, ptRNA67)	This study
AW977	MG1655 Δ7 *rrn* Δ(*lacZYA*) *att7*::*tna*$_p$*tnaC*(*S10P*)(*tnaA*'-'*lacZYA*) (pNK, ptRNA67)	This study
AW978	MG1655 Δ7 *rrn* Δ(*lacZYA*) *att7*::*tna*$_p$*tnaC*(*R23H*)(*tnaA*'-'*lacZYA*) (pNK-A2059C, ptRNA67)	This study
AW979	MG1655 Δ7 *rrn* Δ(*lacZYA*) *att7*::*tna*$_p$*tnaC*(*R23H*)(*tnaA*'-'*lacZYA*) (pNK-A2059G, ptRNA67)	This study
AW980	MG1655 Δ7 *rrn* Δ(*lacZYA*) *att7*::*tna*$_p$*tnaC*(R23H)(*tnaA*'-'*lacZYA*) (pNK-A2059U, ptRNA67)	This study
AW981	MG1655 Δ7 *rrn* Δ(*lacZYA*) *att7*::*tna*$_p$*tnaC*(R23H)(*tnaA*'-'*lacZYA*) (pNK-A2058G, ptRNA67)	This study
AW982	MG1655 Δ7 *rrn* Δ(*lacZYA*) *att7*::*tna*$_p$*tnaC*(*R23H*)(*tnaA*'-'*lacZYA*) (pNK-A752C, ptRNA67)	This study
AW983	MG1655 Δ7 *rrn* Δ(*lacZYA*) *att7*::*tna*$_p$*tnaC*(*R23H*)(*tnaA*'-'*lacZYA*) (pNH153, ptRNA67)	This study
AW984	MG1655 Δ7 *rrn* Δ(*lacZYA*) *att7*::*tna*$_p$*tnaC*(*R23H*)(*tnaA*'-'*lacZYA*) (pNH2609, ptRNA67)	This study
AW985	MG1655 Δ7 *rrn* Δ(*lacZYA*) *att7*::*tna*$_p$*tnaC*(*R23H*)(*tnaA*'-'*lacZYA*) (pNK, ptRNA67)	This study

Table 7. Continued

Strains	Relevant genotype	Source
AW986	MG1655 Δ7 *rrn* Δ(*lacZYA*) *att7*::*tna*$_p$*tnaC*(*S10P*)(*tnaA*'-'*lacZYA*) (pNK-A2058G, ptRNA67)	This study
AW987	MG1655 Δ7 *rrn* Δ(*lacZYA*) *att7*::*tna*$_p$*tnaC*(*R23H*)(*tnaA*'-'*lacZYA*) (pNK-A2058U, ptRNA67)	This study
Plasmids	**Description**	**Source**
pKD3	Template plasmid for gene disruption	(109)
pKD46	Lambda red recombinase plasmid	(109)
ptRNA67	tRNA encoding plasmid	(76)
p*rrnC-sacB*	Wild-type *rrnC* operon; Km^r, and a *sacB* gene, derived from pCS101	(76)
pNK	Wild-type *rrnB* operon; Amp^r, derived from ColE1	(12)
pAW137	Has the *tna*$_p$*tnaC(ΔN2-H22)* with BsaI-XhoI-BsaI linker-*tnaA'-'lacZYA* cloning reporter gene derived from pACYC184	(99)
pAW627	*tnaC-tnaA'-* cloned into pUC18 BamHI site	This study
pAW629	Derived from pAW627, start codon of *tnaC* changed to stop codon (ATG -> TGA)	This study

Creation of the *tnaA'-'lacZ* reporter gene at the *att7* site

Creation of the *tnaA'-'lacZ* reporter genes at the *att7* site was carried out as previously described (99).

tna operon deletion

The *cat* gene from pKD3 was amplified with forward primer, AW269, that contained 50 base pairs of homology from the endogenous *tna* locus of *E.coli* MG1655 from -290 to -240 nucleotides upstream of *tnaC* and reverse primer, AW270, that contains 50 base pairs of homology from 150-200 nucleotides downstream of *tnaB*. The resulting PCR product was used to transform MB4091 cells by electroporation. Transformants were selected for growth on LB containing 25μg/ml chloramphenicol. Transformants were screened to ensure replacement of the *tna* operon by the Cam-cassette using colony PCR and Ehrlich's reagent addition to over night cultures. The resulting strain was designated AW741.

The *tna* operon:::Cam^R loci was transduced to recipient strains containing *tnaC-tnaA'-'lacZYA* (either wild type or mutant versions of *tnaC*) at the att7 locus of AW122 using P1 transduction with $P1_{virAW741}$. P1 lysate preparation and transduction were carried out as previously described (79).

Selection for suppressors that restore induction to TnaC D16E uninducible mutant

Strain AW845 was grown overnight in VB minimal medium plus 0.2% glucose, 0.05% acid-hydrolyzed casein, 0.01% vitamin B1 and 25 μg/ml kanamycin. Cultures were washed once in VB without any supplements and 100 μl of washed culture was plated on VB minimal medium supplemented with 1% lactose, 100 μg/ml Trp, 0.05% acid-hydrolyzed casein, 0.01% vitamin B1 and 25 μg/ml kanamycin. Plates were incubated at 37°C for 6 days. Colonies that formed were picked and each colony was

grown overnight in VB minimal medium plus 0.2% glucose, 0.05% acid-hydrolyzed casein, 0.01% vitamin B1 and 25 μg/ml kanamycin. Mutations that restore induction to the uninducible TnaC(D16E) mutant were desired, so these cultures were screened for Trp inducibility. Overnight cultures were replica plated onto VB plates supplemented with 1% lactose, 0.05% acid-hydrolyzed casein, 0.01% vitamin B1 and 25 μg/ml kanamycin, with or without 100 μg/ml Trp. Those colonies that either grew on the Trp containing plate and not at all on the plate lacking Trp, or those that grew better on the Trp containing plate than they did on the plate lacking Trp were selected for further analysis by Miller Assay. Out of the 1152 total colonies screened by replica plating, 111 showing differential growth were analyzed by Miller Assay of exponentially growing cultures to determine if the LacZ reporter was inducible by Trp. Out of the 111, 13 were confirmed to be inducible by Trp in three independent experiments. To analyze the expression of the *tnaA'-'lacZ* reporter gene Miller assays were performed as described(79). β-gal activity is reported in Miller units.

Sequencing of *tna*$_p$*tnaC-tnaA'-'lacZ* region to identify *cis*-acting mutations that suppress uninducible TnaC(D16E) mutant

The *tna*$_p$*tnaC-tnaA'-'lacZ* region at the *att7* site was first amplified from mutant strains using primers Att7F: 5'-GCGGCGACAACAGTTGCGACGGTGGTACG-3' and AW111: 5'-GCGGTTTTCTCCGGCGCGTAAAAATGCGCTCAGG-3', and the resulting PCR product was sequenced using M13F-200: 5'-CCATTCGCCATTCAGGCTGCGCAAC-3'.

Recreation of second site mutations within TnaC(D16E)

To recreate the D16E/S10P double mutant and the S10P single mutant, annealed oligonucleotides were used to insert TnaC(S10P/D16E) or TnaC(S10P) sequences into pAW137. Synthetic oligonucleotides AW297 and AW298 were used for TnaC(S10P/D16E) and AW299 and AW300 were used for TnaC(S10P). Creation of the *tnaA'-'lacZ* reporter genes at the *att7* site was carried out as previously described (99). To make the D16E/R23H double mutant and the R23H single mutant pAW627 was used as a template for site-directed mutagenesis. Primers AW303 and AW304 were first used to make the R23H change and then primers AW305 and AW306 were used to make the D16E change for the double mutant. The resulting *tnaC-tnaA*'- region was cloned from pUC18 into pRS552 as a BamHI fragment which creates an in-frame translational fusion between *tnaA'*- and -*'lacZ*. The *tnaC-tnaA*'-'*lacZYA* region from the pRS552 derivatives were cloned as SalI fragments into XhoI digested pGRG36. The pGRG36 derivatives were then used for integration at the *att7* site as described previously {McKenzie, 2006 #26;Martinez, 2012 #90}.

Identification of *trans*-acting rRNA mutations that suppress uninducible TnaC(D16E) mutant

To determine whether *trans*-acting mutations were within the rRNA, the p*rrnC-sacB* plasmids were prepared from strains AW854 and AW857. The resulting plasmids were designated pAW854 and pAW857, respectively. pAW854 and pAW857 were transformed into chemically competent AW834 cells and transformants were selected on

LB plates containing 25 μg/ml kanamycin. Two independent transformants from each transformation were selected and subcultured every 12 hours for 72 hours in LB broth containing 25 μg/ml kanamycin. Dilutions of each of the final cultures were plated on LB plates containing 25 μg/ml kanamycin. Resulting colonies were replica plated on LB plates containing either 25 μg/ml kanamycin or 100 μg/ml ampicillin to ensure eviction of pNK and maintenance of pAW854 or pAW857. The resulting strains were designated AW870, AW871, AW872, and AW873. Likewise, pNK was transformed into chemically competent AW854 and AW857 cells. Transformants were selected on LB plates containing 100 μg/ml ampicillin. Two independent transformants of each were selected and cultured overnight in LB broth containing 100 μg/ml ampicillin. Dilutions of the overnight cultures were plated on LB plates containing 5% sucrose, which selects against the p*rrnC-sacB* derived plasmids (pAW854 and pAW857). Resulting colonies were replica plated on LB plates containing either 25 μg/ml kanamycin or 100 μg/ml ampicillin to ensure eviction of p*rrnC-sacB* derived plasmids and maintenance of pNK. The resulting strains were designated AW874, AW875, AW876, and AW877.

After verifying by Miller Assay that the *trans*-acting mutation that conferred Trp-inducibility to the TnaC(D16E) mutant was on the p*rrnC-sacB* plasmids of AW854 and AW857, the *rrnC* operon from pAW854 and pAW857 were sequenced.

RESULTS

Suppressor mutations of the loss-of-function TnaC mutant D16E, were isolated using a combined selection and screen strategy

Considering the conservation and functional importance of D16, this amino acid of TnaC was chosen as a candidate for the combined selection and screen for mutations that could suppress non-functional D16 mutants. Nine different amino acid substitutions at this position abolish TnaC-mediated ribosome arrest in response to L-Trp, demonstrating the importance of this residue (31,39,99). The conservative loss-of-function mutation D16E was chosen for the selection for two reasons. First, the D16E mutation is the result of a single nucleotide change and therefore revertants should be readily obtained. Identification of revertants was used as a positive control to validate the combined selection and screen. Second, because of the importance of D16, we reasoned that it would be more likely to obtain suppressor mutations of D16E, because of the conservative nature of this change (i.e., it extends the side chain by a methylene group).

The strain used for this study has several important characteristics that make the combined selection and screen possible. First, the *tnaC*(*D16E*)-*tnaA*'-'*lacZYA* reporter operon is integrated site-specifically in a single copy in the chromosome. Second, the strain lacks the endogenous *tna* operon. Deleting the endogenous *tna* operon eliminates homologous recombination between the reporter operon and the endogenous *tna* operon, which could restore the wild-type *tnaC* sequence to the reporter operon. Finally, the strain has all seven of the rRNA operons deleted from the chromosome with a wild-type

rRNA operon supplied on a low copy plasmid. This gets rid of the requirement for dominant *trans*-acting suppressor mutations in the rRNA and also allows these mutations to be easily identified.

Strains that acquire a mutation that restores the ability of the D16E mutant to induce expression of the reporter *lac* operon in the presence of L-Trp, should be able to grow on minimal lactose medium containing L-Trp. Using the D16E strain to select for spontaneous mutations that confer growth on minimal lactose medium containing L-Trp, a total of 1152 individual colonies were isolated. Resulting colonies could either be the result of mutations that only confer growth on minimal lactose medium containing L-Trp or mutations that confer growth on minimal lactose medium independent of L-Trp. Since suppressor mutations that restored Trp-induction to D16E were desired, the 1152 colonies that resulted from the selection were screened by replica plating overnight cultures of each on minimal lactose medium with or without L-Trp. Colonies from the replica plates were chosen for further analysis if they met one of two criteria: 1) the colony grew on the plate containing L-Trp and not at all on the plate lacking L-Trp, or 2) the colony grew better on the plate containing L-Trp than it did on the plate lacking Trp.

A total of 111 colonies from the replica plates met the above criteria and were screened by Miller Assay. Out of these 111, 13 were confirmed to be $\geq$ 2-fold Trp-inducible by 3 independent experiments (Table 8). The leader region of the reporter operon from the 13 mutants was sequenced to determine if there were any mutations within TnaC. Based on the *tnaC* sequence, the mutants were divided into 4 classes (Table 9). Revertants were designated as class 1, *trans*-acting mutants were designated

as class 2, and two different *cis*-acting mutants were designated class 3 and class 4. Nearly half of the mutants were revertants, which shows that the combined selection and screening method is a powerful tool that can be used to identify mutations that can restore L-Trp-inducibility to the non-functional D16E mutant, or in principal any other non-functional TnaC mutant.

Table 8. Mutants isolated from growth on minimal lactose medium containing L-Trp selection that restore ≥2-fold Trp-induction to D16E.

Strain	β-galactosidase activity (MU)		Induction ratio (+Trp/-Trp)
	-Trp	+Trp	
Wild-type	8 ± 0	97 ± 8	12.1
D16E	10 ± 1	12 ± 0	1.2
D16E-4E9	66 ± 1	181 ± 4	2.7
D16E-6E11	114 ± 1	179 ± 3	1.6
D16E-6F7	184 ±14	255 ± 21	1.4
D16E-8H11	67 ± 1	181 ± 5	2.7
D16E-11F5	33 ± 4	993 ± 11	30.1
D16E-12A9	51 ± 3	135 ± 5	2.6
D16E-12F12	12 ± 0	550 ± 32	45.8
D16E-13D3	74 ±13	178 ± 19	2.4
D16E-16G12	11 ± 1	450 ± 29	40.9
D16E-17B6	16 ± 1	1021 ±170	63.8
D16E-17E2	30 ± 1	1114 ± 79	37.1
D16E-19G2	26 ± 0	1437 ± 70	55.3
D16E-23E6	64 ± 3	191 ± 4	3.0

[a]Cultures of Δ7 *rrn E. coli* bacterial strains AW819 (Wt), AW845 (D16E), AW854 (D16E-4E9), AW855 (D16E-6E11), AW856 (D16E-6F7), AW857 (D16E-8H11), AW858 (D16E-11F5), AW859 (D16E-12A9), AW860 (D16E-12F12), AW861 (D16E-13D3), AW862 (D16E-16G12), AW863 (D16E-17B6), AW864 (D16E-17E2), AW865 (D16E-19G2), and AW869 (D16E-23E6) were grown in minimal medium plus 0.2% glycerol, 0.05% acid-hydrolyzed casein, 0.01% vitamin B1, 25 μg/ml kanamycin, with (+Trp) or without (-Trp) 100 μg/ml Trp. β-Galactosidase assays were performed in three independent experiments .
[b]Ratio of values for cultures grown with Trp (+Trp) and those grown without Trp (-Trp).

Table 9. Four classes of mutants that restore ≥2-fold Trp-induction to D16E.

Class	Mutation	Strains
1	Revertant D16E -> D16	11F5, 12F12, 16G12, 17B6, 17E2, 19G2
2	Still D16E, no other change in TnaC	4E9, 8H11
3	S10P/D16E	12A9, 13D3
4	D16E/R23S/H	6E11, 6F7, 23E6

Trans-acting mutations

The two mutants in class 2 still have the D16E change within *tnaC* and do not have any other mutations within the *tna* leader region; therefore, the mutation in these strains that restore L-Trp-inducibility to the D16E peptide are *trans*-acting. Structural studies of the TnaC peptide within the ribosomal exit tunnel show that at the time of ribosome arrest D16 is at the constriction site formed by loops of r-proteins L4 and L22 (38,43). Biochemical analysis show that the non-functional D16A mutant fails to protect the 23S rRNA nucleotide U2609 from methylation which is also located near the constriction site (99). Based on the structural and biochemical analyses, we hypothesized that interactions between D16 and components of the ribosome exit tunnel contribute to the ability of the nascent TnaC peptide to respond to L-Trp and cause ribosome arrest, and that the side chain of D16 may be crucial for maintaining this interaction. Thus changes at this position would disrupt this required interaction abolishing ribosome arrest in response to L-Trp.

Due to the predicted position of D16 within the ribosomal exit tunnel we hypothesized that mutations to residues of r-proteins L4 or L22 or to the 23S rRNA within this region may be able to suppress the D16E change restoring L-Trp-mediated

ribosome arrest to the D16E containing nascent peptide. However, no mutations were identified in r-proteins L4 or L22 of the class 2 mutants. Since the rRNA operon in these strains is plasmid-encoded, the rRNA-containing plasmid from the class 2 mutants was replaced by a plasmid encoding a wild-type rRNA. With both of the class 2 mutants, when the plasmid encoding the wild-type rRNA replaced the original rRNA-containing plasmid, induction of the TnaC(D16E) reporter was abolished (data not shown). Also, the rRNA-containing plasmid from the class 2 mutants was used to replace the wild-type rRNA plasmid in a virgin D16E strain. In this case, the rRNA-containing plasmids from both of the class 2 mutants restored induction to the TnaC(D16E) reporter in the virgin D16E strain (data not shown). The results of these experiments suggest that the *trans*-acting mutation that suppresses the non-functional D16E mutation is plasmid-encoded. However, after sequencing the entire rRNA operon from both class 2 mutants, no mutations in this region of the plasmid were identified (data not shown). The nature of these plasmid-encoded *trans*-acting mutations is still unknown and may merely change copy number or expression levels.

C*is*-acting mutations at two different positions within TnaC restore inducibility to D16E

Mutations at two different positions within TnaC were found to suppress the non-functional D16E mutant. That is, in addition to still having the D16E mutation, the class 3 mutants have the second-site mutation S10P and the class 4 mutants have a second-site mutation at R23, either R23S or R23H. Both of the class 3 mutants (S10P/D16E double

mutants) are ~2.5-fold inducible in response to L-Trp (Table 8**)**. Within the class 4 mutants, the *cis*-acting R23S mutants are ~1.5-fold inducible in response to L-Trp and the R23H *cis*-acting mutant is ~3-fold inducible in response to L-Trp (Table 8**)**. Since we are interested in suppressors that restore ≥ 2-fold L-Trp-induction to D16E, the *cis*-acting S10P and R23H mutations will be the focus of the rest of this study.

The *cis*-acting mutations S10P and R23H suppress the loss-of-function TnaC mutant, D16E

To ensure that the second-site mutations within *tnaC* that were isolated from the selection, S10P and R23H, are responsible for restoring L-Trp-mediated ribosome arrest to D16E, strains containing reporter operons with the single S10P and R23H changes in *tnaC* and the double S10P/D16E and D16E/R23H mutations within *tnaC* were constructed. Both the S10P/D16E and D16E/R23H double mutant showed induction in response to L-Trp (~4-fold and ~2.4-fold respectively) (Table 10). These results suggest that either of the single amino acid changes, S10P or R23H, can restore the L-Trp dependent ribosome arrest function to the non-functional D16E mutant. Interestingly, both the S10P and R23H single mutants have high basal LacZ levels (~20-fold over wild-type TnaC basal LacZ levels) but still show a slight induction in response to L-Trp (~1.9-fold and ~1.4-fold, respectively) (Table 10).

Table 10. S10P and R23H are *cis*-acting mutations that suppress the loss-of-function D16E mutation.

Strain	β-galactosidase activity (MU)		Induction ratio (+Trp/-Trp)
	-Trp	+Trp	
Wild-Type	57 ± 2	2175 ± 274	38.2
D16E	38 ± 11	68 ± 25	1.8
S10P	1312 ± 290	2506 ± 244	1.9
R23H	1147 ± 40	1636 ± 317	1.4
S10P/D16E	138 ± 14	568 ± 137	4.1
D16E/R23H	192 ± 32	453 ± 10	2.4

[a]Cultures of *rrn*+ E. *coli* bacterial strains AW153 (Wt), AW821 (D16E), AW888 (S10P), AW922 (R23H), AW909 (D16E/S10P), and AW925 (D16E/R23H) were grown in minimal medium plus 0.2% glycerol, 0.05% acid-hydrolyzed casein, 0.01% vitamin B1, with (+Trp) or without (-Trp) 100 μg/ml Trp. β-Galactosidase assays were performed in three independent experiments . [b]Ratio of values for cultures grown with Trp (+Trp) and those grown without Trp (-Trp).

The constitutive expression of the *lacZ* reporter observed in the S10P and R23H constructs is translation dependent

Two different mechanisms can explain the high basal level of LacZ observed with the S10P and R23H mutants. The first possibility is that the changes at the nucleotide level affect the mRNA secondary structure or other regulatory elements leading to inefficient transcription attenuation in the absence of added L-Trp. The second possibility is that the mutant nascent peptides are causing ribosome arrest in the absence of added L-Trp. Constitutive ribosome arrest is translation-dependent and thus can be tested *in vivo* by eliminating translation of *tnaC* and preventing TnaC-mediated ribosome arrest. If the mutant nascent peptides cause constitutive ribosome arrest, in the absence of translation, premature transcription termination will occur both in the presence and absence of L-Trp leading to a dramatic decrease in LacZ levels under both conditions. To determine if the elevated basal level expression of LacZ in the S10P and

R23H mutants was dependent on the translation of the mutant nascent peptides we created reporter constructs in which the AUG start codon of TnaC was changed to a UGA stop codon (ΔAUG). The elimination of the start codon of wild-type and several mutant versions of *tnaC* dramatically reduce the expression of the *lacZ* reporter gene and eliminate Trp-mediated induction (32,99). As expected, elimination of the start codon of wild-type *tnaC* dramatically decreased the expression of *lacZ* both in the presence and absence of L-Trp, and L-Trp-dependent induction was abolished (Table 11 and 12). Elimination of the start codon of all of the TnaC mutants examined also decreased the expression of *lacZ* in both the presence and absence of L-Trp. In the absence of translation, the L-Trp-dependent induction of the S10P/D16E and D16E/R23H double mutants was also abolished (Table 11 and 12). These results suggest that the high basal level of LacZ observed with the S10P and R23H mutants is translation-dependent, which is consistent with the idea that these mutant nascent peptides cause ribosome arrest *in vivo* in the absence of added L-Trp.

Table 11. High basal LacZ level observed with S10P is translation-dependent.

Strain	β-galactosidase activity (MU)		Induction ratio (+Trp/-Trp)
	-Trp	+Trp	
Wild-type	45 ± 2	2028 ± 65	45.1
Wild-type (ΔAUG)	7 ± 1	7 ± 0	1.0
S10P	903 ±91	3128 ±104	3.5
S10P (ΔAUG)	8 ± 0	8 ± 2	1.0
D16E	27 ± 5	44 ± 2	1.6
D16E (ΔAUG)	7 ± 1	7 ± 0	1.0
S10P/D16E	161 ± 9	688 ± 36	4.3
S10P/D16E (ΔAUG)	10 ± 0	9 ± 1	0.9

[a]Cultures of *rrn*+ E. *coli* bacterial strains AW153 (Wt), AW643 (Wt(ΔAUG)), AW821 (D16E), AW946 (D16E (ΔAUG)), AW888 (S10P), AW940 (S10P (ΔAUG)), AW909 (S10P/D16E), and AW949 (S10P/D16E (ΔAUG)) were grown in minimal medium plus 0.2% glycerol, 0.05% acid-hydrolyzed casein, 0.01% vitamin B1, with (+Trp) or without (-Trp) 100 μg/ml Trp. β-Galactosidase assays were performed in three independent experiments . [b]Ratio of values for cultures grown with Trp (+Trp) and those grown without Trp (-Trp).

Table 12. High basal LacZ level observed with R23H is translation-dependent.

Strain	β-galactosidase activity (MU)[a]		Induction ratio (+Trp/-Trp)[b]
	-Trp	+Trp	
Wild-type	78 ±17	3391 ±179	43.5
Wild-type (ΔAUG)	5 ± 0	5 ± 0	1.0
R23H	521 ±30	1690 ±326	3.2
R23H (ΔAUG)	5 ± 0	5 ± 0	1.0
D16E	31 ± 4	51 ± 6	1.6
D16E (ΔAUG)	5 ± 0	5 ± 0	1.0
D16E/R23H	99 ± 6	512 ± 43	5.2
D16E/R23H (ΔAUG)	6 ± 1	5 ± 0	0.8

[a]Cultures of *rrn*+ *E. coli* bacterial strains AW153 (Wt), AW643 (Wt(ΔAUG)), AW821 (D16E), AW946 (D16E (ΔAUG)), AW922 (R23H), AW961 (R23H (ΔAUG)), AW925 (D16E/R23H), and AW973 (D16E/R23H (ΔAUG)) were grown in minimal medium plus 0.2% glycerol, 0.05% acid-hydrolyzed casein, 0.01% vitamin B1, with (+Trp) or without (-Trp) 100 μg/ml Trp. β-Galactosidase assays were performed in three independent experiments . [b]Ratio of values for cultures grown with Trp (+Trp) and those grown without Trp (-Trp).

The *cis*-acting S10P and R23H mutations increase induction to D16E, but not other non-functional TnaC mutants

Next, we wanted to determine if the S10P and R23H mutations could restore L-Trp-inducibility to other uninducible TnaC mutants, or if this restoration was specific to D16E. The *cis*-acting mutations were combined with two other loss-of-function mutations to D16, D16A (S10P/D16A or D16A/R23H) and D16K (S10P/D16K or D16K/R23H), and a loss-of-function mutation at a different position, W12R (S10P/W12R or W12R/R23H). Only when the S10P mutation was combined with D16E was L-Trp-inducibility increased (Table 13). Although the LacZ levels of the S10P/D16A, S10P/D16K, and S10P/W12R double mutants were higher than the D16A, D16K, and W12R single mutants, none of the double mutants were inducible by L-Trp. The higher levels of LacZ observed with the double mutants is likely a consequence of the S10P mutation. Similar results were obtained when the R23H mutation was combined with the D16 and W12 changes (Table 14). These results suggest that the S10P and R23H mutations increase the L-Trp-mediated ribosome-arrest function of D16E, but not of other loss-of-function TnaC mutants.

Table 13. The ability of S10P to suppress the loss-of-function D16E mutant is allele specific.

Strain	β-galactosidase activity (MU)[a]		Induction ratio (+Trp/-Trp)[b]
	-Trp	+Trp	
Wild-type	52 ± 2	2045 ± 8	39.3
S10P	1016 ±37	3196 ±140	3.1
D16E	27 ± 0	46 ± 2	1.7
S10P/D16E	178 ± 6	731 ± 61	4.1
D16A	61 ± 1	47 ± 1	0.8
S10P/D16A	328 ±41	373 ± 37	1.1
D16K	28 ± 1	21 ± 1	0.8
S10P/D16K	148 ± 5	114 ± 9	0.8
W12R	155 ± 3	91 ± 6	0.6
S10P/W12R	156 ±16	96 ± 7	0.6

[a]Cultures of *rrn*+ *E. coli* bacterial strains AW153 (Wt), AW888 (S10P), AW821 (D16E), AW513 (D16A), AW797 (D16K), AW154 (W12R), AW909 (S10P/D16E), AW952 (S10P/D16A), AW930 (S10P/D16K), and AW933 (S10P/W12R) were grown in minimal medium plus 0.2% glycerol, 0.05% acid-hydrolyzed casein, 0.01% vitamin B1, with (+Trp) or without (-Trp) 100 μg/ml Trp. β-Galactosidase assays were performed in three independent experiments . [b]Ratio of values for cultures grown with Trp (+Trp) and those grown without Trp (-Trp).

Table 14. The ability of R23H to suppress the loss-of-function D16E mutant is allele specific.

Strain	β-galactosidase activity (MU)[a]		Induction ratio (+Trp/-Trp)[b]
	-Trp	+Trp	
Wild-type	68 ± 3	2301 ±82	33.8
R23H	1193 ±43	2383 ±83	2.0
D16E	28 ± 2	51 ± 2	1.8
D16E/R23H	187 ± 8	510 ±15	2.7
D16A	45 ± 2	31 ± 2	0.7
D16A/R23H	464 ±52	403 ±21	0.9
D16K	27 ± 0	20 ± 0	0.7
D16K/R23H	289 ± 8	132 ± 3	0.5
W12R	136 ± 8	50 ± 2	0.4
W12R/R23H	293 ± 6	85 ± 2	0.3

[a]Cultures of *rrn*+ *E. coli* bacterial strains AW153 (Wt), AW922 (R23H), AW821 (D16E), AW513 (D16A), AW797 (D16K), AW154 (W12R), AW925 (D16E/R23H), AW965 (D16A/R23H), AW955 (D16K/R23H), and AW958 (W12R/R23H) were grown in minimal medium plus 0.2% glycerol, 0.05% acid-hydrolyzed casein, 0.01% vitamin B1, with (+Trp) or without (-Trp) 100 μg/ml Trp. β-Galactosidase assays were performed in three independent experiments . [b]Ratio of values for cultures grown with Trp (+Trp) and those grown without Trp (-Trp).

Interestingly, when either the S10P or R23H mutation was combined with other loss-of-function TnaC mutants (D16A, D16K, and W12R), the LacZ levels decreased ~10-fold compared to the S10P or R23H single mutants (Table 13 and 14). This decrease in LacZ levels indicates that both W12 and D16 are required for the constitutive S10P and R23H nascent peptide-mediated ribosome arrest.

Differential response of ribosomes with 23S rRNA changes to TnaC S10P and R23H mutants

Finally, we wanted to examine what effect different 23S rRNA mutations have on the Trp-independent ribosome arrest caused by the S10P and R23H mutant TnaC peptides. We tested the expression of the wild-type, *tnaC*(*S10P*), and *tnaC*(*R23H*) *tnaA*'-'*lacZ* reporter constructs in cells containing wild-type ribosomes or ribosomes with 23S rRNA mutations (Figure 24). As expected, expression of the wild-type reporter was dramatically reduced in cells containing A752C, U2609C, +A751ins, and A2058U ribosomes, and there was little change in the expression of the wild-type reporter in cells containing ribosomes with A2059 mutations or the A2058G mutation. Interestingly, in the Δ7 *rrn E.coli* background, the expression of the S10P and R23H reporters does not appear to be constitutive (Figure 24). Although the basal level of expression of the S10P and R23H reporters is higher than the basal level of expression of the wild-type reporter, the basal level of expression of the mutant reporters is much lower than the induced level of expression, which is not what was observed in the wild-type (*rrn*+) *E.coli* background. As shown with S10P(ΔAUG) (Table 11) and

R23H(ΔAUG) (Table 12), the constitutive phenotype of the S10P and R23H mutants is translation dependent suggesting that these mutant peptides cause ribosome arrest in the absence of added L-Trp. These TnaC mutations may increase the sensitivity of the ribosome to L-Trp such that endogenous levels of L-Trp are sufficient to induce ribosome arrest. One explanation for the difference in the basal level of expression with the S10P and R23H reporter constructs between the two strain backgrounds is that the endogenous levels of L-Trp may be lower in the Δ7 *rrn E.coli* background compared to the wild-type (*rrn*+) *E.coli* background. Therefore, if the TnaC S10P and R23H mutations increase the sensitivity of the ribosome for L-Trp, these reporter constructs would cause more stalling in the absence of added L-Trp in a strain background that produces a higher endogenous amount of L-Trp. The mechanism of how the 23S rRNA mutations affect the TnaC S10P and R23H mutant peptides is still being explored.

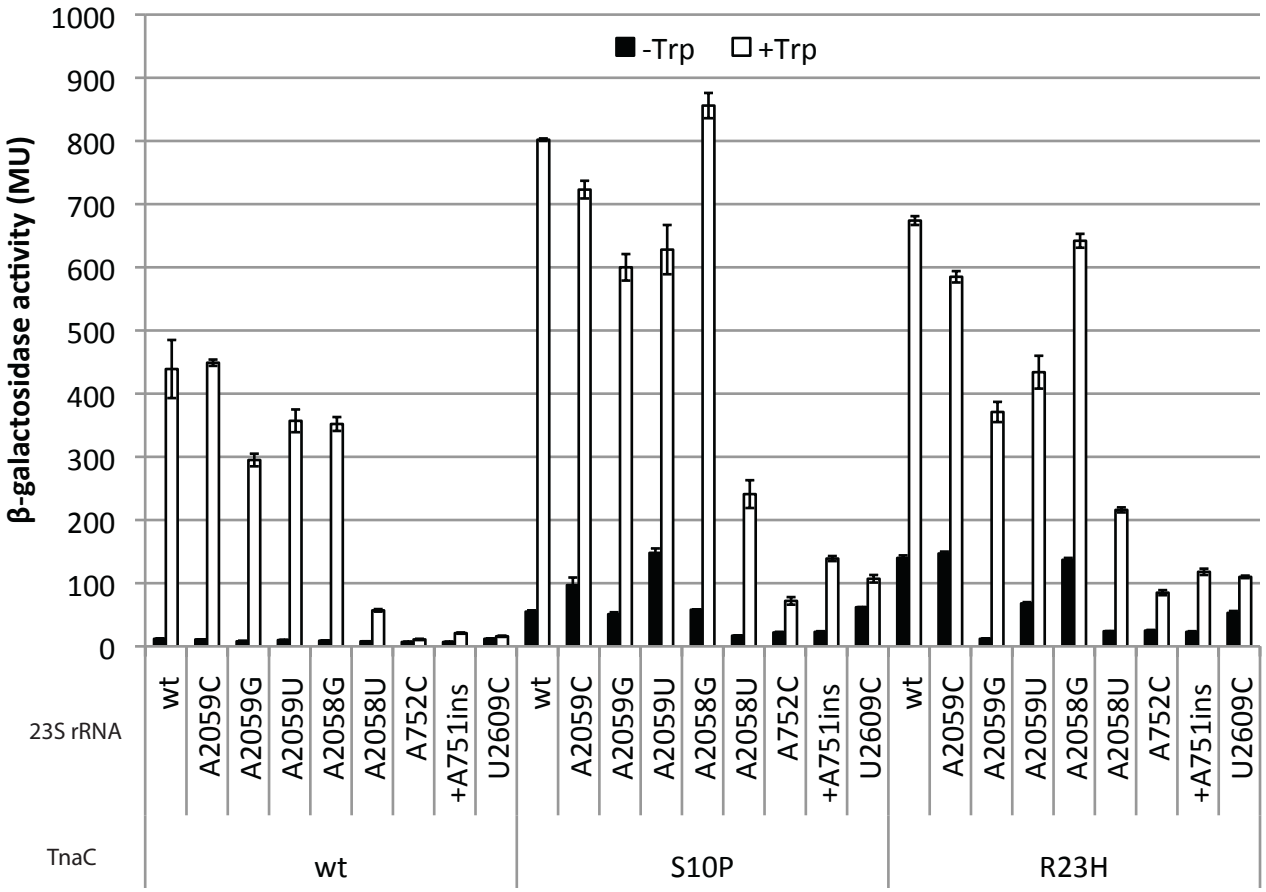

Figure 24. Effects of 23S rRNA mutations on S10P and R23H mutant TnaC peptides. Bacterial cells (Δ7 *rrn*) expressing the indicated 23S rRNAs and *tnaC* alleles were used to analyze expression of β-galactosidase from a *tnaC-tnaA'-'lacZ* protein fusion. The tested cultures were grown in minimal medium containing 0.2% glycerol, 0.05% acid-hydrolyzed casein, 0.01 % vitamin B1, 100μg/ml ampicillin, with (+Trp) or without (-Trp) 100 μg/ml L-Trp. β-Galactosidase assays were performed in three independent experiments.

DISCUSSION

TnaC residue D16 is highly conserved and is required for the L-Trp-dependent ribosome arrest function of TnaC. In this study we identified two second-site mutations within TnaC (S10P and R23H) that partially restore the ribosome arrest function to the non-functional TnaC(D16E) mutant. In addition to eliminating TnaC-mediated ribosome arrest in response to L-Trp, changes to D16 also fail to protect 23S rRNA residue U2609 from chemical methylation (99). The inability to protect U2609 from chemical methylation suggests that changes to the critical D16 residue affect the configuration of the nascent TnaC peptide in the ribosome exit tunnel. The change in the configuration of the nascent peptide may disrupt interactions between components of TnaC and the exit tunnel that are required for L-Trp binding and/or action. The *cis*-acting S10P and R23H mutations may compensate for the altered configuration of TnaC induced by the D16E change, restoring the required contacts between D16E (or other functional residues) and exit tunnel components. The observation that the *cis*-acting mutations can only restore L-Trp-inducibility to D16E, and not other loss-of-function TnaC mutants, is consistent with this idea.

In addition to S10P and R23H acting as suppressors of D16E, we showed that both the single S10P and R23H single TnaC mutants cause translation-dependent constitutive expression of the *lacZ* reporter *in vivo*. These results suggest that the S10P and R23H TnaC peptides cause ribosome arrest even in the absence of added L-Trp. The ability of the S10P and R23H mutant TnaC peptides to change the way mutant ribosomes respond to L-Trp supports the idea that the S10P and R23H changes are

acting at the level of translation. One explanation is that the mutant peptides have an altered conformation in the exit tunnel that mimics the conformation that is normally only induced in the presence of L-Trp, therefore the requirement for L-Trp to function as an inducer is lost in these mutants. Alternatively, the S10P and R23H changes may increase the ribosome and/or nascent peptide's binding affinity for L-Trp such that endogenous levels of L-Trp are sufficient to induce ribosome arrest.

Based on TnaC amino acid sequence alignments neither S10 nor R23 are conserved (39). However, none of the versions of TnaC have a Pro corresponding to *E.coli* position 10 or a His corresponding to *E.coli* position 23. Importantly, the 34 amino acid long TnaC from *Proteus vulgaris*, which is the only other TnaC that has been shown to be functional, has a Lys at *E.coli* position 10 (*P.vulgaris* K18) and a Phe at *E.coli* position 23 (*P.vulgaris* F31) (39,97). Although the amino acids at these positions are not conserved there may be selective pressure against a Pro at *E.coli* position 10 or a His at *E.coli* position 23 so that the regulated expression of the *tna* operon is maintained. It is crucial for the cell that the *tna* operon be tightly regulated so that the L-Trp catabolic genes are only produced under conditions in which glucose is limiting and L-Trp is present in excess.

Yap and Bernstein proposed that in addition to the critical residues that are required for SecM-mediated ribosome arrest, other variable residues are also required to facilitate the positioning of the key functional residues. These variable residues primarily influence the conformation of the nascent peptide in the exit tunnel ensuring that interactions between the essential SecM residues and the components of the exit

tunnel that are required for the ribosome arrest are maintained. They further propose that all RAPs contain both essential, functional residues as well as context-dependent sequence elements (65). Based on the results of genetic and biochemical analyses of S10 and R23, these residues of TnaC are likely context-dependent elements with their primary role being to direct the positioning of the essential TnaC residues so that they can interact with the ribosome exit tunnel components.

The classification of S10 and R23 as context-dependent elements is supported by several observations. By biochemical and structural analyses W12 is shown to be in close proximity to the A750-752 region of the 23S rRNA; this region of the 23S rRNA is functionally important for TnaC-mediated ribosome arrest in response to L-Trp (38,43-45,99). Although changes to the N-terminus of TnaC have little to no effect on Trp-induction, amino acids in the N-terminus may have a role in the proper positioning of W12 (68). This could explain the selective pressure against a Pro residue at *E.coli* position 10. A Pro at this position may impose conformational constraints on the peptide, that as discussed previously, would effect the configuration of the nascent peptide in the exit tunnel, such that regulated expression of the *tna* operon is lost. Genetic and biochemical analyses also show that the spacing between W12 and P24 is essential for maintaining L-Trp inducibility (68). While this region contains all of the essential residues, it also contains residues that are context-dependent and while they may serve minor functions by interacting with ribosomal exit tunnel components, their main function is likely to maintain the required spacing between the critical W12 and P24 residues (31,36,39,44,68).

In summary, the findings presented in this study show that the combined selection and screening method used is a powerful tool for identifying *cis*-acting mutations that can restore L-Trp-inducibility to the non-functional TnaC(D16E) mutant. Our findings also a suggest a possible role for S10 and R23 as context-dependent elements that influence the configuration of the nascent peptide in the ribosome exit tunnel and facilitate the interactions between D16, or other functional TnaC residues, with ribosomal exit tunnel components.

CHAPTER V

GENERAL DISCUSSION AND FUTURE WORK

OVERVIEW AND COMPARISON OF RIBOSOME ARREST PEPTIDES

Ribosome arrest peptides (RAPs) encoded in the 5'-leader region of bacterial transcripts (leader peptides) and upstream open reading frames (uORFs) of eukaryotic transcripts function to stall translating ribosome during their own synthesis. The mechanism by which the nascent peptide-dependent ribosome arrest regulates the expression of other genes encoded in the same transcriptional unit is dependent on the specific nature of the RAP. Ribosomes arrested by the fungal arginine attenuator peptide (AAP) block scanning ribosomes from reaching the downstream gene *arg2*, thus leading to decreased *arg2* expression (6). The stall manifested by the bacterial RAPs SecM, ErmCL, and MifM induce structural rearrangements of the mRNA, which makes the once unavailable Shine Dalgarno (SD) sequence of the downstream gene available for translation initiation by other ribosomes (7,8,12). The ribosome stall mediated by another bacterial RAP, TnaC, positively regulates transcription of the structural genes of the operon by inhibiting factor-dependent transcription termination (4). In the case of the bacterial RAPs, the ribosome stall functions to increase the expression of the genes regulated by the leader peptides.

The bacterial RAPs TnaC, ErmCL, SecM, and MifM all function to stall ribosomes during their own synthesis; however, there is very little sequence similarity between these peptides. All of bacterial RAPs contain residues that are essential for

ribosome arrest but how these residues are recognized by the ribosome and how they cause the arrest is poorly understood. Both TnaC and ErmCL are factor-dependent, meaning that the arrest is induced in response to a small molecule, L-Trp or erythromycin (Ery), respectively. SecM and MifM contain intrinsic arrest sequences. In these cases the ribosome arrest is alleviated only when the nascent peptide is physically pulled from the ribosome by interactions with the cellular secretion/translocation machinery. More studies need to be done before the sequence elements that are required for factor-dependent versus factor-independent ribosome arrest can be identified.

In order for the nascent peptide to induce ribosome arrest, constituents of the ribosome must be recognizing or responding to specific sequence elements of the RAP. The fact that specific residues of the ribosome exit tunnel are required for the function of the Escherichia coli RAPs TnaC, SecM, and ErmCL support this idea. The effect of mutations to ribosomal components have not been studied with the *Bacillus subtilis* RAP, MifM, because this RAP does not function in *E.coli* and the tools have yet to be developed for studying ribosomal mutations in *B.subtilis* (90). The *E.coli* RAPs TnaC, SecM, and ErmCL are all affected by changes to the 23S rRNA nucleotide A2058, suggesting that this nucleotide may be involved in monitoring translation and recognizing components of the RAP involved in ribosome arrest (5,12,44).

Based on the current knowledge, A2058 seems to be the only residue of the ribosomal exit tunnel that is required for the function of all of the *E.coli* RAPs. While TnaC- and SecM-mediated ribosome arrest is abolished by changes to the A748-A752 region of the 23S rRNA, ErmCL-mediated ribosome arrest is not affected by changes to

this region (7,12,44). However, ErmCL is shorter than both TnaC and SecM and is anchored to the exit tunnel through its interactions with A2058 and A2059. Therefore, ErmCL does not reach the region of the exit tunnel where nucleotides A748-A752 are located (7). Finally, both SecM and ErmCL require nucleotides A2503 and A2062 while TnaC (and other Erm variants ErmBL and ErmDL) do not (5). The different requirements for specific residues of the ribosome exit tunnel for RAP function suggest that the sequence components of the RAP essential for ribosome stalling activity are not recognized by the ribosome in the same way. Instead, there are differences in the way that the ribosome responds to the sequence elements of the RAPs that are required for ribosome arrest.

MAJOR FINDINGS OF STUDY

The *tna* operon in *E.coli* contains a 5'-leader region containing the coding sequence for the 24 amino acid RAP TnaC followed by two structural genes *tnaA* and *tnaB* that function in the catabolism of L-tryptophan (L-Trp) (21-23). TnaC stalls ribosomes in response to L-Trp positively regulating the expression of *tnaA* and *tnaB* by preventing premature transcription termination (1). Key residues of both the TnaC peptide and the ribosome required for TnaC-mediated ribosome arrest have been identified through genetic and biochemical analyses (45,64,84). Furthermore, structural analyses of TnaC in the ribosome exit tunnel revealed the position of these key residues, placing the conserved functional residues of TnaC in close proximity to residues of the 23S rRNA that are required for TnaC-mediated ribosome arrest in response to L-Trp

(38,43). These data suggest that interactions between the nascent peptide and ribosomal components play a role in ribosome arrest. However, how the interactions between the nascent TnaC peptide and the ribosome exit tunnel facilitate the ribosome arrest has remained largely unknown. The findings of this study begin to explain how TnaC, the ribosome, and L-Trp function cooperatively to mediate ribosome arrest.

Changes to the highly conserved TnaC residues W12 and D16 as well as mutations in the A748-A752 region (+A751ins and A752C) and U2609 of the 23S rRNA abolish TnaC-mediated ribosome arrest in response to L-Trp. Based on the UV cross-linking data that showed K11 of TnaC is positioned near 23S rRNA nucleotide A750, W12 of TnaC is believed to be located in close proximity to the A748-A752 region and U2609 of the 23S rRNA (44). Taken together, these data suggest that interactions between the crucial W12 residue of TnaC and the region of the ribosome exit tunnel containing nucleotides A748-A752 and U2609 may explain the requirement for these residues in L-Trp-induced ribosome arrest. However, structural analyses of TnaC in the ribosome exit tunnel position W12 within the constriction site of the exit tunnel and instead place TnaC residue K18 in between nucleotides U2609 and A752 (38,43).

In aiming to resolve the conflicting biochemical and structural data regarding the position of W12 within the exit tunnel, how changes to W12, D16, and K18 affect the configuration of the nascent peptide in the exit tunnel was examined. While changes to W12 and D16 abolish TnaC-mediated ribosome arrest in response to L-Trp, changes to K18 had little to no affect on L-Trp induction. Functional TnaC peptides (wild-type and K18A) protected 23S rRNA nucleotide U2609 from chemical methylation while non-

functional TnaC peptides (W12R and D16A) failed to protect U2609 from chemical methylation. The ability of the K18A mutant TnaC peptide to function in L-Trp induction and protection of U2609 from methylation is not consistent with the placement of K18 in this region of the exit tunnel.

Instead, consistent with the TnaC K11 UV cross-linking data, several lines of evidence support the placement of the crucial TnaC residue W12 in close proximity to the region of the 23S rRNA containing nucleotides A748-A752 and U2609. First, both W12 of TnaC and the A748-A752 and U2609 nucleotides are required for TnaC-mediated ribosome arrest. Second, the non-functional W12R mutant peptide fails to protect U2609 from chemical methylation. Finally, U2609 methylation protection is abolished in ribosomes that have lost their ability to respond to functional TnaC due to the +A751ins or A752C mutations in the 23S rRNA. The requirement for W12 and nucleotides in the A748-A752 region for Trp induction and for the protection of U2609 from chemical methylation suggest that interactions between these components may play a role in TnaC-mediated ribosome arrest. Although the results of this study support the placement of W12 instead of K18 near the A748-A752 and U2609 nucleotides, our results likely explain the change in conformation of U2609 in TnaC-containing ribosomes versus empty ribosomes that was observed by cryo-EM (43). The TnaC-induced conformational change of U2609 may be the result of either a direct interaction of W12 with U2609 or interactions between W12 and the A748-A752 region. U2609 forms a base-pair interaction with A752; it is conceivable that interactions between W12 and the A748-A752 region would affect the conformation of U2609.

Another interaction between the TnaC nascent peptide and the ribosome exit tunnel predicted by the structural analyses is between TnaC residue I19 and 23S rRNA nucleotides A2058 and A2059 (38,43). I19 of TnaC is highly conserved and the non-conservative mutations I19N, I19T, I19A, and I19W eliminate L-Trp induction (31,39). Also TnaC-mediated ribosome arrest is affected by changes to A2058 and A2059 (5,12,44). Although the genetic and biochemical data on TnaC residue I19 and the A2058 and A2059 nucleotides is limited and therefore conclusions as to whether or not interactions between these residues contribute to TnaC-mediated ribosome arrest cannot be made, the available data does support a functional role of these positions.

In this study we aimed to further examine the contributions of TnaC residue I19 and the A2058 and A2059 23S rRNA nucleotides in TnaC-mediated ribosome arrest by performing a more extensive mutational analysis of these positions. By making conservative and non-conservative changes to I19, we determined that I19 plays a role in the ability of the ribosome to sense free L-Trp. All of the conservative changes (I19L, I19M, and I19V) maintain L-Trp induction while the non-conservative changes (I19W and I19A) abolish L-Trp induction. While all of the conservative changes maintained L-Trp induction, only I19L required a similar concentration of 1-L-methyl-Trp (1MT) as wild-type TnaC for 50% induction. Both I19M and I19V required a higher concentration of 1MT to reach 50% induction compared to wild-type TnaC. The ability of L-Trp to induce ribosome arrest is influenced by the nature of the residue at position 19 of TnaC, suggesting that this residue participates in the ribosome's ability to sense free L-Trp.

As a result of the mutational and biochemical analyses of nucleotides A2058 and A2059, A2058 was determined to be the most crucial for TnaC-mediated ribosome arrest. While changes to A2059 had little to no effect on L-Trp induction, changes to A2058 impacted L-Trp induced ribosome arrest. The A2058G mutation decreased induction at low concentrations of 1MT but at higher concentrations of 1MT induction reached wild-type levels. More importantly however, the A2058U mutation drastically reduced L-Trp induced ribosome arrest. Interestingly, cells containing the A2058C mutation are not viable suggesting, that along with this nucleotides role in RAP function, it may also play a role in general translation.

After establishing the requirement for TnaC residue I19 and 23S rRNA nucleotide A2058 in TnaC-mediated ribosome arrest, we tested the prediction that there is a genetic interaction between TnaC I19 and the A2058 nucleotide. The TnaC I19 mutations were combined with each of the A2058 and A2059 changes and the effect of these changes on L-Trp induced ribosome arrest was assessed. The I19L TnaC change restored L-Trp sensitivity to the A2058U ribosomes. Furthermore, the compensatory effect of the TnaC I19L mutation was specific to A2058U because I19L was incapable of restoring L-Trp inducibility to U2609C ribosomes. These results support the cryo-EM model and molecular dynamic simulations that place I19 in close proximity to A2058 and A2059 and provide the first evidence of a functional interaction between a RAP and the ribosome exit tunnel (38,43).

The requirement of the crucial D16 residue of TnaC was further explored through the development of a combined selection and screening method that was used to

select for second-site mutations that could restore L-Trp inducibility to the non-functional D16E mutant. Two *cis*-acting mutations, S10P and R23H, which restored L-Trp induction to the D16E mutant peptide, were identified. The compensatory effect of the *cis*-acting mutations was allele specific; they did not restore L-Trp inducibility to other non-functional TnaC mutants. Interestingly, both of the single S10P and R23H TnaC mutants cause L-Trp-independent ribosome arrest *in vivo* that requires both W12 and D16. The restoration of ribosome arrest function to the D16E TnaC mutant by second-site mutations within TnaC suggest that the D16E change may be interfering with an interaction between the nascent TnaC peptide and ribosomal exit tunnel components that can be restored by compensatory mutations. Alternatively, the *cis*-acting S10P and R23H mutations within TnaC may create alternative interactions that allow the D16E mutant peptide to function in ribosome arrest.

The nascent TnaC peptide induces ribosome arrest by inhibiting peptidyl transferase activity. Many of the residues of TnaC and ribosomal components required for TnaC-mediated ribosome arrest are within the ribosome exit tunnel, far from the peptidyl transferase center (PTC). The results of this study begin to explain how these residues contribute to ribosome arrest.

Based on the cryo-EM model of TnaC in the exit tunnel of the ribosome, Seidelt, *et al*. proposed three different relay pathways to explain how a signal could be transmitted from interactions within the exit tunnel to the PTC, to cause inhibition of peptidyl transferase activity. Two of the relay pathways propose that upon L-Trp binding, interactions between the nascent TnaC peptide and ribosomal components

induce conformational changes of exit tunnel components transmitting a signal through 23S rRNA nucleotides in the exit tunnel to those in the PTC. One pathway proposes that the signal is relayed by the side of the exit tunnel containing the A748-A752 and U2609 23S rRNA nucleotides while the other pathway proposes that the other side of the exit tunnel, which contains the A2058 and A2059 nucleotides, relays the signal. The third pathway proposes that upon L-Trp binding the signal is relayed through conformational changes of the nascent TnaC peptide (43).

The results of this study suggest that all three of the proposed relay pathways play a role in transmitting the signal from the ribosome exit tunnel to the PTC. First, changes to TnaC residues W12 and D16 and to 23S rRNA nucleotides A748-A752 abolish the protection of U2609 from chemical methylation and abolish L-Trp induction. These results suggest that these changes affect the configuration of TnaC and/or the ribosomal exit tunnel components constituting this region. The configuration changes may block the relay signal from being transmitted to the PTC through TnaC, the side of the exit tunnel containing 23S rRNA nucleotides A748-A752 and U2609, or both. Second, changes to TnaC residue I19 and 23S rRNA nucleotides A2058 and A2059 affect L-Trp sensitivity and TnaC-mediated ribosome arrest. These results suggest a requirement for these residues in L-Trp binding. However, these changes may also cause conformational changes in these components, which block the relay signal to the PTC that is transmitted from the nascent peptide, the side of the exit tunnel containing the A2058 and A2059 nucleotides, or both. Finally, the identification of *cis*-acting elements, which restore ribosome arrest function to the loss-of-function D16E TnaC

mutant suggest that the nascent peptide plays a role in relaying the signal from the ribosome exit tunnel to the PTC. Taken together, these results support the requirement for all three relay pathways proposed by Seidelt *et al*. in inhibition of peptidyl transferase activity resulting in TnaC-mediated ribosome arrest. Interestingly, relay pathways through the RAP and/or exit tunnel components have been proposed for other RAPs, most notably ErmCL and SecM (7,12,43,85).

FUTURE WORK

While the results of this study begin to explain how residues of both TnaC and the 23S rRNA lining the exit tunnel contribute to ribosome arrest in response to L-Trp, further experiments are still needed before the molecular mechanism of TnaC-mediated ribosome arrest can be fully understood. Previous genetic and biochemical analyses identifying the residues involved as well as the structural analyses which allow predictions on possible interactions and conformational changes that are required to induce ribosome arrest provide a starting point for further investigation. All of the proposed interactions between the crucial TnaC residues and ribosomal components need to be tested experimentally. The methods used in this and other studies provide a means to determine if these interactions are functionally important. Most importantly however, the binding site of L-Trp has yet to be elucidated. Once the L-Trp binding site is determined, how changes to TnaC and the ribosomal exit tunnel and PTC components affect L-Trp binding and/or action can be determined. The answers to these remaining questions will allow the development of a model to explain the molecular mechanism of

L-Trp induced TnaC-mediated ribosome arrest. This model will also be useful for comparing the mechanisms by which other RAPs induce ribosome arrest.

REFERENCES

1. Stewart, V. and Yanofsky, C. (1985) Evidence for transcription antitermination control of tryptophanase operon expression in *Escherichia coli* K-12. *J Bacteriol*, **164**, 731-740.

2. Narayanan, C.S. and Dubnau, D. (1987) Demonstration of erythromycin-dependent stalling of ribosomes on the *ermC* leader transcript. *J Biol Chem*, **262**, 1766-1771.

3. Alexieva, Z., Duvall, E.J., Ambulos, N.P., Kim, U.J. and Lovett, P.S. (1988) Chloramphenicol induction of cat-86 requires ribosome stalling at a specific site in the leader. *Proc Natl Acad Sci U S A*, **85**, 3057-3061.

4. Gong, F. and Yanofsky, C. (2002) Analysis of tryptophanase operon expression *in vitro*. *J Biol Chem*, **277**, 17095-17100.

5. Vazquez-Laslop, N., Ramu, H., Klepacki, D., Kannan, K. and Mankin, A.S. (2010) The key function of a conserved and modified rRNA residue in the ribosomal response to the nascent peptide. *EMBO J*, **29**, 3108-3117.

6. Wang, Z. and Sachs, M.S. (1997) Ribosome stalling is responsible for arginine-specific translational attenuation in *Neurospora crassa*. *Mol Cell Biol*, **17**, 4904-4913.

7. Vazquez-Laslop, N., Thum, C. and Mankin, A.S. (2008) Molecular mechanism of drug-dependent ribosome stalling. *Mol Cell*, **30**, 190-202.

8. Chiba, S., Lamsa, A. and Pogliano, K. (2009) A ribosome-nascent chain sensor of membrane protein biogenesis in *Bacillus subtilis*. *EMBO J*, **28**, 3461-3475.

9. Ruan, H., Shantz, L.M., Pegg, A.E. and Morris, D.R. (1996) The upstream open reading frame of the mRNA encoding S-adenosylmethionine decarboxylase is a polyamine-responsive translational control element. *J Biol Chem*, **271**, 29576-29582.

10. Degnin, C.R., Schleiss, M.R., Cao, J. and Geballe, A.P. (1993) Translational initiation mediated by a short upstream open reading frame in the human Cytomegalovirus gpUL4 (gp48) transcript. *J Virol*, **67**, 5514-5521.

11. Cao, J. and Geballe, A.P. (1995) Translational inhibition by a human Cytomegalovirus upstream open reading frame despite inefficient utilization of its AUG codon. *J Virol*, **69**, 1030-1036.

12. Nakatogawa, H. and Ito, K. (2002) The ribosomal exit tunnel functions as a discriminating gate. *Cell*, **108**, 629-636.

13. Calvo, S.E., Pagliarini, D.J. and Mootha, V.K. (2009) Upstream open reading frames cause widespread reduction of protein expression and are polymorphic among humans. *Proc Natl Acad Sci U S A*, **106**, 7507-7512.

14. Fritsch, C., Herrmann, A., Nothnagel, M., Szafranski, K., Huse, K., Schumann, F., Schreiber, S., Platzer, M., Krawczak, M., Hampe, J. *et al.* (2012) Genome-wide search for novel human uORFs and N-terminal protein extensions using ribosomal footprinting. *Genome Res*, **11**, 2208-2218.

15. Melnikov, S., Ben-Shem, A., Garreau de Loubresse, N., Jenner, L., Yusupova, G. and Yusupov, M. (2012) One core, two shells: bacterial and eukaryotic ribosomes. *Nat Struct Mol Biol*, **19**, 560-567.

16. Ramakrishnan, V. (2002) Ribosome structure and the mechanism of translation. *Cell*, **108**, 557-572.

17. Zhang, L., Sato, N.S., Watanabely, K. and Suzuki, T. (2003) Functional genetic selection of the decoding center in E. coli 16s rRNA. *Nucleic Acids Symp Ser*, **3**, 319-320.

18. Yusupov, M.M., Yusupova, G.Z., Baucom, A., Lieberman, K., Earnest, T.N., Cate, J.H.D. and Noller, H.F. (2001) Crystal structure of the ribosome at 5.5 Angstrom resolution. *Science*, **292**, 883-896.

19. Voss, N.R., Gerstein, M., Steitz, T.A. and Moore, P.B. (2006) The Geometry of the ribosomal polypeptide exit tunnel. *J Mol Biol*, **360**, 893-906.

20. Ban, N., Nissen, P., Hansen, J., Moore, P.B. and Steitz, T.A. (2000) The complete atomic structure of the large ribosomal subunit at 2.4 Angstrom resolution. *Science*, **289**, 905.

21. Deeley, M.C. and Yanofsky, C. (1981) Nucleotide sequence of the structural gene for tryptophanase of *Escherichia coli* K-12. *J Bacteriol*, **147**, 787-796.

22. Sarsero, J.P., Wookey, P.J., Gollnick, P., Yanofsky, C. and Pittard, A.J. (1991) A new family of integral membrane proteins involved in transport of aromatic amino acids in *Escherichia coli*. *J Bacteriol*, **173**, 3231-3234.

23. Newton, W.A. and Snell, E.E. (1964) Catalytic properties of tryptophanase, a multifiunctional pyridoxal phosphate enzyme. *Proc Natl Acad Sci U S A*, **51**, 382-389.

24. Ren, D., Bedzyk, L.A., Ye, R.W., Thomas, S.M. and Wood, T.K. (2004) Stationary-phase quorum-sensing signals affect autoinducer-2 and gene expression in *Escherichia coli*. *Appl Environ Microbiol*, **70**, 2038-2043.

25. Winzer, K., Hardie, K.R. and Williams, P. (2002) Bacterial cell-to-cell communication: sorry, can't talk now -- gone to lunch! *Curr Opin Microbiol*, **5**, 216-222.

26. Bhatt, S., Anyanful, A. and Kalman, D. (2011) CsrA and TnaB coregulate tryptophanase activity to promote exotoxin-induced killing of *Caenorhabditis elegans* by enteropathogenic *Escherichia coli*. *J Bacteriol*, **193**, 4516-4522.

27. Botsford, J.L. and DeMoss, R.D. (1971) Catabolite repression of tryptophanase in *Escherichia coli*. *J Bacteriol*, **105**, 303-312.

28. Stewart, V., Landick, R. and Yanofsky, C. (1986) Rho-dependent transcription termination in the tryptophanase operon leader region of *Escherichia coli* K-12. *J Bacteriol*, **166**, 217-223.

29. Gong, F. and Yanofsky, C. (2001) Reproducing *tna* operon regulation in vitro in an S-30 system. *J Biol Chem*, **276**, 1974-1983.

30. Konan, K.V. and Yanofsky, C. (1997) Regulation of the *Escherichia coli tna* operon: Nascent leader peptide control at the *tnaC* stop codon. *J Bacteriol*, **179**, 1774-1779.

31. Gish, K. and Yanofsky, C. (1995) Evidence suggesting *cis* action by the TnaC leader peptide in regulating transcription attenuation in the tryptophanase operon of *Escherichia coli*. *J Bacteriol*, **177**, 7245-7254.

32. Konan, K.V. and Yanofsky, C. (2000) Rho-dependent transcription termination in the *tna* operon of *Escherichia coli*: Roles of the *boxA* sequence and the *rut* site. *J Bacteriol*, **182**, 3981-3988.

33. Platt, T. and Richardson, J.P. (1992) In Yamamoto, S. L. M. a. K. R. (ed.), *Transcriptional regulation*. Cold Spring Harbor Laboratory Press, Cold Spring Harbor, NY, pp. 365-388.

34. Platt, T. (1994) Rho and RNA: models for recognition and response. *Mol Microbiol*, **11**, 983-990.

35. Yanofsky, C. and Horn, V. (1995) Bicyclomycin sensitivity and resistance affect Rho factor-mediated transcription termination in the *tna* operon of *Escherichia coli*. *J Bacteriol*, **177**, 4451-4456.

36. Gollnick, P. and Yanofsky, C. (1990) tRNA(Trp) translation of leader peptide codon 12 and other factors that regulate expression of the tryptophanase operon. *J Bacteriol*, **172**, 3100-3107.

37. Yanofsky, C., Konan, K.V. and Sarsero, J.P. (1996) Some novel transcription attenuation mechanisms used by bacteria. *Biochimie*, **78**, 1017-1024.

38. Trabuco, L.G., Harrison, C.B., Schreiner, E. and Schulten, K. (2010) Recognition of the regulatory nascent chain TnaC by the ribosome. *Structure*, **18**, 627-637.

39. Cruz-Vera, L.R. and Yanofsky, C. (2008) Conserved residues Asp16 and Pro24 of TnaC-tRNAPro participate in tryptophan induction of *tna* operon expression. *J Bacteriol*, **190**, 4791-4797.

40. Gong, F., Ito, K., Nakamura, Y. and Yanofsky, C. (2001) The mechanism of tryptophan induction of tryptophanase operon expression: Tryptophan inhibits release factor-mediated cleavage of TnaC-peptidyl-tRNA^{Pro}. *Proc Natl Acad Sci U S A*, **98**, 8997-9001.

41. Konan, K.V. and Yanofsky, C. (1999) Role of ribosome release in regulation of *tna* operon expression in *Escherichia coli*. *J Bacteriol*, **181**, 1530-1536.

42. Tanner, D.R., Cariello, D.A., Woolstenhulme, C.J., Broadbent, M.A. and Buskirk, A.R. (2009) Genetic identification of nascent peptides that induce ribosome stalling. *J Biol Chem*, **284**, 34809-34818.

43. Seidelt, B., Innis, C.A., Wilson, D.N., Gartmann, M., Armache, J.-P., Villa, E., Trabuco, L.G., Becker, T., Mielke, T., Schulten, K. *et al.* (2009) Structural insight into nascent polypeptide chain-mediated translational stalling. *Science*, **326**, 1412-1415.

44. Cruz-Vera, L.R., Rajagopal, S., Squires, C. and Yanofsky, C. (2005) Features of ribosome-peptidyl-tRNA interactions essential for tryptophan induction of *tna* operon expression. *Mol Cell*, **19**, 333-343.

45. Cruz-Vera, L.R., New, A., Squires, C. and Yanofsky, C. (2007) Ribosomal features essential for *tna* operon induction: tryptophan binding at the peptidyl transferase center. *J Bacteriol*, **189**, 3140-3146.

46. Schlunzen, F., Zarivach, R., Harms, J., Bashan, A., Tocilj, A., Albrecht, R., Yonath, A. and Franceschi, F. (2001) Structural basis for the interaction of antibiotics with the peptidyl transferase centre in eubacteria. *Nature*, **413**, 814-821.

47. Weisblum, B. (1995) Erythromycin resistance by ribosome modification. *Antimicrob Agents Chemother*, **39**, 577-585.

48. Nobeli, I., Laskowski, R.A., Valdar, W.S.J. and Thornton, J.M. (2001) On the molecular discrimination between adenine and guanine by proteins. *NAR*, **29**, 4294-4309.

49. Bottger, E.C., Springer, B., Prammananan, T., Kidan, Y. and Sander, P. (2001) Structural basis for selectivity and toxicity of ribosomal antibiotics. *EMBO Rep*, **2**, 318-323.

50. Horinouchi, S. and Weisblum, B. (1980) Posttranscriptional modification of mRNA conformation: Mechanism that regulates erythromcin-induced resistance. *Proc Natl Acad Sci U S A*, **77**, 7079-7083.

51. Mayford, M. and Weisblum, B. (1989) *ermC* leader peptide: Amino acid sequence critical for induction by translational attenuation. *J Mol Biol*, **206**, 69-79.

52. Vazquez-Laslop, N., Klepacki, D., Mulhearn, D.C., Ramu, H., Krasnykh, O., Franzblau, S. and Mankin, A.S. (2011) Role of antibiotic ligand in nascent peptide-dependent ribosome stalling. *Proc Natl Acad Sci U S A*, **108**, 10496-10501.

53. Toh, S.-M., Xiong, L., Bae, T. and Mankin, A.S. (2008) The methyltransferase YfgB/RlmN is responsible for modification of adenosine 2503 in 23S rRNA. *RNA*, **14**, 98-106.

54. Brundage, L., Hendrick, J.P., Schiebel, E., Driessen, A.J.M. and Wickner, W. (1990) The purified *E. coli* integral membrane protein SecYE is sufficient for reconstitution of SecA-dependent precursor protein translocation. *Cell*, **62**, 649-657.

55. Oliver, D., Norman, J. and Sarker, S. (1998) Regulation of *Escherichia coli secA* by cellular protein secretion proficiency requires an intact gene X signal sequence and an active translocon. *J Bacteriol*, **180**, 5240-5242.

56. Oliver, D.B. and Beckwith, J. (1982) Regulation of a membrane component required for protein secretion in *Escherichia coli*. *Cell*, **30**, 311-319.

57. McNicholas, P., Salavati, R. and Oliver, D. (1997) Dual regulation of *Escherichia coli secA* translation by distinct upstream elements. *J Mol Biol*, **265**, 128-141.

58. Schmidt, M.G. and Oliver, D.B. (1989) SecA protein autogenously represses its own translation during normal protein secretion in *Escherichia coli*. *J Bacteriol*, **171**, 643-649.

59. Nakatogawa, H. and Ito, K. (2001) Secretion monitor, SecM, undergoes self-translation arrest in the cytosol. *Mol Cell*, **7**, 185-192.

60. Yen, M.R., Harley, K.T., Tseng, Y.H. and Jr., M.H.S. (2001) Phylogenetic and structural analyses of the oxa1 family of protein translocases. *FEMS Microbiol Lett*, **204**, 223-231.

61. Xie, K. and Dalbey, R.E. (2008) Inserting proteins into the bacterial cytoplasmic membrane using the Sec and YidC translocases. *Nat Rev Microbiol*, **6**, 234-244.

62. Rubio, A., Jiang, X. and Pogliano, K. (2005) Localization of translocation complex components in *Bacillus subtilis*: Enrichment of the signal recognition particle receptor at early sporulation septa. *J Bacteriol*, **187**, 5000-5002.

63. Chiba, S. and Ito, K. (2012) Multisite ribosomal stalling: A unique mode of regulatory nascent chain action revealed for MifM. *Mol Cell*, **47**, 863-872.

64. Yang, R., Cruz-Vera, L.R. and Yanofsky, C. (2009) 23S rRNA nucleotides in the peptidyl transferase center are essential for tryptophanase operon induction. *J Bacteriol*, **191**, 3445-3450.

65. Yap, M.-N. and Bernstein, H.D. (2009) The plasticity of a translation arrest motif yields insights into nascent polypeptide recognition inside the ribosome tunnel. *Mol Cell*, **34**, 201-211.

66. Dunkle, J.A., Xiong, L., Mankin, A.S. and Cate, J.H.D. (2010) Structures of the *Escherichia coli* ribosome with antibiotics bound near the peptidyl transferase center explain spectra of drug action. *Proc Natl Acad Sci U S A*, **107**, 17152-17157.

67. Deeley, M.C. and Yanofsky, C. (1982) Transcription initiation at the tryptophanase promoter of *Escherichia coli* K-12. *J Bacteriol*, **151**, 942-951.

68. Gong, F. and Yanofsky, C. (2002) Instruction of translating ribosome by nascent peptide. *Science*, **297**, 1864-1867.

69. Cruz-Vera, L.R., Sachs, M.S., Squires, C.L. and Yanofsky, C. (2011) Nascent polypeptide sequences that influence ribosome function. *Curr Opin Microbiol*, **14**, 160-166.

70. Fang, P., Spevak, C.C., Wu, C. and Sachs, M.S. (2004) A nascent polypeptide domain that can regulate translation elongation. *Proc Natl Acad Sci U S A*, **101**, 4059-4064.

71. Hood, H.M., Spevak, C.C. and Sachs, M.S. (2007) Evolutionary changes in the fungal carbamoyl-phosphate synthetase small subunit gene and its associated upstream open reading frame. *Fungal Genet Biol*, **44**, 93-104.

72. Spevak, C.C., Ivanov, I.P. and Sachs, M.S. (2010) Sequence requirements for ribosome stalling by the arginine attenuator peptide. *J Biol Chem*, **285**, 40933-40942.

73. Schuwirth, B.S., Borovinskaya, M.A., Hau, C.W., Zhang, W., Vila-Sanjurjo, A., Holton, J.M. and Cate, J.H. (2005) Structures of the bacterial ribosome at 3.5 A resolution. *Science*, **310**, 827-834.

74. Sachs, M.S. and Geballe, A.P. (2002) Biochemistry. Sense and sensitivity--controlling the ribosome. *Science*, **297**, 1820-1821.

75. Garza-Ramos, G., Xiong, L., Zhong, P. and Mankin, A. (2001) Binding site of macrolide antibiotics on the ribosome: new resistance mutation identifies a specific interaction of ketolides with rRNA. *J Bacteriol*, **183**, 6898-6907.

76. Zaporojets, D., French, S. and Squires, C.L. (2003) Products transcribed from rearranged *rrn* genes of *Escherichia coli* can assemble to form functional ribosomes. *J Bacteriol*, **185**, 6921-6927.

77. Brosius, J., Dull, T.J., Sleeter, D.D. and Noller, H.F. (1981) Gene organization and primary structure of a ribosomal RNA operon from *Escherichia coli*. *J Mol Biol*, **148**, 107-127.

78. McKenzie, G. and Craig, N. (2006) Fast, easy and efficient: site-specific insertion of transgenes into Enterobacterial chromosomes using Tn7 without need for selection of the insertion event. *BMC Microbiol*, **6**, 39.

79. Miller, J. (1972) *Experiments in Molecular Genetics* Cold Spring Harbor, NY: Cold Spring Harbor Laboratory.

80. Yanofsky, C., Horn, V. and Gollnick, P. (1991) Physiological studies of tryptophan transport and tryptophanase operon induction in *Escherichia coli*. *J Bacteriol*, **173**, 6009-6017.

81. Wilson, D.N. and Beckmann, R. (2011) The ribosomal tunnel as a functional environment for nascent polypeptide folding and translational stalling. *Curr Opin Struct Biol*, **21**, 274-282.

82. Moazed, D. and Noller, H.F. (1989) Interaction of tRNA with 23S rRNA in the ribosomal A, P, and E sites. *Cell*, **57**, 585-597.

83. Gustafsson, C. and Persson, B.C. (1998) Identification of the *rrmA* gene encoding the 23S rRNA m1G745 methyltransferase in *Escherichia coli* and characterization of an m1G745-deficient mutant. *J Bacteriol*, **180**, 359-365.

84. Cruz-Vera, L.R., Gong, M. and Yanofsky, C. (2006) Changes produced by bound tryptophan in the ribosome peptidyl transferase center in response to TnaC, a nascent leader peptide. *Proc Natl Acad Sci U S A*, **103**, 3598-3603.

85. Bhushan, S., Meyer, H., Starosta, A.L., Becker, T., Mielke, T., Berninghausen, O., Sattler, M., Wilson, D.N. and Beckmann, R. (2010) Structural basis for translational stalling by human Cytomegalovirus and fungal Arginine Attenuator Peptide. *Mol Cell*, **40**, 138-146.

86. Lebars, I., Yoshizawa, S., Stenholm, A.R., Guittet, E., Douthwaite, S. and Fourmy, D. (2003) Structure of 23S rRNA hairpin 35 and its interaction with the tylosin-resistance methyltransferase RlmAII. *EMBO J*, **22**, 183-192.

87. Youngman, E.M., Brunelle, J.L., Kochaniak, A.B. and Green, R. (2004) The active site of the ribosome is composed of two layers of conserved nucleotides with distinct roles in peptide bond formation and peptide release. *Cell*, **117**, 589-599.

88. Gregory, S.T. and Dahlberg, A.E. (1999) Erythromycin resistance mutations in ribosomal proteins L22 and L4 perturb the higher order structure of 23 S ribosomal RNA. *J Mol Biol*, **289**, 827-834.

89. Chiba, S., Kanamori, T., Ueda, T., Akiyama, Y., Pogliano, K. and Ito, K. (2011) Recruitment of a species-specific translational arrest module to monitor different cellular processes. *Proc Natl Acad Sci U S A*, **108**, 6073-6078.

90. Vazquez-Laslop, N. and Mankin, A.S. (2011) Picky nascent peptides do not talk to foreign ribosomes. *Proc Natl Acad Sci U S A*, **108**, 5931-5932.

91. Ramu, H., Mankin, A. and Vazquez-Laslop, N. (2009) Programmed drug-dependent ribosome stalling. *Mol Microbiol*, **71**, 811-824.

92. Ito, K., Chiba, S. and Pogliano, K. (2010) Divergent stalling sequences sense and control cellular physiology. *Biochem Biophys Res Commun*, **393**, 1-5.

93. Ito, K. and Chiba, S. (2013) Arrest peptides: cis-acting modulators of translation. *Annu Rev Biochem*, **82**, 171-202.

94. Hirakawa, H., Kodama, T., Takumi-Kobayashi, A., Honda, T. and Yamaguchi, A. (2009) Secreted indole serves as a signal for expression of type III secretion system translocators in enterohaemorrhagic *Escherichia coli* O157:H7. *Microbiology*, **155**, 541-550.

95. Kamath, A.V. and Yanofsky, C. (1992) Characterization of the tryptophanase operon of *Proteus vulgaris*. Cloning, nucleotide sequence, amino acid homology, and in vitro synthesis of the leader peptide and regulatory analysis. *J Biol Chem*, **267**, 19978-19985.

96. Kamath, A. and Yanofsky, C. (1997) Roles of the *tnaC-tnaA* spacer region and Rho factor in regulating expression of the tryptophanase operon of *Proteus vulgaris*. *J Bacteriol*, **179**, 1780-1786.

97. Cruz-Vera, L.R., Yang, R. and Yanofsky, C. (2009) Tryptophan inhibits *Proteus vulgaris* TnaC leader peptide elongation, activating *tna* operon expression. *J Bacteriol*, **191**, 7001-7006.

98. Stewart, V. and Yanofsky, C. (1986) Role of leader peptide synthesis in tryptophanase operon expression in *Escherichia coli* K-12. *J Bacteriol*, **167**, 383-386.

99. Martinez, A.K., Shirole, N.H., Murakami, S., Benedik, M.J., Sachs, M.S. and Cruz-Vera, L.R. (2012) Crucial elements that maintain the interactions between the regulatory TnaC peptide and the ribosome exit tunnel responsible for Trp inhibition of ribosome function. *NAR*, **40**, 2247-2257.

100. Brosius, J., Ullrich, A., Raker, M.A., Gray, A., Dull, T.J., Gutell, R.R. and Noller, H.F. (1981) Construction and fine mapping of recombinant plasmids containing the *rrnB* ribosomal RNA operon of *E. coli*. *Plasmid*, **6**, 112-118.

101. Sigmund, C.D., Ettayebi, M., Borden, A. and Morgan, E.A. (1988) In Harry F. Noller, J. K. M. (ed.), *Methods in Enzymology*. Academic Press, Vol. 164, pp. 673-690.

102. Cardinale, C.J., Washburn, R.S., Tadigotla, V.R., Brown, L.M., Gottesman, M.E. and Nudler, E. (2008) Termination factor Rho and Its cofactors NusA and NusG silence foreign DNA in *E. coli*. *Science*, **320**, 935-938.

103. Hansen, J.L., Moore, P.B. and Steitz, T.A. (2003) Structures of five antibiotics bound at the peptidyl transferase center of the large ribosomal subunit. *J Mol Biol*, **330**, 1061-1075.

104. Shimizu, Y., Kanamori, T. and Ueda, T. (2005) Protein synthesis by pure translation systems. *Methods*, **36**, 299-304.

105. Kannan, K. and Mankin, A.S. (2011) Macrolide antibiotics in the ribosome exit tunnel: species-specific binding and action. *Ann N Y Acad Sci*, **1241**, 33-47.

106. Lu, J., Hua, Z., Kobertz, W.R. and Deutsch, C. (2011) Nascent peptide side chains induce rearrangements in distinct locations of the ribosomal tunnel. *J Mol Biol*, **411**, 499-510.

107. Bhushan, S., Hoffmann, T., Seidelt, B., Frauenfeld, J., Mielke, T., Berninghausen, O., Wilson, D.N. and Beckmann, R. (2011) SecM-stalled ribosomes adopt an altered geometry at the peptidyl transferase center. *PLoS Biol*, **9**, e1000581.

108. Abou-Nader, M. and Benedik, M.J. (2010) Rapid generation of random mutant libraries. *Bioengineered*, **1**, 337-340.

109. Datsenko, K.A. and Wanner, B.L. (2000) One-step inactivation of chromosomal genes in Escherichia coli K-12 using PCR products. *Proc Natl Acad Sci U S A*, **97**, 6640-6645.

APPENDIX

CONTIRBUTIONS

Several of my collaborators carried out specific experiments, the results of which are used in this work. The purpose of this Contributions section is to explicitly state my contributions and the contributions of others.

I constructed all strains with an "AW" designation and all plasmids with a "pAW" designation. The following plasmids: pNKA2058G, pNKA2058T, pNKA2059C, pNKA2059G, and pNKA2059T, described in Chapter III, were constructed in Dr. Luis Rogelio Cruz-Vera's laboratory. All other plasmids and strains are referenced accordingly.

I carried out all of the Miller Assays, with the exception of the results shown in Chapter II, Table 3. I also developed the combined selection and screen method used in Chapter IV, and carried out all experiments in this chapter.

The following experiments were carried out in Dr. Luis Rogelio Cruz-Vera's laboratory: puromycin assays described in Chapters II and III, methylation protection assays described in Chapter II, primer extension experiments described in Chapter II, Miller Assays of 23S rRNA U2609 and A752 double mutants shown Table 3 of Chapter II, and TnaC-tRNA^{Pro} accumulation experiments described in Chapter III.

The 2D-DIGE analysis described in Chapter III was performed by Dr. Lewis M. Brown at the Comparative Proteomics Center, Columbia University in collaboration

with Dr. Alexander Mankin's laboratory. Researchers in Dr. Alexander Mankin's laboratory also carried out all of the toeprinting experiments described in Chapter III.